SPOWIND | Interreg Euro-MED | Co-funded by the European Union

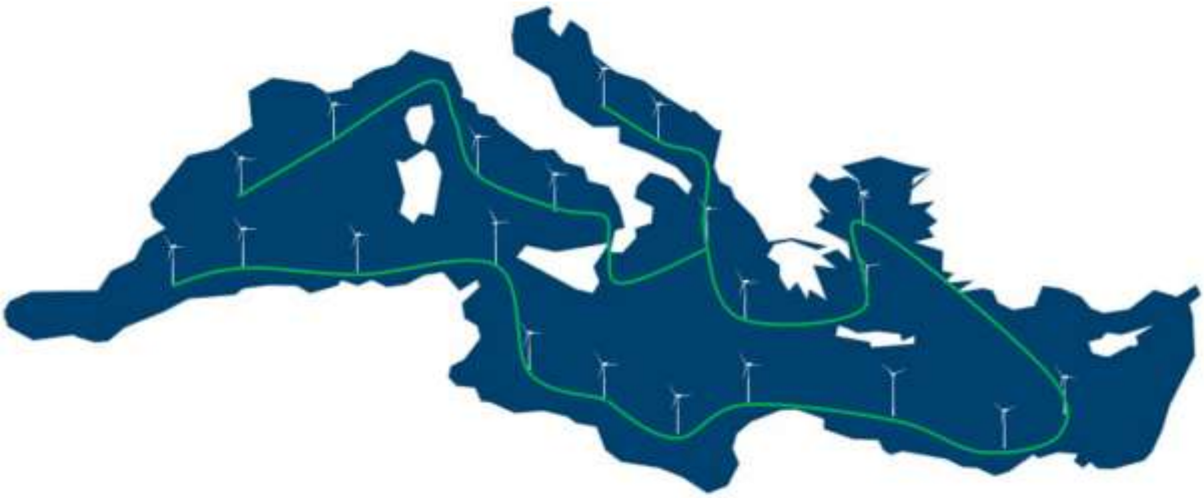

February 2025

Power-to-X technologies and opportunities

https://spowind.interreg-euro-med.eu/

SPOWIND

Deliverable Euro-MED0200199

Project acronym	SPOWIND
Project title	Spatial Planning for Offshore Wind Industry Development
Project mission	Strengthening an innovative sustainable economy
Project priority	1 - Smarter MED
Specific objective	RSO1.1 - Developing and enhancing research and innovation capacities and the uptake of advanced technologies
Type of project	Thematic
Project duration	01/01/2024 – 31/03/2026 (27 months)

Deliverable title	Power-to-X technologies and opportunities
Deliverable number	D.3.2.1
Deliverable type	Report,
Work package number	WP3
Work package title	Energy carriers and transfer
Activity name	Power-to-x solutions for offshore wind farms
Activity number	3.2
Partner in charge (author)	SAP
Partners involved	POLITO, SAP, ICCS

Document history

Versions	Date	Document status	Delivered by
Version 1.0	08/01/2025	Draft	SAP
Version 2.0	30/01/2025	V2	SAP
Version 1.0	25/02/2025	Final	SAP

Table of contents

Abbrevations

Abbreviation	Full Form
AHP	Annual Hydrogen Production
ANP	Annual Ammonia Production
CAPEX	Capital Expenditure
CF	Capacity Factor
E_{annual}	Annual Energy Production
EEL	Electrolyzer Efficiency
E_{el}	Electrical Energy Input
HHV	Higher Heating Value
HVDC	High-Voltage Direct Current
HVAC	High-Voltage Alternating Current
LCOA	Levelized Cost of Ammonia
LCOE	Levelized Cost of Energy
LCOH	Levelized Cost of Hydrogen
LCOT	Levelized Cost of Transport
LH_2	Liquid Hydrogen
NH_3	Ammonia
OPEX	Operational Expenditure
OWF	Offshore Wind Farm
PtX	Power-to-X
SOEC	Solid Oxide Electrolyzer Cell

Executive summary

This deliverable provides a comprehensive review and techno-economic assessment of Power-to-X (PtX) solutions integrated with offshore wind farms, focusing particularly on hydrogen and ammonia pathways. The study addresses both the technical feasibility and economic viability of coupling large-scale offshore wind generation with electrolysis and subsequent conversion, transport, and utilization options.

Context and Objectives

- Offshore wind is a key pillar of Europe's decarbonization strategy, with the EU targeting up to 450 GW by 2050.
- Power-to-X technologies (hydrogen, ammonia, synthetic fuels, etc.) are explored as strategies to overcome transmission constraints, provide long-term storage, and decarbonize hard-to-abate sectors.
- The report's objective is to assess PtX integration from a technical, infrastructural, economic, and regulatory perspective, aligning with WP3 objectives of SPOWIND.

Key Findings

1. Hydrogen Production
    - Green hydrogen via electrolysis is the most mature PtX option for offshore integration.
    - Electrolyzer technologies compared include Alkaline (AEL), Proton Exchange Membrane (PEMEL), and Solid Oxide Electrolyzers (SOEC), each with distinct advantages (cost, efficiency, operating conditions).
    - Offshore electrolysis can reduce reliance on costly HVDC export cables, while onshore electrolysis benefits from easier access and economies of scale.
2. Ammonia as a Carrier
    - Ammonia offers higher volumetric energy density than hydrogen and leverages an already mature global infrastructure (shipping, storage, fertilizer industry).
    - Offshore ammonia production is particularly attractive for long-distance

export markets.

- Safety and environmental concerns (toxicity, NOx emissions, marine impact) require robust handling frameworks.

3. Infrastructure and Substructures
    - Both bottom-fixed and floating platforms are assessed for offshore PtX substations.
    - Floating solutions enable deployment in deep waters, expanding resource accessibility.
    - Case studies (VindØ Island, BrintØ Hydrogen Island, Lhyfe floating electrolyzer, North Sea Wind Power Hub, etc.) illustrate real-world pilots and concepts.
4. Economic Analysis
    - CAPEX, OPEX, and transport costs were quantified for hydrogen and ammonia supply chains.
    - Pipelines are favorable for near-to-midshore delivery, while shipping (particularly ammonia) becomes more competitive for long-range export.
    - Sensitivity analysis highlights that declining electrolyzer costs and efficiency improvements could make offshore PtX increasingly competitive within the next decade.
5. Safety, Standards, and Regulations
    - The report reviews international, European, and national regulatory frameworks for hydrogen and ammonia handling.
    - Identifies gaps in permitting and safety standards, particularly for offshore PtX facilities.

Conclusions

- No single PtX pathway is universally optimal; the best solution depends on distance to shore, scale, infrastructure availability, and target market.
- Hydrogen pipelines are cost-effective at medium distances; ammonia export is

preferable for long-haul transport; hybrid configurations provide resilience and flexibility.

- Integrating PtX with offshore wind not only reduces curtailment and transmission bottlenecks but also unlocks new business models and accelerates Europe's decarbonization goals.

1. INTRODUCTION

1.1 Background on the Significance of Offshore Wind Farms

Wind power produces roughly 5% of the world's electricity [1] , with most installations located onshore. However, Offshore wind farms offer the advantage of higher wind speeds and consistency, resulting in greater energy production per turbine compared to onshore installations. The harsh marine environment presents technical challenges and increases costs. Despite these challenges, offshore wind energy is increasingly recognized for its potential to significantly reduce greenhouse gas emissions and contribute to a sustainable energy future. The European Union, for instance, has set an ambitious target of installing around 450 gigawatts of offshore wind capacity by 2050 to help achieve its net-zero emissions goals. [2] . Offshore wind farms offer several advantages over traditional onshore installations, including higher and more consistent wind speeds, reduced visual impact, and easier maintenance access. These benefits make them an attractive option for large-scale renewable energy generation and integration into the grid.

1.2 Introduction to Power-to-X (PtX) Technologies and Their Relevance in the Offshore Wind Industry

Power-to-X (PtX) technologies enable the conversion of renewable energy into various energy carriers, such as hydrogen, methane, methanol, and synthetic fuels. These energy carriers can serve as clean alternatives to fossil fuels in various sectors, including transportation, power generation, and industrial processes. PtX technologies are especially beneficial in the offshore wind industry as they can stabilize the grid and utilize excess energy produced by wind turbines. By converting excess energy into hydrogen or other fuels, PtX technologies can reduce the need for long-distance transmission lines and enhance energy security. This approach enables the transportation of energy to areas where it is needed, making it a valuable solution for integrating offshore wind clusters into weak grids [3].

The report aims to comprehensively review the significance and role of PtX technologies in the offshore wind industry. It will discuss the benefits of PtX technologies and the challenges associated with implementing these technologies in offshore environments.

1.3 Power-To-X (Ptx) Technologies

Power-to-X (PtX) technologies convert electrical power, often from renewable sources, into other forms of energy or materials for various applications. The "X" represents different end products based on the specific technology. Here are key PtX technologies and their products:

- **Power-to-Gas (PtG):** Converts excess electricity into hydrogen gas via water electrolysis, usable as transportation fuel or chemical feedstock.
- **Power-to-Liquid (PtL):** Uses electricity to produce liquid fuels like methanol or synfuels through chemical processes.
- **Power-to-Chemicals (PtC):** Converts electricity into chemical feedstocks such as ammonia or ethylene, which are essential for producing various chemicals and materials.
- **Power-to-Heat (PtH):** Utilizes excess electricity to generate heat for district heating or industrial processes.

These technologies facilitate the integration of renewable energy into different sectors by converting excess electricity into useful forms of energy, feedstocks, or products. This report specifically examines Power-to-Gas technologies, particularly hydrogen and ammonia, due to their techno-economic advantages over other solutions, as identified in the literature review.

HYDROGEN:

Hydrogen (H2) is a highly promising clean fuel due to its abundance, lightweight nature, and high energy content per unit of weight compared to any fossil fuel. However, current hydrogen production processes rely heavily on fossil fuels such as natural gas and coal, accounting for 6% and 2% of global consumption, respectively. This results in the release of approximately 900 million tons of CO2 equivalent annually. Despite these challenges, hydrogen has gained significant attention as a potential alternative energy source due to its high energy density, transportability, and versatility. With ongoing technical developments, hydrogen is expected to play a crucial role in achieving decarbonization goals and establishing itself as the future clean energy carrier [4].

Offshore Power-to-Hydrogen is an option that involves generating hydrogen using electricity from offshore wind farms. Besides its storage potential, hydrogen is a vital component in the chemical and petroleum industries, comprising most of the global demand of around 50 million tons annually [5].

Hydrogen is a versatile gas that can be produced through electrolysis and has numerous applications, including use as an energy source for transportation and mixing into the natural gas grid. It is currently used in fuel refining and fertilizer production. Although hydrogen production has historically relied on fossil fuels and emitted significant CO2, recent advancements in electrolysis and renewable energy production have made it possible to produce green hydrogen at a competitive price. As governments prioritize reducing carbon emissions and decreasing dependence on fossil fuels, demand for green hydrogen is expected to rise substantially in the coming years. Incentives and policies are driving significant research into green hydrogen production globally, with the aim of producing carbon-free hydrogen that can compete with traditional production methods. The figure below illustrates the production of hydrogen on an offshore facility:

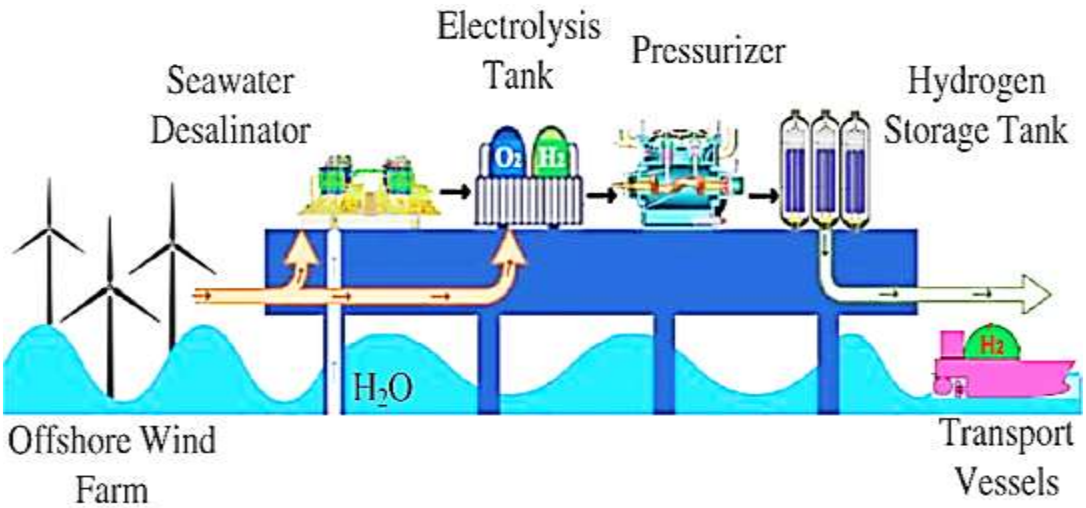

Figure 1: Illustration of Hydrogen Production from an Offshore wind farm.

European offshore wind plants are exploring new methods to profitably integrate variable and intermittent electricity into the grid due to low power prices. One promising solution is hydrogen production using excess wind energy that would otherwise be wasted. Electrolyzers in hybrid plants can utilize this excess electricity from offshore wind farms to produce hydrogen at different times of the day.

Rising concerns for decarbonized energy systems require heightened attention to alternative pathways beyond electricity to dramatically decrease greenhouse gas emissions [6]. Recent advances in electrolyser performance and cost reductions have now allowed investors to revisit the role of hydrogen in a low-carbon energy economy [7]. Coupling hydrogen production with offshore wind is not new, however, represents an emerging area of importance not only for wind farm developers to increase revenues, but also for decarbonization strategies, as wind-based hydrogen production could have a much lower carbon abatement cost than other carbon mitigation strategies.

The shifting economics of offshore wind power offer a lucrative business opportunity for hydrogen producers to use curtailed near-shore wind electricity as electrolysis feedstock. This approach provides several benefits, including improved market access, long-term storage options, and reliable power sources for hydrogen production in existing locations. Hydrogen (H2) boasts high energy density, eco-friendliness, and the ability to store large amounts of energy for extended periods. It allows for cost-effective long-distance energy transportation via pipelines, ships, or trucks in gaseous, liquefied, or other forms, compared to power transmission lines [8]. Hydrogen can serve as a form of energy storage and act as an energy carrier, as it has a much higher energy density than batteries and is easily storable.

Given the significant growth and technical advances in the offshore wind sector, combining hydrogen with offshore wind energy can address challenges like high transmission system installation costs and transmission losses. Hydrogen's high energy density and storage ease make it an efficient energy storage and transportation option, surpassing batteries. As offshore wind energy grows and advances, integrating hydrogen can help overcome transmission-related challenges. Fuel cell electric vehicles (FCEVs) can provide comparable mobility services to conventional cars with potentially low carbon emissions. Producing hydrogen from excess wind power is more carbon-efficient than curtailing wind due to renewable hydrogen's lower carbon footprint. With the current hydrogen supply chain relying heavily on coal steam reformation, there is significant potential to shift global industrial hydrogen production to renewable feedstock.

Ammonia:

Using ammonia to convert excess power from offshore wind farms offers a practical solution due to its easy storage and transport as a liquid, unlike hydrogen, which has a lower volumetric energy density and it is costly to transport. Ammonia can be utilized for fertilizer production, power generation, long-term energy storage, and transportation. For offshore ammonia production, it can be transported to shore via tanker ships at regular intervals or through pipelines. Given the high transportation costs of hydrogen, it is not an economically competitive option compared to ammonia.

The global ammonia market is substantial, with a production rate of 180 million tons per year, primarily for fertilizer use. This established market underscores ammonia's suitability and economic viability for energy applications [9]. It can also be used for energy storage to balance temporal and geographical mismatch between energy demand and supply.

Ammonia (NH3) is the second most commonly produced chemical in the world. The infrastructure involved in its production, transportation, and distribution is already technologically mature and cost-effective. Ammonia has the highest H2 net volumetric density, potentially the highest total energy efficiency, and offers higher utilization flexibility. It can be used directly or decomposed to release the contained H2 [10]. As the costs of electrolyzers and renewable electricity continue to decrease, the production of ammonia using renewable energy can become economically viable. Additionally, ammonia production at offshore wind farms can take advantage of economies of scale and proximity to energy sources, reducing transportation costs.

Ammonia offers a viable Power-to-Gas solution for offshore wind farms, enhancing renewable energy utilization and contributing to a sustainable energy future. Its high energy density, existing infrastructure, and versatility make it an attractive option for energy storage and transportation. By addressing challenges and maximizing benefits, ammonia can be pivotal in the transition to a low-carbon energy system.

Transmitting electricity generated far offshore to onshore demand centers poses significant challenges due to the prohibitive cost of long-distance submarine power cables. To overcome this, we propose using offshore wind energy to produce green ammonia directly, which can then be transported to shore via ships or pipelines. This approach is technically feasible, as ammonia production from electricity requires only water and air as input materials.

Ammonia can be obtained by a catalytic reaction from hydrogen and nitrogen. Figure 2 illustrates the value chain of ammonia production from hydrogen. The reaction is typically carried out over an iron catalyst at temperatures around 400–600 °C and pressure ranging from 200 to 400 bar.

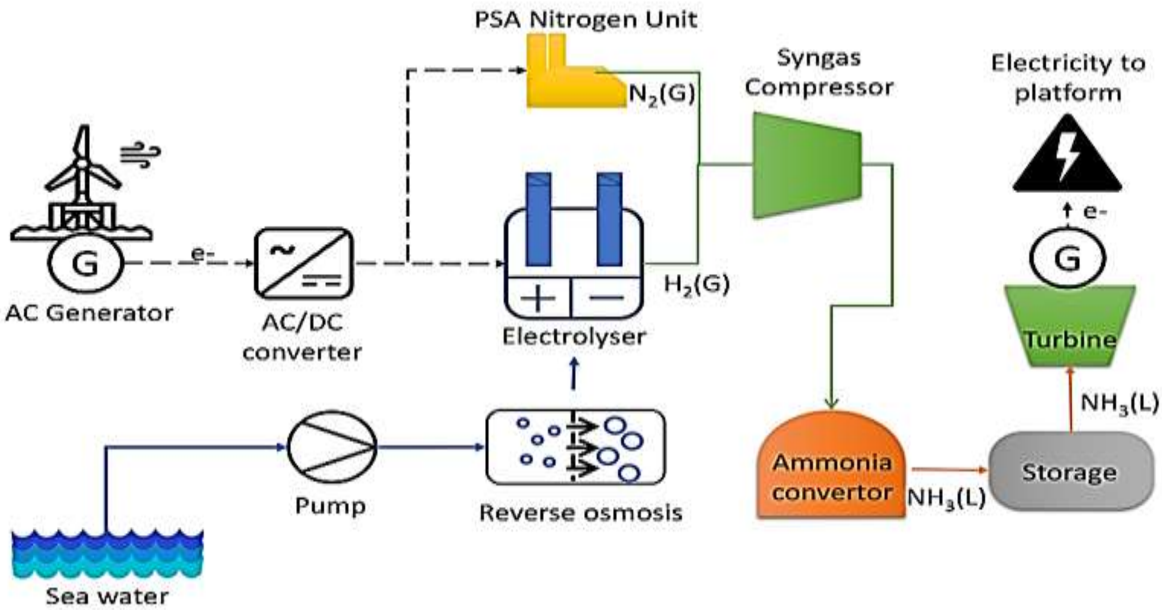

Figure 2 Ammonia production from hydrogen

Another approach developed by Haldor Topsøe involves using a combination of the solid oxide electrolysis cell (SOEC) and the HB process. In this method, the SOEC is used to separate the hydrogen from water and nitrogen from the air/steam mixture, eliminating the need for an air separation unit. Ammonia has an energy density of 6 kWh/kg, which is comparable to natural gas, and it can be easily liquefied by compression to 8 barg at atmospheric temperature. Ammonia produced from renewable sources can be synthesized using a completely carbon-free process [11].

In terms of regulations and environmental risk, it's important to note that ammonia is a toxic chemical with severe health consequences. Releasing ammonia into the sea can have a detrimental impact on the environment as it is harmful to aquatic life. Additionally, the combustion of ammonia may generate NOx and N2O, both of which are powerful greenhouse gases.

2. INTEGRATION OF PTX WITH OFFSHORE WIND FARMS

Benefits of integrating PtX with offshore wind

Incorporating Power-to-X (PtX) technologies into offshore wind farms brings several advantages that boost the energy system's efficiency, reliability, and sustainability. These benefits include better energy storage, improved grid stability, and considerable economic benefits. Integrating PtX technologies with offshore wind farms optimizes grid integration and guarantees a consistent supply of renewable energy. This is achieved through the use of cutting-edge technologies like energy storage and power-to-gas systems, which manage wind energy variability and ensure a dependable electricity supply [12].

PtX technologies can store excess energy generated by offshore wind farms during periods of low energy demand. This stored energy can then be used to power gas turbines, reducing the need for fossil fuels and enhancing the overall efficiency of the energy system. PtX integration can help mitigate grid congestion and ensure a stable supply of renewable energy, which is particularly important for offshore wind farms located far from the main grid. It requires efficient transmission and distribution infrastructure.

Economic Benefits: PtX integration can create economic opportunities by providing a route to market for renewable energy. This can include the production of renewable hydrogen for use in transportation, power generation, and industrial processes.

Decarbonization: PtX integration can help decarbonize hard-to-abate sectors such as shipping, aviation, and industrial processes by using renewable energy to produce low-carbon fuels.

System Integration: PtX integration can facilitate system integration by enabling the efficient use of renewable energy across different sectors, including power, heat, and gas systems, thereby enhancing the overall efficiency and flexibility of the energy system.

Reduced Emissions: PtX integration can help reduce greenhouse gas emissions by using renewable energy to produce low-carbon fuels, contributing to the overall goal of achieving net-zero emissions by 2050.

Increased Flexibility: PtX integration can provide increased flexibility in the energy system by enabling the efficient use of renewable energy across different sectors, including power, heat, and gas systems, thereby enhancing the overall efficiency and flexibility of the energy system.

New Business Models: PtX integration can create new business models by providing a route to market for renewable energy, including the production of renewable hydrogen for various sectors such as transportation, power generation, and industrial processes.

Improved Energy Security: PtX integration can improve energy security by providing a reliable and sustainable source of energy, thereby enhancing the overall resilience and security of the energy system.

Enhanced Sustainability: PtX integration can enhance sustainability by using renewable energy to produce low-carbon fuels, contributing to the overall goal of achieving net-zero emissions by 2050 and supporting the transition to a low-carbon economy [13].

3. ELECTROLYZER TECHNOLOGIES FOR OFFSHORE WIND FARMS

3.1 Introduction

An electrolyzer is a device that utilizes DC electricity and demineralized water to split water molecules into hydrogen and oxygen atoms through a chemical reaction, producing high-purity oxygen and hydrogen. Although various electrolyzer technologies function slightly differently, they all consist of an anode and cathode separated by an electrolyte. The two primary electrolyzer technologies employed for commercial hydrogen production are Alkaline Electrolyzers (AEL) and Proton Exchange Membrane Electrolyzers (PEMEL) [14]. Another technology undergoing intense research and development is Solid Oxide Electrolyzer (SOE), which promises high efficiencies and flexibility, but at the cost of both high operating temperatures (700 to 900 °C) and durability.

3.2 Alkaline Electrolyzer

AELs are currently the most cost-effective technology and have the longest lifespan, partly due to their extensive history in the industry, spanning roughly 100 years. While advancements are anticipated, PEMEL and SOE development are likely to progress more rapidly. However, AELs have certain limitations, such as slower reaction times to production changes, complex maintenance requirements for the alkaline fluid, a minimum operating threshold for safety reasons, longer start-up times, and lower current density compared to PEMEL, approximately five times lower. [15]. In addition, the output pressure of the hydrogen produced is lower, which requires higher compression for transport and storage, reducing the advantage the lower CAPEX provided initially.

3.3 Proton Exchange Membrane Electrolyzer

PEM electrolyzers (PEMELs) are more recent than alkaline electrolyzers (AELs) and come with several advantages, such as faster start-up times, higher current densities resulting in smaller electrolyzer footprints, higher hydrogen purity (>99.8%), the ability to operate beyond nominal power, and higher output pressure. The report provides [14] a comparison between PEMEL and AEL revealing notable differences in efficiency, capital expenditure (CAPEX), and electrical consumption. By 2025, projections show improvements in both technologies. AEL's efficiency is expected to rise from 65% to 68%, while PEMEL's efficiency is projected to increase from 57% to 64%.

Regarding CAPEX, AEL is anticipated to decrease from 750 €/kW to 480 €/kW, and PEMEL from 1200 €/kW to 700 €/kW by 2025. In terms of electrical consumption, AEL currently consumes around 51 kWh/kg of hydrogen, which is expected to decrease to 49 kWh/kg by 2025. Similarly, PEMEL's current consumption of approximately 58 kWh/kg is projected to drop to 52 kWh/kg by 2025. During shutdown periods, both technologies require minimal energy to maintain system operation, which is crucial for offshore or off-grid electrolyzers. However, a backup power source is necessary when coupled with renewable power sources due to their intermittent nature. Despite PEMEL's significant advancements in efficiency, output pressure, ramp-up and ramp-down times, and CAPEX, it remains more expensive than AEL and has a shorter lifespan [14].

3.4 Solid Oxide Electrolyzer

Solid Oxide Electrolysis Cells (SOECs) present a promising solution for generating hydrogen offshore, thanks to their impressive efficiency and ability to operate at high temperatures. Unlike conventional electrolysis methods, SOECs use solid oxide materials as electrolytes, which enables them to convert electrical energy into chemical energy more efficiently. This feature is especially beneficial when it comes to harnessing offshore wind energy, which can be unpredictable at times. By using SOECs, hydrogen can be produced effectively even when wind conditions are variable. However, SOECs do have some challenges to overcome, such as high initial costs, material degradation at high temperatures, and the need for sophisticated thermal management systems. Following table illustrated technical features of the electrolyzers discussed:

Table 1 Resume of principal technical features for electrolyzers [16],[17],[18]

Parameter	Alkaline	PEM	SOEC
Energy Requirements [kWwh/KgH2]	51	58	41
Nominal System Efficiency (LHV)	63-70	56-60	74-81

[%]*			
Current Density [A/cm²]	0.2-0.6	1-2.5	0.3-1.0
Load Range [% nominal Load]	20-10	~10-200	-100/+100
Stack Lifetime [h]	80000	40000-80000	8000-20000
Max. Nominal power Stack [MW]	2-4	2-3	<0.01
CAPEX [€/MW]	500-1400	1100-1800	2800-5600
Operating Temperature [C]	60-90	50-80	700-1000
Typical Output Pressure	1-30	30-50	1-15
Plant Footprint [m²/MWe] |	26-95	~19-48	--

3.5 Electrolyzer Auxiliaries

The electrolyzer auxiliaries' system are composted by the following elements:

1. **Power Conversion Systems**
   a. These systems are responsible for converting the variable AC power generated by wind turbines into the DC power required by the electrolyzers. They ensure a stable and efficient power supply to the electrolysis process

2. **Water Purification Systems - Desalination**
   a. High-purity water is essential for the electrolysis process to avoid contamination and damage to the electrolyzers. Water purification systems, including filters and reverse osmosis units, ensure the water meets the necessary quality standards [16]

3. **Hydrogen Storage and Handling Systems**
   a. Hydrogen produced by electrolysis needs to be safely stored and handled. Storage systems may include high-pressure tanks, cryogenic storage for liquid hydrogen, or metal hydrides for solid-state storage. Proper handling systems, including safety valves and monitoring systems, are crucial to prevent leaks and ensure safe operation

4. **Control and Monitoring Systems**
   a. Advanced control systems are essential for monitoring the operation of the electrolyzer substation. These systems manage the power supply, electrolysis process, and storage systems, ensuring optimal performance and safety. Real-time data monitoring helps in predictive maintenance and operational efficiency.

5. **Safety Systems**
   a. Given the flammable nature of hydrogen, robust safety systems are integrated into the substation design. These include gas detectors, ventilation systems, emergency shutdown mechanisms, and fire suppression systems to manage and mitigate risks associated with hydrogen production and storage.

6. **Infrastructure and Support Systems**
   a. The overall infrastructure includes the physical platforms (fixed or floating foundations), structural supports, and ancillary systems necessary for the operation of the substation in the harsh offshore environment. This includes corrosion-resistant materials, robust structural designs, and systems to withstand marine conditions.

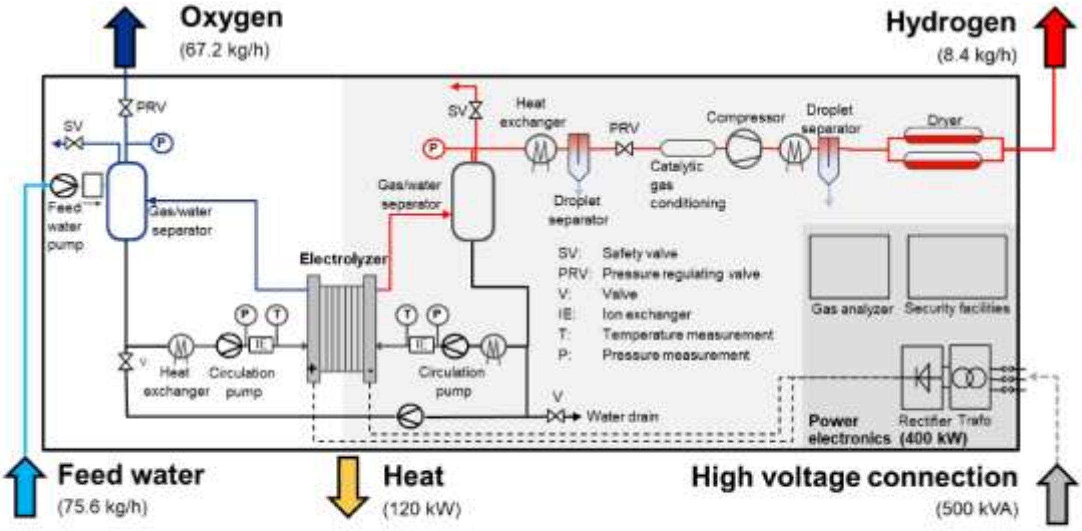

Figure 3 Layout of H2 electrolyser

Figure 4 Render of substation of electrolyser

3.6 Types of Foundations for Offshore Electrolyzer Substations

Bottom-fixed Foundations

Including monopiles and gravity-based structures, are directly anchored to the seabed. These foundations are typically used in shallower waters (< 50 m) (Figure 5), where the seabed provides a solid and stable base. Monopiles are long steel tubes driven into the seabed, while gravity-based structures rely on their weight and a wide base to remain stable on the seafloor. These foundations require precise engineering to ensure stability and durability.

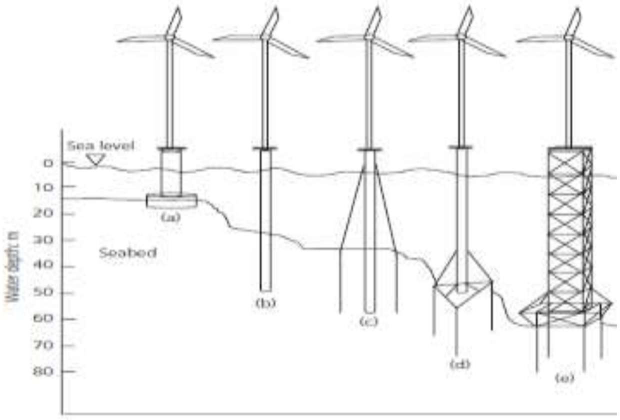

Figure 5 Illustration of bottom-fixed substructure design depending on the bathymetry level deployment

Common materials used include steel for monopiles and reinforced concrete for gravity-based structures. These materials are chosen for their strength, corrosion resistance, and ability to withstand the mechanical stresses of an offshore environment. The installation process often involves significant seabed preparation to ensure a stable and level base for the foundation.

Figure 6 Bottom fixed foundation example a centralized electrolyzer

Table 2 Adv vs Dis in the bottom fixed substructure scenario for electrolyzer

Aspect	Advantages	Disadvantages
Stability & Load Capacity	High stability and load-bearing capacity: Provides a stable base capable of supporting heavy structures and equipment.	Limited depth suitability: Generally suitable for depths up to 50 meters, with diminished practicality beyond this.
Reliability	Proven reliability: Extensively used and tested in various offshore applications, ensuring durability.	Requires thorough testing: Despite proven reliability, each new application may require extensive validation.
Environmental Impact	Less disruptive installation compared to more extensive structures: Installation may be more contained within a specific area.	Significant environmental impacts: Seabed disturbance, potential harm to marine ecosystems, and alteration of local water flow and sediment patterns.
Suitability	Suitable for shallow waters: Ideal for applications within 50 meters depth.	Not practical for deeper waters: Beyond 50 meters, alternatives like floating foundations might be needed.

Floating Foundations

Floating foundations, such as spar buoys and semi-submersibles, are designed to float on the water's surface and are anchored by mooring lines to the seabed. These foundations are particularly suitable for deeper waters where traditional fixed-bed foundations are not feasible. Spar buoys are long, cylindrical structures that provide buoyancy, while semi-submersibles use a platform supported by multiple pontoons. Regarding the offshore wind turbine application as shown in there are at least four main designs: Barge, Semi-submersible, SPAR, Tension leg platform (TLP).

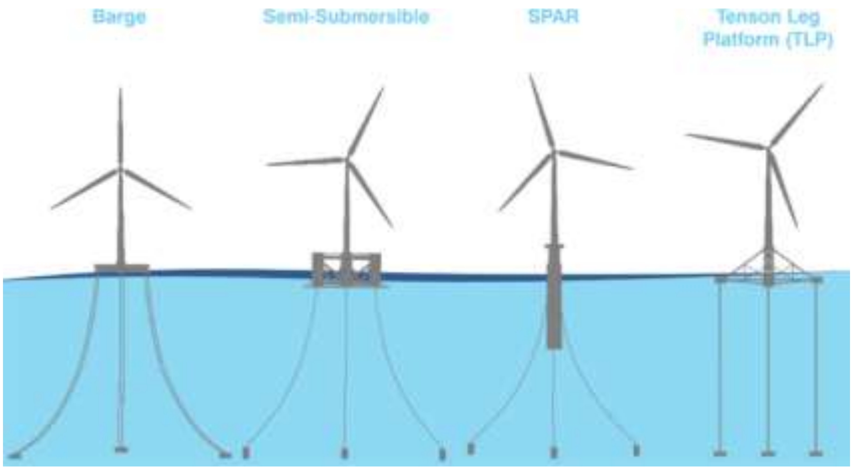

Figure 7 Floating offshore wind turbine type substructure

Floating foundations are engineered for buoyancy and stability. They typically use high-strength steel and composite materials to ensure structural integrity. Mooring systems, which can include chains, wires, or synthetic ropes, are critical for maintaining the position of the floating foundation and must be designed to withstand dynamic marine conditions such as waves, currents, and wind [17].

Table 3 Adv vs Dis in the floating substructure scenario for electrolyzer

Aspect	Advantages	Disadvantages
Suitability	Suitable for deeper waters: Ideal for depths exceeding 50 meters, allowing exploitation of wind resources in deeper offshore areas.	Limited to deep waters: Not suitable for shallow waters where traditional fixed-bed foundations may be more effective.

Environmental Impact	Less invasive to the seabed: Minimal seabed disturbance during installation, reducing impact on marine ecosystems.	Potential for ecological disturbance: Although minimal, still may impact marine life through noise and movement.
System Complexity	Simplifies installation in deep waters: Avoids the need for extensive seabed preparation.	Complex and costly mooring systems: Requires complex and expensive mooring systems for anchoring.
Maintenance	Potentially fewer disruptions to marine life during installation.	Increased maintenance: Subject to dynamic movements and environmental conditions, leading to higher maintenance needs.

Floating substructure proposal:

Following, two examples of floating substructure for offshore electrolysis are presented. As it is possible to see, they are inspired by the offshore wind world, in particular by semisubmersible platforms. In Figure 8, a three columns semisubmersible platform is shown: the entire complex of balance of plant plus electrolyzer is installed on one column, while the others can be used as an access for vessels (e.g., maintenance ships). On the other hand, in Figure 9, a 4 columns platform is presented, with the balance of plant and the electrolyzer that are installed using all the available space. Figure 8 Floating substructure example for electrolyser

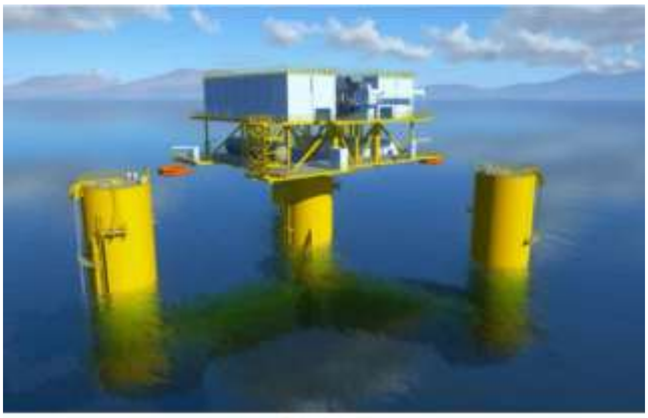

Figure 8 Floating substructure example for electrolyser, 3 columns.

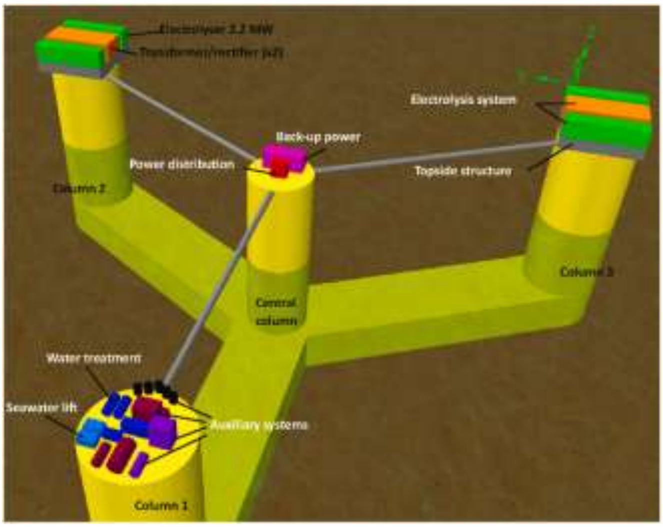

Figure 9: Floating substructure example for electrolyzer, 4 columns (Al., 2024).

3.7 Power-to-X hubs and islands: project examples

Vindø island: The artificial island will be built in the Danish part of the North Sea, around 100 km from the coast. This location offers optimal conditions for generating clean, green energy using wind turbines. The island is planned to be established by 2033 and will connect 3 GW of offshore wind power. Over time, the island will connect up to 10 GW of offshore wind power and will host energy storage systems, Power-to-X technology, accommodation facilities, O&M (operation and maintenance) facilities, and HVDC converters for transmission and interconnectors.[18]

North Sea Wind Power Hub: The North Sea Wind Power Hub (NSWPH)[19], is an ambitious new approach to integrating renewable energy. Currently, climate policy is primarily national, segmented by energy sectors, and progresses incrementally. The NSWPH adopts a markedly different perspective. It is transnational, integrated, and represents a significant step forward in the expansive development of offshore wind in the North Sea. The hub-and-spoke concept links the energy systems of North-West Europe into a well-planned and coordinated network while connecting substantial amounts of offshore wind. It has unique characteristics:

- Transnational: Connecting multiple countries through a hub-and-spoke concept.

- Hybrid: Combining interconnection with the integration of offshore wind.
- Cross-sector: Integrating different energy sectors and energy carriers.

The future energy system needs long-term flexibility: the ability to deliver electricity when renewable sources are not producing enough. Renewable electricity can be converted into green hydrogen, which aids integration in various ways. Electrolysis, by converting renewable electricity into hydrogen, supports a more extensive and effective deployment of offshore wind generation than would be possible without it.

Figure 10 Different hub-and-spoke configuration

BrintØ island

In 2022, CIP proposed the construction of an artificial island dedicated to large-scale production of green hydrogen from offshore wind, named "BrintØ" (Hydrogen Island), in the Danish part of the North Sea. The island is anticipated to supply an unprecedented amount of green hydrogen by 2030, playing a crucial role in securing Europe's future green energy supply.

BrintØ is planned to be located in the Danish part of Dogger Bank. Figure 11 BINTO energy island , an area expected to become a central hub for the future development of offshore energy infrastructure in the North Sea. This 20,000 km² sandbank offers some of the world's best conditions for producing low-cost green electricity due to its shallow waters and strong wind resources. The overall project will include four main components: offshore wind farms, an artificial island, Power-to-X facilities, and a hydrogen export pipeline. The island is planned to be connected to 10 GW of offshore wind capacity. The energy produced will be sufficient to power approximately 10 million European households. As an artificial island, it will serve as a hub for connecting surrounding offshore wind farms. The island will house large-scale hydrogen production facilities and an operations and maintenance (O&M) harbor for servicing the offshore wind farms. The hydrogen production facilities on the island will convert renewable energy into green hydrogen through Power-to-X technology. At full capacity (10 GW), the island is expected to produce around 1 million tonnes of green hydrogen annually, which corresponds to roughly 7% of Europe's projected hydrogen demand by 2030.[20]

Figure 11 BINTO energy island illustration

Lhyfe floating eletrolyzer

Since 2022, off the coast of Le Croisic, at Centrale Nantes' offshore pilot site, SEM-REV, Lhyfe is developing the first offshore hydrogen production facility in the world. Lhyfe and Centrale Nantes aim to demonstrate the reliability of an electrolyser at sea to make offshore renewable hydrogen feasible. The offshore pilot site meets all necessary conditions – including the presence of Marine Renewable Energy (MRE) sources and stringent environmental criteria – to validate the offshore hydrogen production technology before considering large-scale industrial deployment in 2024. The facility features a wind turbine with a rated power of 2 MW and an electrolyser with a capacity of **440 kg per day**. Energy and risk management specialists DNV have already started safety studies to identify key risks.[21]

Figure 12 SEM-REV test site: (2 MW) FOWT connected with H2 elestrolyzer floating substation

Table 4 Various Offshore hydrogen production Projects. Dara taken from sources [22] [23] [24] [25] [26] [27] [28] [29] [30] [31]

Name	Capacity	Site	Nation	Operational time
Offshore Hydrogen Production of Lhyfe and Centrale Nantes [21]	10–100 MW	SEM-REV, Centrale Nantes' offshore test site	France	2022
OYSTER of ITM Power, Ørsted and Siemens Gamesa [22]	MW scale	Grimsby	UK, EU	2024
Esbjerg Offshore Wind-to-Hydrogen Project, Swiss energy company H2 Energy Europe [23]	1 GW	Esbjerg	Denmark	2024
Hyport Oostende Hydrogen Project of DEME Group and H2 Energy [3]	50 MW	Oostende	Belgium	2025
AquaVentus Project [4]	10 GW	Helgoland	Germany	2035
DOLPHYN Project [5]	4 GW	Northern North Sea	Scotland, UK	2035

Name	Capacity	Site	Nation	Operational time
Bantry Bay green energy facility of Zenith Energy and EI-H2 [26]	3.2 GW	Bantry Bay	Ireland	2028
Salamander Project [28]	5 GW	Peterhead	UK	2028

3.8 Conclusion and preliminary substructures sizing

As shown in the previous sections the development of an actual commercial let substructure design is not so ready. There are several proven technologies which could support the electrolyzer facilities synthetized in the APPENDIX. The module selected is a Siemens product for industrial use, Sylyzer 300, with an area of 15x7x8 m and a total weight around of 2.1 tons per modules. Similarly, we found that the substructure of a wind turbine with 5 MW rated power with mass property detailed in appendix.

As preliminary computation the selected substructure can handle the number of electrolyzer equivalent mass equal to the WT weight of 700 tons as:

$$n_{H_2} = \frac{Mass_{WT}}{Mass_{H2}} = \frac{700\ tons}{48\ tons} \cong 14$$

Which corresponds to an equivalent of holding input power of:

$$P_{H_{2tot}} = P_{H_{2_i}} * n_{H_2} \cong 240\ MW$$

The proposed procedure can be scaled up to newer substructure deigned to hold several weight capacities form 2 MW to 15 MW WT, allowing the varsity of possible sizes of the electrolyzer.

Once defined the Electrolyzer commercial size is implemented in the SPOWIND project, it will be applied a more detailed dimensioning framework.

3.9 Offshore POWER-TO-X substation – centralized

Centralized Bottom-fixed POWER to X substructure proposal design

Herein is presented the jacket structure design to hold a 5 MW wind turbine from [32]. This structure must be capable of withstanding the electrolyzer and its balance of plant, including the desalination system, and converters. In the APPENDIX B and in [8], [9] it is possible to explore the main design data ad approaches.

Centralized Floating POWER to X substructure proposal design

For the case of elevated bathymetries, floating solution must be adopted for the installation of the elctrolyzer and its balance of plant. In the APPENDIX B is presented the main design data. Additional information can be found in [10].

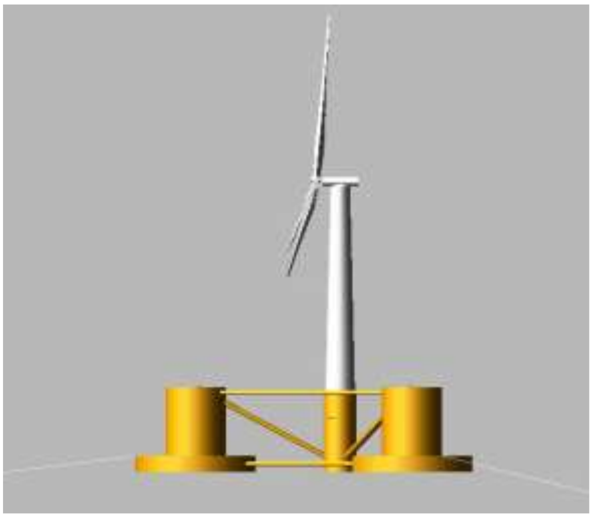

Figure 13 OC4 reference Semisubmerisible FOWT support structure [33]

3.10 Offshore POWER-TO-X substation – decentralized design

For the case of decentralised production, the floating platform already used for the turbine can be adapted to host the electrolyzer and its balance of plant as per [5], [11], (Figure 14). An additional solution could be to host the power to X system inside the tower, in a configuration similar to Figure 15.

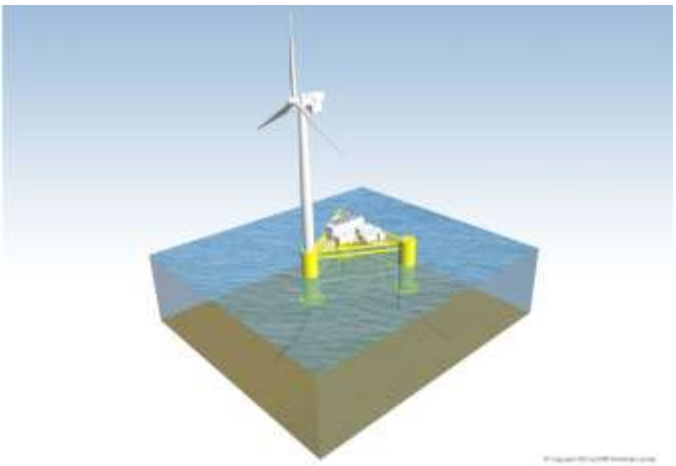

Figure 14: Example of decentralised Power to X system using turbine platform.

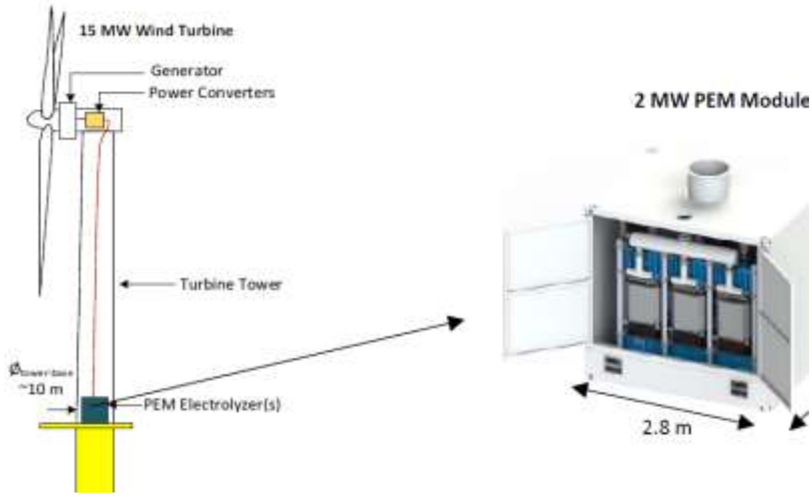

Figure 15: Example of Power to X system inside the tower [5].

3..11 OFFSHORE ENVIRONMENT CHALLENGES

The main concern about the coupling of offshore wind farms and electrolyzers are related to the environment in which the installation takes place (Figure 16). For example, the ocean/sea offers a more stable wind resource, but still it is subject to peaks and lows, which have to be handled by the electrolyzer if battery/grid connection is not present. In addition to this, if the wind farm is located where the water depth does not allow the use of fixed structures, also the floating structure motion must comply with the requirements of the electrolyzer. Hence, the aim of this paragraph is to analyse the main critical issues that must be addressed for the successful implementation of the technology.

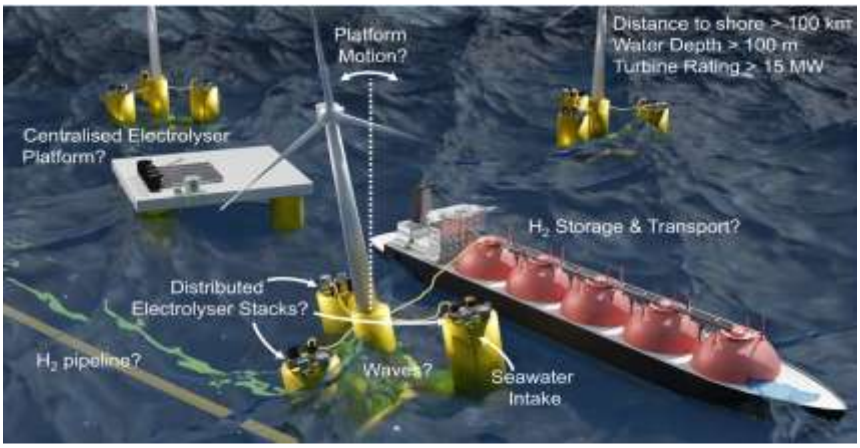

Figure 16 Illustration of Power to X combination configuration

The first issue is related to the **production of clean water**, since the current technologies do not allow the use of sea water which is corrosive and most non-precious metals will dissolve at anode potentials and will produce metal chlorides and oxychlorides. Sea water also contains a large variety of biological and dissolved solids, which can foul the membrane and electrodes. Another issue is that cations in seawater will exchange with the proton exchange membrane, resulting in much lower conductivity. Similar issues arise with anions in anion exchange membrane electrolysers. Salt precipitation is also a problem in all electrolysers because the salts left behind after water is consumed by the electrolysis process. As previously discussed, chlorine evolution, as well as the increase in cathode pH and decrease in anode pH, will lead to additional energy consumption. The increase in cathode pH will cause the precipitation of Mg and Ca hydroxides and bicarbonates (upon reacting with carbon dioxide from the atmosphere) or those present in seawater.[34] Another issue related to the desalination is the waste disposal of this process, which has to be carefully taken into account.

Another problem that could emerge is related to the **intermittent power supply:** since current electrolysers are designed for steady-state scenarios, operating from intermittent renewable energy can be challenging, therefore new design or control strategies should be implemented. Fluctuating power (Figure 17) may cause start and stop cycling. This cycling of the cell potential or current can affect electrode materials which will increase the maintenance periods for the electrolysers and decrease the durability. Moreover, if power drops below electrolyser minimum operating threshold, the device will shut down and it might take a few minutes to restart from cold which can lead to a significant amount of wind power during the start-up period will need to be curtailed or will be unused with consequent revenue loss.[34] **From this perspective, PEM electrolyzers appear to be better, since they have a shorter start-up from cold window** and also better ramp-up time and flexibility with respect to Alkaline technologies.

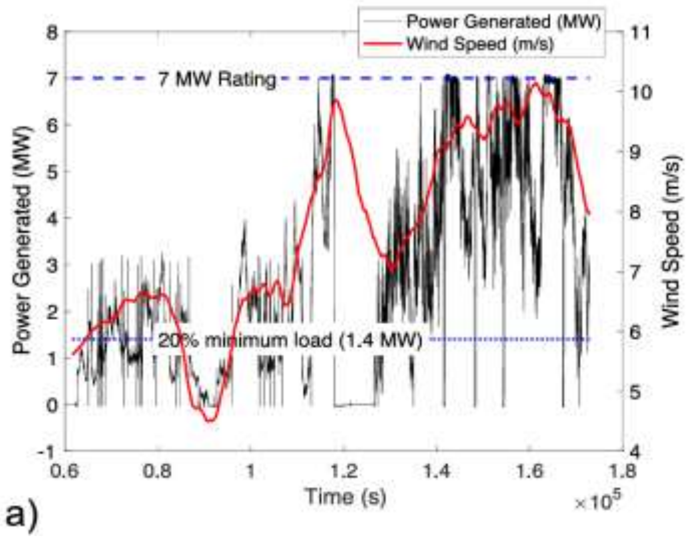

Figure 17 Time series of energy production of 7 MW wind turbine

For Alkaline and PEM electrolyzers if the fluctuating power from renewable energy drops below **a minimum load**, gas impurity will increase which could lead to explosive mixtures. Therefore, at minimum loads, the stacks will be switched off and the renewable power wasted. For PEM electrolyzers the minimum load threshold is lower than for the Alkaline. Load changes can also impact the temperature and pressure of the electrolyser which may require higher energy need for hydrogen to be produced and can cause greater degradation due to potential fluctuations.[34]

Finally, **device orientation** can also be a variable that should be managed properly. Both **oxygen and hydrogen bubble dynamics** and the performance of the liquid gas separators **could be impacted by device orientation** (Figure 18), caused by the motion of the offshore platform. Nevertheless, there is no study that focuses in detail on this particular issue, while currently, Europe's first offshore electrolyzer completed 6 months of tests with encouraging results: the offshore production was equal to the onshore one.[35]

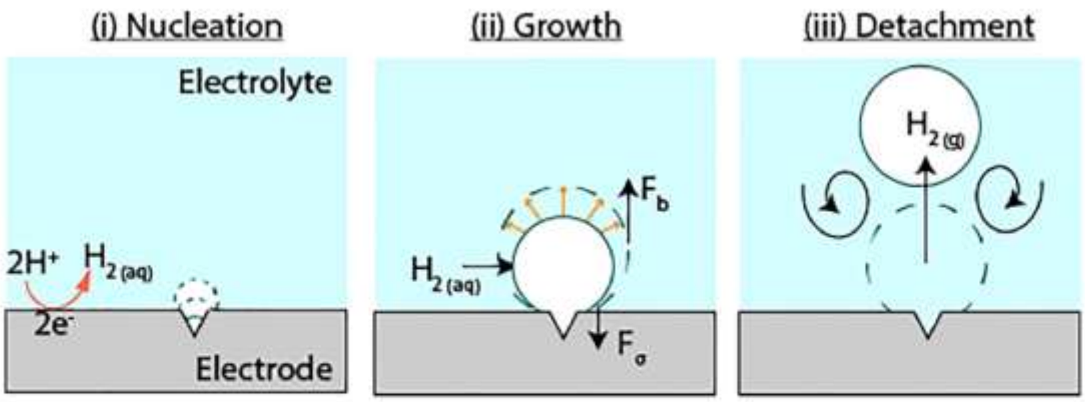

Figure 18 stages of bubble evolution: (1) the nucleation, (2) growth, and (3) detachment of bubbles on an electrode [36]

4. SYSTEMATIC REVIEW OF STUDIES ON OFFSHORE HYDROGEN PRODUCTION

The case study by Dinh et al. [37] examines a hypothetical 101.3 MW wind farm located in a potential offshore wind development area off the East Coast of Ireland. The cost projections for the wind farm and electrolysis plant in this study are based on reference costs from literature and are estimated for the year 2030. The wind farm employs proton exchange membrane (PEM) electrolyzers and underground hydrogen storage. The specific site is located 15 km offshore from Arklow, County Wicklow, with water depths between 30 and 40 meters below mean sea level. The annual wind speed at the site is 8.13 m/s, derived from SEAI's Wind Atlas (2006) and the M2 buoy's hourly wind speed data over 18 years (2002-2019). The study recommends a minimum capacity of 100 MW for economically viable hydrogen production from an offshore wind farm. The projected lifetime operating hours of the PEM electrolyzer stack in 2030 are estimated to range between 60,000 and 110,000 hours [38]. The study shows that the offshore wind farm and hydrogen production project at the chosen site, along with the specifications of wind turbines and electrolysers, are projected to be profitable in 2030 with a hydrogen price of Eur 5/kg and underground storage terms ranging from 2 days to 45 days.

Wang et. al, [39] conducted a techno-economic analysis for green offshore ammonia plants. The researchers examined various factors, including wind profiles, plant capacities, distances to shore, and water depths, to determine the minimum achievable costs for ammonia production. Their findings indicate that this method could be cost-competitive, particularly as offshore wind turbine costs are projected to decrease in the future. The study aimed to select the optimal configuration from a set of design options while also optimizing the operational schedule. One proposed option involves transmitting electricity generated by offshore wind farms to the mainland via submarine power cables. This electricity can then be utilized for onshore ammonia production. However, the results show that producing ammonia using offshore wind energy in this setup is only cost-competitive when the average wind speed is 11 m/s and the distance to shore is less than 600 km [39].

The choice of power transmission cable depends on the distance to shore. For distances under 80 km, High Voltage Alternating Current (HVAC) is used, while High Voltage Direct Current (HVDC) is preferred for longer distances. At an 80 km distance, HVAC is recommended for ammonia demands between 50 and 300 t/day, while HVDC is preferred for larger demands. In all cases, a hydrogen fuel cell is utilized to convert hydrogen to electricity as needed, with neither batteries nor an ammonia genset being employed. This indicates that ammonia is not used as an energy storage medium.

As the distance to shore increases, both cable length and transmission loss rise, necessitating more electricity generation. Consequently, the costs of wind turbines and power cables escalate, with power cable costs experiencing a more significant increase. When the distance increases from 600 to 2000 km, power transmission's contribution to the Levelized Cost of Ammonia (LCOA) rises from 35% to 56%, making it the most expensive component for long distances.

Another approach for offshore ammonia production involves situating the ammonia plant adjacent to the offshore wind farm. The ammonia produced is then transported to onshore demand points via pipelines or ships, thereby eliminating the requirement for underwater electricity transmission. When the average wind speed is 11 m/s, the Levelized Cost of Ammonia (LCOA) is consistently lower than the reference ammonia price for all cases with an ammonia demand of 300 t/day or more, irrespective of the distance to shore.

In comparison to onshore ammonia production, cost reduction can be achieved in most cases, with the cost savings increasing significantly as the distance to shore increases. Across all instances, an average relative cost reduction of 26% is obtained, while cost reductions of more than 50% are achieved in most cases with a distance to shore of 2000 km. Additionally, there is virtually no curtailment needed in this system, which allows the system to meet the same ammonia demand with a considerably smaller wind farm compared to the case of onshore ammonia production.

The ammonia production plant costs depend on the depths which need to be considered to make it an economically competitive choice. Fixed-bottom wind turbines are used at water depths of 60 m or less, while floating wind turbines are required in deeper waters (blue background) [40]. For water depths less than 168 meters, a jackup platform is cost-effective, while a semisubmersible platform is needed for deeper waters. Using a floating structure like a ship is not chosen due to higher costs. Floating wind turbines have a practical water depth limit of 700-1300 meters, with 1000 meters commonly considered the maximum depth [41].

Fixed bottom technology is currently the most prevalent for offshore wind energy, with 24,952 MW installed in Europe, compared to just 62 MW of floating wind by the end of 2020. The report indicates that the levelized cost of electricity (LCOE) for floating technology is presently 175 €/MWh, while fixed bottom technologies have a lower LCOE of 90 €/MWh. It is projected that by 2050, the LCOE for both technologies will converge to 35 €/MWh [42]. Oneway to eliminate the platform cost is to use existing platforms. Specifically, one could repurpose abandoned oil and gas platforms of which there are currently more than 12,000 platforms worldwide [43]. Besides the cost savings, this could also help reduce various environmental risks associated with abandoned platforms that were not properly decommissioned.

Maritime transportation of ammonia incurs significant costs. Offshore ammonia production could potentially function as refueling stations for ships, thereby lowering fuel expenses. The proposed green offshore ammonia setup offers greater cost-effectiveness than underwater electricity transmission, with potential cost savings of over 50% for plants situated 2000 km from shore. The system's cost is influenced by factors such as water depth and the choice of offshore wind turbines and platforms. Future reductions in offshore wind turbine costs could make this system competitive with existing land-based green ammonia plants in terms of cost.

A Study carried by Calado et. al, [44] reviews integrating hydrogen solutions into offshore wind power. The study evaluates two hydrogen production system configurations: one with an offshore electrolyzer and onshore hydrogen storage (offshore scenario), and another with the electrolyzer situated onshore. Both systems have the option to incorporate a fuel cell to supply electricity during peak demand and stabilize the grid's frequency. The operator can manage power distribution and buy electricity from the grid during low-price periods to produce hydrogen, offering load flexibility to the grid operator. Since the electricity for electrolysis is sourced from wind farms, hydrogen production is carbon emission-free.

Offshore Electrolyzer Scenario Offshore wind farms incur significant costs for transporting electricity to shore through cables, transformers, and power electronics. With a High Voltage Alternating Current (HVAC) transmission system, losses range from 1% to 5% for wind farms with 500 to 1000 MW nominal power located 50–100 km from shore [45]. HVDC systems have losses ranging from 2% to 4%, but transporting hydrogen through a pipeline incurs under 0.1% losses and lower initial costs compared to underwater electrical cables. Since the output pressure of a PEMEL is around 30 bar [46], In order to transport the hydrogen to shore, additional compression is needed. The hydrogen compressor and export pipeline must be sized based on the distance to shore, the operating pressure of the electrolyzer, the flow of hydrogen, and the pressure drop along the pipeline. A study conducted by North Sea Energy [46] estimated the necessary pipeline diameter and pressure, considering an output pressure of 68 bar and a maximum travel speed of 20 m/s. The results indicate that for a 1 to 2 GW wind farm located 50 to 200 km from shore, the minimum pipeline diameter ranges from 0.25 to 0.41 m, and the minimum input pressure ranges from 83 to 100 bar. The offshore electrolyzer scenario is shown in figure 17:

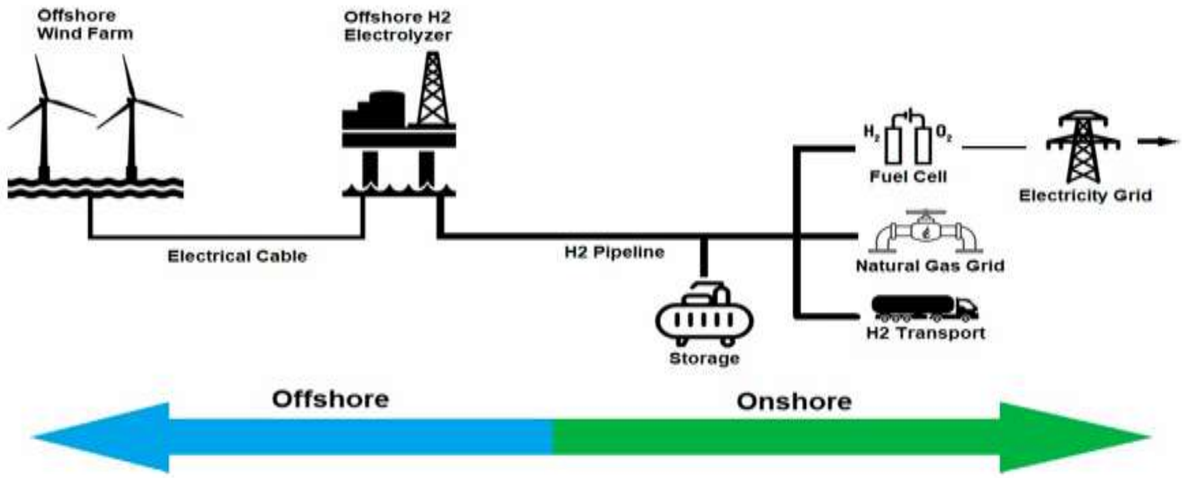

Figure 19 offshore electrolyzer scenario

When determining the size of a PEM electrolyzer (PEMEL) for a wind farm, it is not necessary for its nominal power to correspond to the wind farm's nominal power, as the wind farm may not consistently operate at full capacity. From an economic standpoint, it might be more advantageous to slightly undersize the electrolyzer. Factors like energy consumption for water purification, hydrogen compression for transmission, and wake and array losses reduce the actual available power for the electrolyzer. A backup power source is required for the electrolyzer during rare shutdown periods to maintain its stand-by mode, which consumes a minimal amount of power. These shutdown periods are infrequent and brief, as the PEMEL can function at 1% nominal power with reduced efficiency.

Onshore Electrolyzer Scenario

The hybrid system approach involves transmitting the generated energy to shore as electricity through conventional cables. Once onshore, the energy can either be sold directly to the grid or utilized for hydrogen production. The primary advantage of this system lies in its flexibility. When electricity market prices are high, investors can sell the electricity directly to the grid. Alternatively, when prices are low or grid-level curtailment is required, the energy can be diverted to an electrolyzer to produce hydrogen. Curtailment takes place when electricity production surpasses consumption, necessitating a decrease in production. This overview pertains to the onshore electrolyzer system, refer to Figure 18:

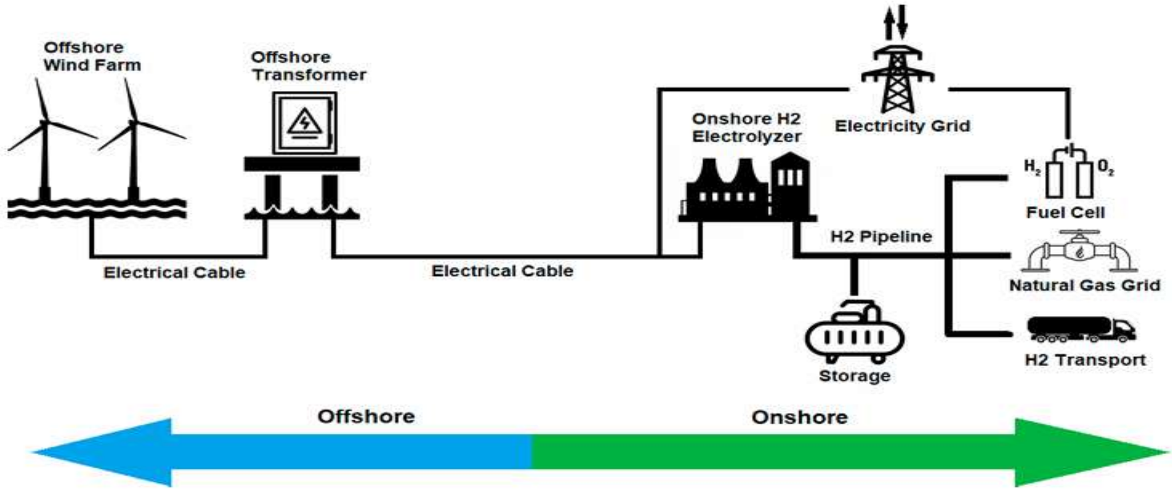

Figure 20 onshore electrolyzer scenario

In this onshore approach, the electrolyzer and sensitive equipment are housed in a building for protection from the elements and to improve the working environment for maintenance personnel. The simplified access to the electrolyzer offsets the increased maintenance and reduced power density, making both AEL and PEMEL viable options when installed on land. HVDC is more expensive and becomes beneficial only for offshore wind farms far from shore or with high nominal powers [47]. HVAC systems with longer transmission lines require more costly line-reactive compensators to address capacitive losses. In comparison, HVDC transmission incurs significantly lower costs, particularly for longer distances. The break-even distance for HVDC to become preferable is around 50–100 km for underground and underwater cables [47].

The study finds that a real-time pricing scheme results in lower $_{\text{LCOH2}}$, as the electrolyzer can decrease consumption during high-energy-price periods. Including storage is also a viable alternative to enhance flexibility, particularly when underground storage can be implemented. An optimal capacity factor ranges between 0.9 and 1, minimizing consumption during peak hours while ensuring high utilization of the CAPEX. For example, Patagonia has significant wind potential, averaging 4100 to 5200 full load hours and resulting in an LCOE of electricity as low as 25.6 €/MWh. In 2018, Philipp-Matthias Heuser et al. examined a potential connection between Japan and Patagonia. The proposed plan involved producing and liquefying hydrogen in Patagonia and shipping it to Japan. The analysis estimated an $_{LCOH2}$ of 2.16 €/kg at the electrolyzer output. The cost increases by 0.57 €/kg for transport to the shipping port and an additional 0.58 €/kg for hydrogen liquefaction and storage in liquid form, resulting in a final $_{LCOH2}$ of 3.31 €/kg. The cost of transport to Japan is 1.13 €/kg, making the cost of hydrogen upon arrival in Japan 4.44 €/kg [48].

Another article comparing the scenarios described above was written by Pengfei Xiao et al. [49] in 2020, where the model was developed for a wind farm in Denmark. Here, the electricity price for the scenarios varied from 80 /MWh to 160 /MWh, depending on the time of day, with the hydrogen price fixed at 6.27 /kg in the scenarios where hydrogen was produced. The article concluded that the hybrid approach yields greater economic interest compared to the other scenarios, with most of the hydrogen being produced at night when the electricity price is lower.

A slightly different approach was taken by Peng Hou et al. [50] , where a 72 MW offshore wind farm was being considered for the production of hydrogen, with two potential operating scenarios. The first scenario involves converting all energy to hydrogen in an electrolyzer, storing it, and then converting it back to electricity in a fuel cell for sale to the grid during peak hours. In the second scenario, electricity generated by wind turbines could either be sold to the grid or used to power an electrolyzer, with the option to purchase energy from the grid when prices are very low. Using Denmark's 2015 electricity prices, the study found that the first scenario was not economically feasible due to the low round-trip efficiency of the electrolyzer and fuel cell. However, for the second scenario with a 50% capacity factor for the electrolyzer, the DPB (Discounted Payback Period) was calculated to be 24.4, 5.5, and 2.6 years, with the nominal power of the electrolyzer being 5.5, 13.5, and 23.4 MW for hydrogen prices of 2, 5, and 9 $/kg, respectively.

Regarding the applications of hydrogen, Rodica Loisel et al. [51] developed a model with an offshore wind farm off the coast of Saint Nazaire, France. The paper simulated the economic viability of each application individually, then combined the two applications (for example, P2P and P2G), and presented a final scenario where all applications considered were implemented. In all scenarios, the electrolyzer's nominal power was considerably lower than the wind farm nominal power; consequently, most of the energy produced was sold directly to the electricity grid at wholesale prices, with the remaining energy being reserved for secondary and tertiary reserves. The study concluded that the most econom ically viable approach was P2G, with a hydrogen price of 4.2 /kg.

The cost of hydrogen is mainly influenced by the cost of electricity and the required infrastructure. As a result, AEL generally has a lower levelized cost of hydrogen ($_{LCOH2}$) than PEMEL due to lower costs. This also applies to the source of electricity: locations with lower electricity prices, such as the electricity grid in Ontario, solar PV in Chile, or onshore wind in Patagonia, tend to have lower $_{LCOH2}$ values. An analysis in California found that producing and selling hydrogen was more profitable than producing and storing hydrogen for later use in electricity generation [52].

A study by Scolaro et. al, [53] investigates whether participating in an ancillary service market is cost competitive for offshore wind-based hydrogen production. The study also determines the optimal size of a hydrogen electrolyzer relative to an offshore wind farm. It examines two scenarios: Scenario 1 assumes the current capacity of the WindFloat Atlantic wind farm to be 25.2 MW, while Scenario 2 considers a long-term commercial phase of 150 MW integrated into a developed hydrogen economy with pipelines for H2 distribution. In both scenarios, a readily available PEM electrolyzer system is employed, and the benefits of selling complementary oxygen are estimated. Wind resource availability and different wind conditions for the location are estimated using the wind energy atlas. Correlations between renewable energy production and wholesale electricity price in the Iberian market are established by processing 2019 data and accounting for seasonal variations.

For each scenario, two cases are analyzed. Case A assumes hydrogen production only at night, whereas Case B allows for production during both nights and afternoons. Results indicate that Case B and oxygen sales contribute to a more economically feasible project. For Case B, assuming a H2 selling price of 8 €/kg, a discount rate of 10%, and a corporate tax of 21%, results show that only Scenario 2 is profitable due to long-term lower costs. Scenario 1 appears feasible only with government incentives. The ratio between the hydrogen plant power and wind farm capacity (PPR) significantly impacts H2 production, with results showing a minimum in H2 cost for a ratio of approximately 30% [54].

Kim et. al, [55] In his study conducted a comparative economic analysis to verify feasible equipment placements of offshore wind-based H2 production systems in various possible cases with different electrolyzer types, wind speeds, and offshore distances. An analysis was conducted to determine suitable equipment placements for offshore wind-based H2 production systems under different scenarios involving various electrolyzer types, wind speeds, and offshore distances. Generally, the unit cost of H2 production increases with longer offshore distances and lower wind speeds. The unit H2 cost ranges from $1.64 to $3.13 per kgH2, $2.27 to $4.17 per kgH2, and $3.43 to $4.46 per kgH2 for cases using AEC, PEC, and SEC electrolyzers, respectively. In Ulsan, where the average wind speed is 7.81 m/s, the unit H2 cost ranges from $2.316 to $3.008, $3.202 to $4.069, and $3.849 to $4.457 per kgH2 with AEC, PEC, and SEC, respectively. The use of AEC indicates feasibility when compared with the H2 price targets ($2.48 to $3.30 per kgH2) in the H2 economy activation roadmap announced by the Republic of Korea. In the Magallanes region, where the average wind speed is 16.84 m/s, the unit H2 cost ranges from $1.766 to $2.447, $2.609 to $3.465, and $3.522 to $4.111 per kgH2 with AEC, PEC, and SEC, respectively. The use of AEC indicates competitiveness when compared with the current price range of conventional H2 production [55].

T. Nguyen et al. [56] performed a techno-economic analysis on grid-connected hydrogen production where several hydrogen storage solutions and electricity pricing schemes were analyzed. The analysis compared different methods for transporting hydrogen. The cost of producing hydrogen ($_{LCOH2}$) depends on real-time pricing, allowing the electrolyzer to adjust its consumption based on electricity prices. The lowest $_{LCOH2}$ obtained is 2.49–2.74 €/kg for an alkaline electrolyzer (AEL) and 2.26–3.01 €/kg for a PEMEL.

The analysis compared various hydrogen transportation methods and found that using compressed hydrogen pipelines or producing hydrogen onshore from transmitted electricity are more cost-effective than transporting liquefied hydrogen or hydrogen carriers via ships. The selected electrolyzer technology was PEMEL, optimally sized between 80% and 90% of the wind farm's nominal power. The $_{LCOH2}$ reaches a value of €3.5 per kg, with a discounted payback period of 9 to 15 years for hydrogen selling prices of €7 and €5 per kg, respectively, considering a wind farm with a minimum capacity of 150

MW [57].

Offshore electrolyzer systems situated 50 km from shore have an $_{LCOH2}$ of 8.98 €/kg in 2020, 4.37 €/kg in 2030, and 2.68 €/kg in 2050. Onshore systems that purchase electricity from the grid achieve a lower $_{LCOH2}$ of 5.84 €/kg in 2020, 3.42 €/kg in 2030, and 2.57 €/kg in 2050. Although renewable hydrogen is feasible, it is currently more expensive. AEL-driven hydrogen production costs €8.38/kg H2, which is only three times the cost of SMR+CCS-generated hydrogen. PEMEL-driven hydrogen production is higher, ranging from €10.49/kg to €10.91/kg H2. Both costs are lower than operating an onshore electrolyzer of the same size using grid electricity. Utilizing low-cost, low-carbon generators to power electrolyzers offers both environmental and economic benefits. Including salt-cavern storage increases $_{LCOH2}$ by less than €0.50/kg H2 for both AEL and PEMEL scenarios.[1]

Based on the literature review, it is clear that the cost of green hydrogen depends primarily on the electricity markets, distance to the shore, windfarm capacity, and the type of electrolyzer used. In order for green hydrogen to be competitive with hydrogen produced through steam methane reforming (SMR), government incentives may also be required.

Summary of Some Ongoing Pilot Projects/ Case Studies highlighting diverse applications and benefits of integrating Power-to-X solutions with offshore wind farms. From enhancing energy storage and grid stability to providing economic and environmental advantages is presented below:

4.1 CASE STUDIES

Table 5 Case Studies

Project	Objective	Hydrogen Production	Outcome	Refs

1. HyDeploy Project, United Kingdom (December 2023) **Overview:** Blending hydrogen into the natural gas network to demonstrate the feasibility of using hydrogen from renewable sources in existing infrastructure. **Location:** Keele University, Staffordshire, UK.	To blend up to 20% hydrogen by volume into the existing natural gas supply, demonstrating safe use in homes and businesses without requiring modifications.	The initial phase uses hydrogen produced through steam methane reforming, with plans to transition to green hydrogen produced via electrolysis using renewable energy sources like offshore wind in future phases.	**Demonstrated Safety and Feasibility**: Successfully showed that hydrogen can be blended into the natural gas grid without safety or operational issues. **Pathway for Renewable Integration:** Paves the way for future projects where hydrogen produced from offshore wind can be integrated into the gas network, enhancing the use of renewable energy	[58]
2. HEAVENN Project, Northern Netherlands January 2020 **Overview:** The HEAVENN (Hydrogen Energy Applications in Valley Environments for Northern Netherlands)	To develop a comprehensive hydrogen value chain that includes production, storage, distribution, and utilization in various sectors such as transportation, industry, and	Green hydrogen is produced using electrolysis powered by renewable energy, including offshore wind farms in the North Sea.	**Comprehensive Integration:** Demonstrates the potential of hydrogen to link various sectors, enhancing the overall efficiency and sustainability of the energy system. **Economic and Environmental Benefits:** Expected to	[59]

project is an ambitious effort to create a fully integrated hydrogen economy in the Northern Netherlands, leveraging renewable energy sources, including offshore wind. **Location:** Northern Netherlands, including Groningen and Drenthe.	heating.		reduce CO_2 emissions significantly and create numerous jobs, contributing to regional economic growth. **Scalability:** Provides a scalable model for other regions to integrate renewable energy with hydrogen production and utilization.	

North Sea Wind Power Hub February 2019 **Overview:** The North Sea Wind Power Hub (NSWPH) project is aimed at creating a large-scale renewable energy hub in the North Sea, incorporating offshore wind and PtG solutions. **Location:** North Sea, involving collaboration between Denmark, Germany, and the Netherlands.	To develop an interconnected offshore wind farm cluster with a capacity of up to 180 GW till 2050, coupled with PtG technologies to produce green hydrogen.	Green hydrogen is produced from electrolysis powered by offshore wind farms.	**Massive Renewable Integration:** Aims to provide large-scale renewable energy supply, significantly contributing to the EU's climate goals. **Energy Export and Storage:** Facilitates the export of green hydrogen to different parts of Europe, addressing energy storage and transport challenges. **Grid Stability:** Enhances grid stability by converting intermittent wind energy into storable hydrogen, which can be used to balance supply and demand.	[60]
H2RES Project, Denmark May 2021 **Overview:** The H2RES project is Denmark's first offshore wind-to-hydrogen project,	To produce green hydrogen using offshore wind power and explore its applications in various sectors.	The project utilizes electricity from an offshore wind farm to power electrolyzers for hydrogen	**Demonstration of Feasibility:** Proves the technical feasibility of offshore wind-to-hydrogen production. **Versatile Applications:** The	[61]

demonstrating the integration of offshore wind energy with hydrogen production. **Location:** Avedøre Holme, near Copenhagen, Denmark.		production.	produced hydrogen is intended for use in transportation, industry, and potentially for heating, showcasing the versatility of hydrogen as an energy carrier. **Scalability:** Serves as a model for scaling up offshore wind-to-hydrogen projects, contributing to Denmark's ambitious renewable energy targets.	
HySeas III, Scotland July 2018 **Overview:** HySeas III is a project focused on developing the world's first sea-going ferry powered by hydrogen produced from renewable sources, including offshore wind.	To build and operate a hydrogen-powered ferry, integrating green hydrogen produced from wind and tidal energy.	Utilizes excess renewable electricity from local wind and tidal energy to produce hydrogen via electrolysis.	**Maritime Sector Decarbonization:** Demonstrates the potential of hydrogen to decarbonize the maritime sector, reducing reliance on fossil fuels. **Renewable Integration:** Highlights the effective use of excess renewable energy for hydrogen production,	[62]

Details: **Location:** Orkney Islands, Scotland.			addressing issues of energy curtailment. **Local Economic Benefits:** Supports local industry and job creation in renewable energy and hydrogen technology sectors.	

5. SAFETY & ENVIRONMENTAL CONSIDERATIONS

5.1 HYDROGEN

Hydrogen is a clean and efficient energy carrier with unique physical and chemical properties that make it an attractive option for energy storage, transport, and use. However, it's important to handle hydrogen with care due to its high flammability and potential for fire/explosion risks. Hydrogen is stored in high-pressure cylinders or tubes made of steel, aluminum, composite materials, or vacuum-insulated tanks. When transporting hydrogen, it's crucial to follow all safety regulations and guidelines to prevent accidents or injuries [63]. Hydrogen is a colorless, odorless, and tasteless gas that is highly flammable in air and can ignite at concentrations as low as 4%. It has the lowest density of all gases and is fourteen times lighter than air. Hydrogen occurs in nature in the form of diatomic molecules (H2) and can be obtained from various sources such as natural gas, water, and biomass. It has a low boiling point (−252.8 ◦C) and a low freezing point (−259.14 ◦C), which means it must be stored and transported at very low temperatures, typically below −253 ◦C, to maintain it in a liquid state. Hydrogen can also easily evaporate and form a flammable mixture with air, which can cause explosions if ignition occurs.

Hydrogen reacts with oxygen to form water, which releases a significant amount of energy, making it an excellent fuel for power generation, transportation, and industrial applications. However, the high laminar flame speed of hydrogen implies significant safety issues, leading to significant explosion severity and the possible transition from deflagration to the detonation mode of propagation (DDT) [64]. Therefore, it's important to carefully design and implement safety measures when working with hydrogen to prevent accidents and mitigate any potential hazards.

Challenges in the **area of safety** as follows:

Hydrogen safety issues include low ignition energy, high reactivity, boil-off tendency, wide flammability limits, deflagration-to-detonation transition, high burning velocity, colorless and odorless nature, high reactivity with materials, and low gas density and diffusivity. These factors require careful handling and investment in safety measures [65]:

- Handling hydrogen requires special equipment and procedures due to its high flammability and risk of leaks.
- Hydrogen embrittlement can cause problems with equipment and infrastructure.
- Transporting hydrogen safely over long distances can be challenging due to its low energy density.
- Public awareness and education are important to prevent accidents and ensure proper handling.
- Boil-off is a safety concern when storing liquid hydrogen due to various phenomena.
- Hydrogen flames are difficult to detect, and its low molecular weight can cause embrittlement and accidental leaks, posing a safety risk.
- Electrical hazard: high electrical currents used during electrolysis can cause electric shocks, short circuits, and fires.

- Chemical exposure: electrolysis uses electrolytes that can result in chemical exposure.
- Typical accidents: fire in chlorine electrolyser cells, hydrogen explosion, hydrogen–oxygen explosion, membrane perforation in a PEM-FC cell, destruction of a PEM FC short stack, deflagration of H2/O2 with a short circuit, fire, hydrogen gas holder explosion due to a malfunction in the electrolyser.

Hydrogen transportation

Hydrogen transportation poses several safety issues that need to be addressed to ensure a safe process for both workers and the public. Hydrogen gas is highly flammable and can easily ignite, which can lead to potential accidents and explosions. The transportation of hydrogen involves the use of high-pressure containers and pipelines, which can pose safety risks if they are not properly maintained. To mitigate these risks, it is essential to follow strict safety protocols and perform regular maintenance checks. Hythane, a mixture of hydrogen and natural gas, is another form of hydrogen fuel that is being explored for transportation. Hythane has a lower risk of explosion compared with pure hydrogen, making it a potentially safer option for transportation. However, it is still important to handle and transport hythane with care to prevent accidents.

Hydrogen storage

Hydrogen storage methods include compressed gas, liquid, and solid-state storage. Compressed gas storage involves storing hydrogen gas in high-pressure tanks (350-750 bar) to increase storage density. Liquid hydrogen storage requires cooling hydrogen gas to a very low temperature (-253°C) and storing it in insulated tanks. Cryocompressed hydrogen (CcH2) storage combines cryogenic temperatures with pressurization (250-350 atm) in a container, unlike current cryogenic containers that store liquid hydrogen (LH2) at near-ambient pressure. Solid-state storage physically or chemically stores hydrogen in solid materials like carbon nanotubes or metal hydrides. Liquid organic carriers use a chemical cycle of hydrogenation and dehydrogenation steps. Heat is required for dehydrogenation in both liquid and solid chemical storage systems, with typical reaction conditions for exothermic hydrogenation being high pressure (1 to 5 MPa) and temperatures from 373 to 523 K [66]. Table 2 shows safety issues in the different storage technologies for hydrogen.

Table 2. Main safety issues concerning hydrogen storage.

Storage	Safety Issues
Compressed hydrogen	High pressure, strong interaction with materials, high frequency of occurrence of release.
Cryogenic hydrogen	Low temperature, strong interaction with materials, difficult thermal management, blow-out, ground release for the high density, freezer burns, complex phenomena close to the release point.
Cryo-compressed hydrogen	High pressure, low temperature, strong interaction with materials, difficult thermal management, blow-out, ground release for the high density, freezer burns, complex phenomena close to the release point.
LOHC	Formic acid: corrosive chemical that causes severe burns to the skin and eyes. DBT: low flammability, and toxicity is not well defined since it is a mixture of different regioisomers.
Chemical storage	Methanol: toxic (ingestion of 56.2 g per person and for inhalation a concentration of 4000–13,000 ppm), low FP, low BP. Ammonia: toxic (the lethal dose after 10 min of exposure is already estimated to be 2700 ppm, with severe irritation already estimated to be 220 ppm. The lethal dose of ammonia after 8 h of exposure can be as low as 390 ppm) and flammable.

To ensure safe use of hydrogen, safety systems such as gas detection and emergency shutdown must be custom-designed and installed in all production, transport, storage, and utilization facilities. Proper safety training and protocols for workers and careful material selection for tanks can minimize risks. Developing and implementing regulatory frameworks and standards for hydrogen safety is crucial to meet safety requirements and mitigate risks effectively. Some Global and regional Standards in the utilization of Hydrogen are listed below:

Current standards and configurations for the permitting and operation of hydrogen refuelling stations [67]

Global standards

The ISO hydrogen standards are developed by the following technical committees.

- ISO/TC 197 Hydrogen technologies
- ISO/TC 220 Cryogenic vessels
- ISO/TC 58 Gas cylinders
- ISO/TC 22/SC 41 Gaseous fuels-specific issues

For the production area, ISO covers both hydrogen production from fossil fuels and generation from water electrolysis. Additionally, there is a specific standard concerning the safety of hydrogen separation and purification systems (**ISO 19983**).

Several standards for hydrogen components and equipment are currently being developed, with LH2 technology having more published standards. ISO TC 197 [68] is actively working on standards for hydrogen fuel stations and vehicles. The ISO 19880 [69] series provides specifications and guidelines for designing, building, operating, and maintaining hydrogen fueling stations, ensuring safety, efficiency, compatibility, and commercial viability. There are nine relevant standards that are related to safety procedures and considerations, as well as explosive gas atmospheres, grouped into four main standard categories:

IEC 60079, IEC 80079, IEC 60204, and IEC 60529.

SAE standards are also in use for hydrogen applications, with the SAE FC Standards Committee developing technical standards for hydrogen refueling operations and connecting devices. The main standard for fueling protocols is SAEJ2601 [70], which provides specifications for dispensing hydrogen fuel to vehicles, ensuring safe and efficient transfer and promoting compatibility between different stations and vehicles. The standard covers safety and performance requirements, self-diagnosis procedures, and is continuously updated to keep up with advances in hydrogen technology. Adoption of SAEJ2601 supports the expansion of the hydrogen fuel cell sector.

European standards

CEN and CENELEC are responsible for generating and publishing standards in Europe, including ISO standards implementation. They provide technical requirements for product safety, quality, and interoperability. CEN and CENELEC have developed several hydrogen-related standards covering safety, storage, transport, and use. These standards are voluntary but widely referenced and adopted by European, national, and industry standards. CEN and CENELEC regularly review and update these standards to keep up with technology and safety advancements in five main categories: Production and supply storage, compression, dispensing, and general applications.

Concerning hydrogen supply, there are several standards for gas supply systems, with operating pressure less or over 16 bar, as well as the consequences of the injection/ transport of hydrogen into the gas infrastructure and the main requirements of transportable gas cylinders.

Storage-related standards are focused both on gaseous hydrogen (**EN 17533**) and liquid hydrogen storage (**EN 1797**) via cryogenic tanks.

The procedures of hydrogen dispensing are assessed from multiple perspectives.

EN 17127 [71] covers outdoor dispensing stations, while hydrogen refuelling procedures and equipment for train uses are still in development**. EN ISO 16380 and 17268** additionally discuss connectivity with fuel-cell electric vehicles, while **EN 17124** deals with hydrogen quality.

Italian National Regulatory Framework

Italy's abundant clean energy sources and extensive natural gas transmission network make it an ideal location for green hydrogen expansion. Its strategic position in the Mediterranean also makes it a potential hub for hydrogen trade between hydrogen-producing regions in the Middle East and Africa and hydrogen-consuming regions in the north. However, despite this potential, several regulatory and other barriers need to be addressed to fully develop green hydrogen in Italy.

The Italian technical committee UNI/CT 056/GL 01, which also functions as the national mirror group for CEN/CLC/JTC 6, is the only technical committee in Italy that mirrors ISO/TC 197 for hydrogen technology. The committee focuses on the systems, equipment, and connections required for producing and utilizing hydrogen from renewable sources.

Italy has recognized hydrogen as an alternative fuel through the National Decree n. 1657 of December 16, 2016, which implements the EU Directive 2014/94/EU. The decree mandates Italy to establish a sufficient network of hydrogen refueling stations by December 31, 2025. However, the lack of implementing legislation for the Ministerial Decree of August 31, 2006, has significantly hindered the expansion of hydrogen refueling stations in Italy.

The 2018 revised Decree permits a supply pressure of 700 bar and aligns with ISO 19880, addressing the absence of implementing regulations in the Ministerial Decree of August 31, 2006. In Italy, the National Fire Corps is responsible for safety and fire prevention assessments. However, certain hydrogen-related activities are currently prohibited, including the storage and distribution of liquid hydrogen, the use of pipeline-supplied hydrogen, and the implementation of mitigation strategies such as passive or active ventilation systems. Additionally, safety distances must be evaluated based on the equipment's working pressure, and there is no established methodology for calculating safety distances in case of ignited or un-ignited hydrogen leaks.

The only national standards accessible are those developed by **UNI** (Ente Nazionale Italiano di

Unificazione), and they are as follows:

UNI ISO 14687:2020, Hydrogen fuel quality Product specifications, which incorporates ISO 14687:2019.

UNI ISO 19880e1:2020, Gaseous hydrogen Fueling stations, which incorporates ISO 14687:2019. - Part 1: Basic specifications, which include ISO 19880e1:2020.

UNI ISO/TR 15916:2018, Fundamental safety considerations for hydrogen systems, which incorporates ISO/TR 15916:2015.

5.2 AMMONIA SAFETY CONSIDERATIONS

Ammonia is a colorless gas with a distinct odor, stored and transported in liquid form. Leaks can occur during production, storage, or transportation due to equipment damage or aging, leading to poisoning, fire, or explosion accidents. Ammonia has a relatively high boiling point of 240 K at 0.1 MPa, making long-term storage possible. Converting hydrogen gas to ammonia is cheaper than liquefying hydrogen, and ammonia can be used as a carbon-free fuel. However, safety risks are widely recognized in the maritime industry.

Hydrogen can be produced through water electrolysis, using surplus renewable energy. It is a highly sustainable clean energy source that can significantly aid the decarbonization of the transportation and energy sectors. However, direct usage of hydrogen fuel for transportation has security and storage challenges due to its extremely low boiling point (20.28 K) and wide flammability range (4-75% concentration in air).

Several alternatives to transport hydrogen have been proposed over time, one of which is ammonia. Ammonia offers several advantages over hydrogen, including lower energy storage costs, simpler production methods, higher volumetric energy density, better handling and distribution capabilities, and greater commercial viability [72].

Regarding safety, ammonia's flammability risk is lower than other hydrogen energy carriers and carbon-based fuels due to its high flash point. However, its health hazards, such as frostbite and toxicity, are significant and comparable to those of liquid hydrogen, LNG, and carbon monoxide. The tolerance concentration in ACGIH is used to rank toxicity.

Explosion and fire

Ammonia has flammability limits of 15% to 28% at standard atmospheric conditions, which can cause potential fire and explosion hazards if mixed with air and an ignition source is present. However, ammonia has a higher flash point and auto-ignition temperature, a slower fuel reaction, and a higher minimum ignition energy of 8.0 MJ compared to other alternative fuels. Additionally, ammonia has a relatively low laminar burning velocity of 0.07 m/s, making it more difficult to ignite than other fuels. The calorific value of hydrogen is more than six times that of ammonia, suggesting a higher risk of hydrogen explosion. Therefore, the probability of fire and explosion of ammonia is lower compared to other alternative fuels [73].

Health and safety

Although ammonia has a lower risk of fire and explosion compared to other low-flammability fuels, it presents unique hazards such as suffocation and cryogenic burns when exposed to normal atmospheric conditions. Ammonia is a toxic and basic gas that can cause asphyxiation, with the severity of its effects depending on the exposure route, dose, and duration. Exposure to high concentrations of ammonia can immediately cause burns to the eyes, nose, throat, and respiratory tract, as well as corrosive injuries such as skin burns, blindness, lung damage, and even death. Therefore, ammonia requires more careful management in terms of toxicity than other fuels.

Concentration of Ammonia - Toxicity

Typically, the ammonia concentration in the blood is less than 50 μmol/L. Ammonia is produced from protein waste products and is metabolized by the liver into urea or glutamine, which is then excreted in the urine. Inhaled ammonia, not naturally produced by the body, usually exists as a gas or vapor. It quickly reacts with moisture in the skin, eyes, mouth, respiratory tract, and mucous membranes to form ammonium hydroxide. This compound causes tissue necrosis by destroying cell membranes, leading to cellular protein decomposition and water extraction, which triggers an inflammatory response and further damage.

Ammonia concentrations above 100 μmol/L can cause consciousness disturbances, while levels exceeding 200 μmol/L may lead to coma or convulsions. Inhalation of ammonia gas can obstruct the airways, making breathing difficult, and may result in laryngitis or bronchitis [74].

Corrosion

Ammonia is highly corrosive and can cause chemical corrosion, leading to structural damage. It particularly corrodes materials such as copper, brass, and zinc alloys, forming green or blue corrosion products. To minimize the risk of corrosion when using ammonia as a fuel, it is essential to avoid these materials in the construction of storage tanks, engines, and fuel systems.

Ammonia can also cause stress corrosion cracking (SCC), a phenomenon where metals exposed to a combination of stress and corrosive environments suffer from structural damage.

Ammonia instrumentations should aim for zero leakage due to serious safety concerns. Dilution devices should be used before venting, and direct venting should only be allowed in case of fire. Ammonia has a lower density than air and is soluble in water, making it prone to absorption by moisture and settling in case of a leak. These factors must be considered when assessing the potential risk of ammonia dispersion.

Ammonia remover

- **Water**

Water is commonly used to reduce ammonia vapor pressure and prevent its diffusion in case of a leak. In outdoor ammonia storage facilities, water sprinklers are typically used as a detoxification system, collecting ammonia water in a dike after spraying water on the leaked ammonia. In enclosed spaces, a water curtain can be installed to absorb leaked ammonia and prevent its diffusion. Airborne ammonia above certain concentrations is hazardous, and water can be used to remove it from the air.

- **Zirconium phosphate**

The ammonia vapor concentration of 1000 ppm can be reduced to less than 1 ppm using insoluble zirconium phosphate in the presence of water.

- **Water + Zirconium**

It is assumed that the presence of water helps the movement of ammonia adsorbed on the surface of zirconium phosphate into the interlayer nano space of zirconium phosphate.

Regulatory Framework for ammonia, taken from [73]

Table 5. Regulatory frameworks for ammonia in the maritime sector.

Organization	Content
IMO	Regulates the safety of ships using low-flashpoint fuels (below 60 °C). The IGF code [46] also provides specific requirements for the design and installation of ammonia supply systems. Hazard identification and risk assessment are also required for the initial design phase. The international standard for the safe carriage by sea of bulk liquefied gas (IGC code) [47] is useful for designing ammonia storage systems. ISO 8217:2017 standardizes the requirements for ammonia as a marine fuel suitable for onboard systems. The International Convention for the Safety of Life at Sea (SOLAS) regulates the use of low-flashpoint fuels for marine vessels.
Korean Register (KR) [48]	Provides general application and arrangement requirements for ships using ammonia as fuel, focused on the safe design, installation, and operation of ammonia-fueled ships. The KR also sets standards for ventilation systems to prevent the toxic and corrosive effects of ammonia in the case of leakage.
DNV GL [49,50]	Covers the specific requirements for the design of ammonia fuel gas supply systems as stated in the IGF Code. The DNV GL serves as a technical reference for the safety of ammonia-fueled ships for designers, ship owners, and operators.
American Bureau of Shipping (ABS) [51]	Provides a guide for both existing and new construction vessels using ammonia and other low-flash point fuels. These regulations provide a safety handling plan and training schedule to prevent accidents caused by humans.
International Association of Classification Society (IACS) [52]	Focuses on survey, repair, and maintenance procedures during the voyage and berthing of ammonia-fueled vessels.
European Maritime Safety Agency (EMSA) [53]	Provides standards relevant to elements of ammonia supply chain systems, including production, transportation, storage, and end-user utilization.
The Society of International Tanker and Terminal Owners (SIGTTO) [54]	Provide detailed guidelines for bunkering procedures with low-flashpoint fuels, specifically for the planning and implementation of ship-to-ship, port-to-ship, and truck-to-ship bunkering.
Society for Gas as a Marine Fuel (SGMF) [55,56]	Provides overall guidelines and detailed implementations for the aforementioned safety zones, as well as best practices for utilizing gases as fuel for marine vessels.
Singapore Quantitative Risk Assessment Technical Guidance [57]	Presents the primary reference document for choosing location-specific input parameters and for presenting the outcomes.

International regulations

Several international regulations ensure the safe transport of ammonia on ships. These include the International Code for the Construction and Equipment of Ships Carrying Dangerous Chemicals in Bulk (IBC Code) [75] for aqueous ammonia and the International Code for the Construction and Equipment of Ships Carrying Liquefied Gases in Bulk (IGC Code) for anhydrous ammonia.

For using ammonia as a fuel in shipping, the primary regulation is the IGF Code, adopted in 2017, which outlines general requirements for low-flashpoint fuels and specific requirements for natural gas. In 2020, the IMO approved the Interim Guidelines for the Safety of Ships Using Methyl/Ethyl A_{LCOH2}ol as Fuel. Additionally, the IMO correspondence group is developing specific regulations for ammonia [76]. The following table summarizes international regulations on ammonia use as a marine fuel:

Summary of various international regulations on using ammonia as a marine fuel.

Reference No.	Document title	Summary
MSC 104/15/9 (IMO, 2021)	Development of non-mandatory guidelines for the safety of ships using ammonia as fuel	Proposes a new output to develop non-mandatory guidelines for the safety of newly built ships using ammonia as a fuel
MSC 104/15/10 (IMO, 2021a)	Hazard identification of ships using ammonia as a fuel	Provides the results of hazard identification of ships using ammonia as a fuel
MSC 104/15/30 (IMO, 2021b)	Necessity of deliberations on operational safety measures and fire safety measures	Points out the necessity of careful deliberations on operational safety measures and fire safety measures for ammonia-fuelled ships
CCC 7/3/9 (IMO, 2021c)	Report from the correspondence group and proposal for developing guidelines for the use of ammonia and hydrogen as a fuel	Provide comments on the progress made in the report from the correspondence group on the development of technical provisions for the safety of ships using low-flashpoint fuels and propose to include the development of two separate guidelines for the safety of ships using ammonia and hydrogen as fuel in the work plan of the CCC Sub-Committee
CCC 7/INF.8 (IMO, 2020)	Forecasting the alternative marine fuel: ammonia	Introduces the outline of the outlook of ammonia as green ship fuel
CCC 8/13/1 (IMO, 2022a)	Development of guidelines for the safety of ships using ammonia as fuel	Provides information on possible issues to be considered for developing guidelines for the safety of ships using ammonia as fuel and proposes the way forward
CCC 8/13/2 (IMO, 2022)	Comments on document CCC 8/13	Proposes a review of the environmental effect which will be considered in future discussions
CCC 8/13 (IMO, 2022b)	Report of the Correspondence Group (safety information for the use of ammonia)	Provides the report of Correspondence Group on the development of technical provisions for the safety of ships using low-flashpoint fuels, regarding the collection of the safety information for the use of ammonia.

ISO standards

The ISO has developed various standards related to ammonia, covering topics such as the design and installation of storage tanks and the measurement of liquefied gas concentrations. For example, ISO 7103:1982 provides a global standard for obtaining representative samples of industrial liquefied anhydrous ammonia from different containers and guidelines for handling this hazardous substance with a boiling point of -33.3°C under standard atmospheric pressure. Additionally, PGS 12:2014 [77] outlines proper procedures for storing and handling ammonia, emphasizing the importance of secure storage and handling due to its toxicity, corrosiveness, and potential for asphyxiation. To ensure safe storage and disposal, storage areas should be well-ventilated with leak detection systems, and employees should wear appropriate personal protective equipment, including respirators, safety goggles, and gloves.

EU legislation

The Seveso Directives are the main EU legislation aimed at preventing, preparing for, and responding to major accidents involving dangerous substances on land. They were established after a chemical factory explosion in Seveso, Italy, exposed residents to high levels of dioxin, a human carcinogen and potent endocrine disruptor. Seveso establishments handle, produce, use, or store hazardous materials, such as refineries, petrochemical sites, oil depots, or explosives depots. The first Seveso Directive (82/501/EEC) was adopted in 1985 and introduced preventive measures and notifications to reduce the risk of hazardous activities. The Seveso II Directive (96/82/EC) was enacted in 1997 and took into account lessons learned from later accidents such as Bhopal, Toulouse, and Enschede. The latest Seveso III Directive (2012/18/EU) was adopted in 2012, reflecting changes to Union legislation on chemical classification and expanding citizens' rights to access information and justice. The Seveso directives primarily apply to land-based facilities.

Class rules and guidelines

Major classification societies have developed their own rules and guidelines for ammonia-fuelled ships in 2021 and 2022. The following list of classification societies and their documents were used in the gap analysis.

- LR (2021) [108]
- ABS (2021) [109]
- ABS (2021) [110]
- ABS (2022) [111]
- BV (2022) [112]
- DNV AS (2021) [113]
- KR (2021) [114]
- NK (2021) [115]
- RINA (2021) [116]

Although most directives are broadly consistent with the IGF code, there are currently no international standards applicable to ammonia fuelled ships. Therefore, the following sub-sections provide a detailed understanding of the safety requirements and guidelines that ammonia fuelled ships must comply with by comparing the differences between classification guidelines and the IGF code. International Regulations for Ammonia Transport and Use as Fuel on Ships summarized in the table below:

Table 6 International Regulations for Ammonia Transport and Use as Fuel on Ships

Regulation	Year	Scope
IBC Code (International Code for the Construction and Equipment of Ships Carrying Dangerous Chemicals in Bulk)	2004	Governs the transport of aqueous ammonia
IGC Code (International Code for the Construction and Equipment of Ships Carrying Liquefied Gases in Bulk)	2014	Governs the transport of anhydrous ammonia
IGF Code (International Code of Safety for Ships Using Gases or Other Low-Flashpoint Fuels)	2017	Sets general requirements for low-flashpoint fuels, including specific requirements for natural gas
Interim Guidelines for the Safety of Ships Using Methyl/Ethyl A_{LCOH2}ol as Fuel	2020	Provides safety guidelines for ships using methyl/ethyl a_{LCOH2}ol as fuel

The IBC Code and IGC Code ensure the safe transport of ammonia, either aqueous or anhydrous, on ships. The IGF Code, adopted in 2017, is the main regulation for using ammonia as a fuel in shipping, covering low-flashpoint fuels generally and natural gas specifically. Additional specific regulations for ammonia as a fuel are currently being developed by the IMO correspondence group.

6. Economic Analysis Of Hydrogen Production From Offshore Wind

6.1 Introduction

Hydrogen demand– estimated at 339 TWh in Europe in 2019 is expected to increase drastically by 2050 and could reach up to 2300 TWh in 2050 according to the European Hydrogen Backbone initiative [78]. At present, hydrogen is primarily produced through steam methane reforming, a method that results in significant greenhouse gas emissions. To establish hydrogen as a viable solution for a sustainable future, it is essential that its production becomes largely carbon-free. Water electrolysis is a promising approach for generating clean hydrogen on a large scale, as it can be powered by decarbonized electricity sources such as renewable or nuclear energy. However, to facilitate the shift from gray/black to low-carbon hydrogen, it is crucial to reduce production costs. Offshore wind turbines are currently being explored as a potential method for generating hydrogen, as they offer less restrictions on sea usage and provide the advantage of more consistent and stronger winds compared to onshore turbines.

The production of hydrogen from offshore wind farms is a relatively new research area. A few recent studies have provided an overview of the current state of water-to-hydrogen (W2H) technology and identified three primary connection schemes for such projects: onshore, centralized offshore, and decentralized offshore electrolysis [79] [80].

6.2 Connection Schemes Considereds

In this work, three connection schemes have been defined for hydrogen production, which are onshore electrolysis, centralized offshore electrolysis, and decentralized offshore electrolysis, as shown in figure:

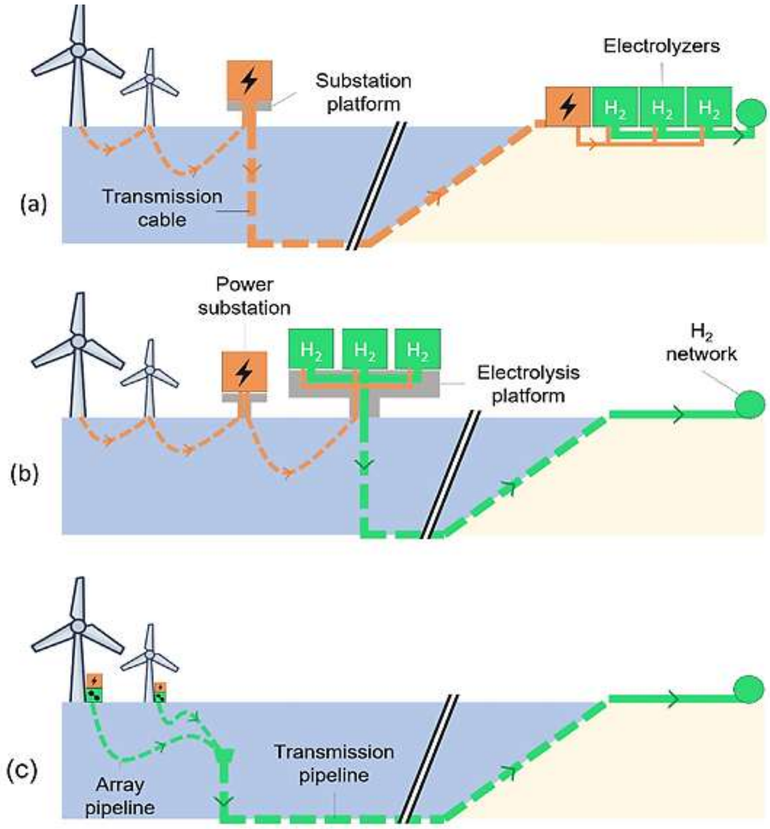

Figure 21 connection schemes for hydrogen production onshore electrolysis (a), centralized offshore electrolysis (b), and decentralized offshore electrolysis (c), source [81]

Scheme 1 - Centralized Offshore Electrolysis:

Another approach to hydrogen production is to generate it directly offshore. Due to the size of electrolyzers, they require their own platform. One option is to install them on a central platform within the wind farm. This configuration utilizes efficient and cost-effective pipelines to transport hydrogen to the shore.

Scheme 2 - Decentralized Offshore Electrolysis:

An alternative option for offshore production is to place an electrolyzer near each wind turbine. In this configuration, hydrogen is transported through individual inter-array pipelines between the turbines to a manifold before being sent onshore via a rigid pipeline. This configuration eliminates the need for massive platforms and results in minimal losses and costs.

6.3 Methodology of Economic Analysis

The Levelized Cost of Hydrogen (LCOH) is a metric used to assess and compare the profitability of hydrogen production from offshore wind farms. It is calculated based on the lifetime costs and energy production over the entire lifespan of the project, as illustrated in Eq. (1).

$$LCOH = \sum l_{\;t=0} \frac{\frac{CAPEXt+OPEXt+DECEXt}{(1+r)^t}}{\sum L_{\;t=0} \frac{Et}{(1+r)^t}} \qquad (1)$$

where $CAPEX$, $OPEX$, and $DECEX$ represent the capital, operational, and decommissioning costs, respectively (e), E represents the energy produced or the amount of hydrogen produced (kg), l is the lifetime of the project (y), and r is the rate of return considered in the economic evaluation (%).

To calculate the LCOH, we must first model $CAPEX$, $OPEX$, and $DECEX$. $CAPEX$ comprises equipment costs, EC, and installation costs, IC, while $OPEX$ includes material costs, MC, and logistics costs, LoC.

Equipment Costs

Wind Turbines

The costs associated with wind turbines, including both the foundation and turbine equipment, are an important factor in the overall economic assessment. Since this analysis is comprehensively covered in WP2, here we only provide a brief reference. The turbine and foundation costs, directly related to the number of turbines, are taken as inputs from WP2 for the techno-economic modeling in this deliverable.

Regarding foundations, three options are considered:

- Monopile for shallow water, i.e., less than 25 meters deep

• Jacket for water depths between 25 and 55 meters

• Floating for waters deeper than 55 meters

The rated cost of the foundations is modeled based on the work of Bosch et al. taking into account the water depth, h (m), as presented in Eq. (5). This equation provides a reliable estimate of the foundation cost as a function of water depth.

$$RC_{TF}(h) = c_1 \cdot h^2 + c_2 \cdot h + c_3 \cdot 10^3 \qquad (5)$$

The values of the coefficients $c1$, $c2$, and $c3$ vary depending on the type of foundation and tend to decrease over time, as presented in Table 7

Table 7 Coefficients used for foundation costs of wind turbines, taken from [74]

		Turbine foundation		
		Monopile	Jacket	Floating
2020	c_1	201	114	0
	c_2	613	−2270	774
	c_3	812	932	1481
2030	c_1	181	103	0
	c_2	552	−2043	697
	c_3	370	478	1223
2050	c_1	171	97	0
	c_2	521	−1930	658
	c_3	170	272	844

In the case of decentralized offshore electrolysis, the wind turbine foundations need to be modified to accommodate the electrolyzers, such as by adding a dedicated platform. As the foundation cost is determined by the weight to be supported, this modification is accounted for by an additional cost set at 20% of the foundation cost, since the power density of the electrolyzers is estimated to be 20% of the power density of the wind turbine (based on estimates from [82]).

Offshore Platforms

The dedicated platforms required for offshore electrolyzers and power substations have costs that are modeled in a similar manner to wind turbines. These costs encompass the expenses related to platform equipment, denoted as PE, as well as the platform foundations, represented by PF.

$$EC_{OP} = EC_{PE} + EC_{PF} \quad (6)$$

The choice of platform for accommodating equipment depends on the water depth at the site. For shallow waters with a depth below 30 meters, **sand islands** are typically used as they significantly lower investment costs as the size of the wind farm increases. The equation for the cost of a sand island, denoted as EC_{SI}, is presented in Eq.(7) and depends on the volume of sand V_{SI} (m^3) and the area to be protected A_{SI} (m^2), as defined by Singlitico et al. [83]. For substations and electrolyzers, a footprint of $5m^2/MW$ and $20m^2/MW$, respectively, is assumed based on [83] [84].

$$EC_{SI} = C_{SI,V} \cdot V_{SI}(h) + C_{SI,A} \cdot A_{SI}(h) \quad (7)$$

Cost parameters for sand islands, $C_{SI,V}$ = 3.26 (€/m^3), and $C_{SI,A}$ = 804.00 (€/m^2), taken from [83].

The modelling of **jacket (shallow to intermediate water depths, ranging from about 50 to 300 meters depth) and floating platform (deep waters, usually in water depths greater than 300 meters)** foundation costs is presented in Eq. (8).

$$EC_{PF}=RC_{PF}(h) \cdot P^*_{WF} + UC_{PF}(h) \quad (8)$$

		Platform foundation	
		Jacket	Floating
RC	c_2	233	87
	c_3	47	68
UC	c_2	309	116
	c_3	62	91

Coefficients used for the foundation costs of Platforms [82]

The equipment costs of the **power substation**, denoted as EC_{PS}, depend on the capacity of the wind farm and the type of substation (HVAC or HVDC), as shown in Eq. (9).

$$EC_{PS} = RC_{PS} \cdot P_{WF} + UC_{PS} \cdot 10^3 \qquad (9)$$

The substation cost hypotheses are presented in Table, taken from [82]

	HVDC	HVAC	
RC_{PS}	102.93	22.87	(€/kW)
UC_{PS}	31.75	7.06	(M€)

De

Electrolysis Plant

Electrolyzers

Proton exchange membrane (PEM) electrolyzers are the preferred option for offshore hydrogen production because they produce hydrogen at higher pressures and require a limited footprint and operating temperature [83]. The installation cost for 2030 according to the report [85] estimates the total installed costs of a 1-GW green-hydrogen plant are estimated at EUR 730 million (730 €/ kW installed capacity) for a plant using AWE technology, and at EUR 830 million (830 €/kW installed capacity) for a plant using PEM technology. When expressed in terms of hydrogen production, the estimated total installation costs would be 1580 €/(kg/day) for AWE technology and 1770 €/(kg/ day) for PEM technology. The cost for electrolyzers C_{EL} (€/kW) is given by eq. 10.

$$C_{EL} = RC_{EL} \cdot P_{EL} \qquad (10)$$

Where,

$$RC_{EL} = (k_0 + k \cdot p^{\alpha-1}{}_{EL}) \cdot (Y / Y0)^{\beta} + RC_0 \qquad (11)$$

Where k_0 and k are constants, P_{EL} is the rated power of the electrolyzer (kWe), and Y and Y_0 are the installation year and reference year, respectively as shown in table. RC_0 is an additional fixed cost that accounts for the electrolyzer-to-system costs, such as connection and sealing, which decrease over time and are aligned with values found in the literature [84].

Table 8 Cost parameters of electrolysis systems, Source [86]

k_0	673.73	(€)
k	10,876.93	(€)
α	0.662	–
Y_0	2020	–
β	−104.45	–

Figure 22. evolution of the cost of the electrolyzer as a function of the rated power of the system for the years 2020,2030, and after 2040, taking into account the parameter values listed in Table 8, Source [86].

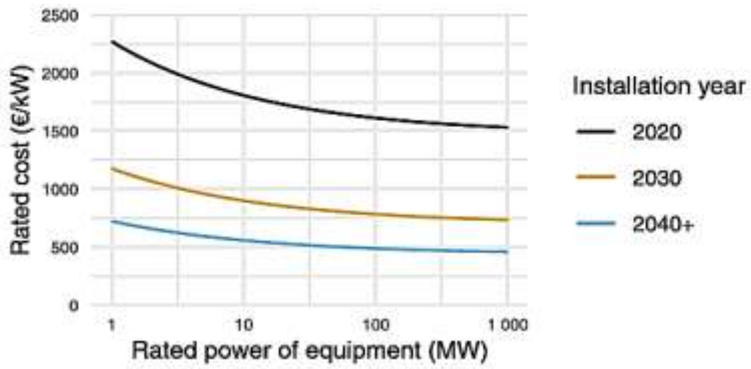

Desalinator

Offshore hydrogen production necessitates seawater desalination to provide the substantial amount of freshwater required for electrolysis. The cost of the desalination system, denoted as $ECDS$, is estimated using Eq. (12) [83]

$$CAPEX_{DS} = RC_{DS} \cdot \quad V_{H20} \qquad (12)$$

Where RC_{DS} is the rated cost of the desalinator, costs 800 to 1500 (€/(m³/h)) [87], and $\dot{V}H2O$ is the nominal flow rate of water (m³/h). The desalinator is sized at 80% of the electrolyzers' rated power (kW), taking into account a small buffer tank for freshwater. The nominal flow rate of water is then related to the rated power of the electrolyzer by Eq. (13), where the nominal water consumption of the electrolyzers, $\dot{v}H2O$, is estimated to be 0.263 m³/MWh [82].

$$V_{H2O} = \dot{v}_{H2O} \cdot 0.8 \cdot P_{\mathrm{EL}} \qquad (13)$$

Compressor

The Capex of the compressor is determined from the compressor's duty(or power) required for the service, which is a function of the gas mass flow rate (and its intrinsic properties), temperature, and the desired compression ratio, as shown in equation (taken from [87]:

$$Power_{Compressor}[watts] = m\,\frac{RT_{in}}{MW}\frac{\gamma}{\gamma-1}\frac{Z_1+Z_2}{2}\;\frac{1}{\eta_{iso}\,\eta_m}\left[\left(\frac{P_2}{P_1}\right)^{\frac{Z_1+Z_2}{2}}-1\right]$$

Where m [kg/s] is the gas mass flow rate; $P2$ [bar] and $P1$[bar] are the discharge and suction pressures, respectively; Z and $Z1$ are the gas compressibility factor at suction and discharge; Tin[K] is the inlet temperature, γ the specific heat ratio; MW is the molecular mass of the gas, ηiso & ηm correspond to the isentropic and mechanical efficiency of the compressor, respectively, and R is the universal gas constant. For the offshore electrolysis case, the suction pressure is determined from 2 design variables: the electrolyzer operating pressure (assumed 30 bar) and the allowed pressure losses in the transfer pipeline to the collection point (assumed 2 bar). On the other hand, on experts' suggestion, the discharge pressure is set to 100 bar. The reasoning for this decision is that this pressure corresponds to a reasonable transmission for offshore pipelines operating in the North Sea. Likewise, the available pipeline cost (explained in the later section) was obtained for pipelines operating around this pressure; higher pressures will increase the required thickness of the pipeline, for which no data costs were available. In addition, 100 bars is found to be sufficient discharge pressure to ensure that the produced hydrogen enters the gas network at the required injection pressure (80 bar) [87].

On the other hand, for the onshore electrolysis case, a compression system was also included to increase the electrolysis pressure (~30 bar) to 80 bar, which is the expected injection pressure to the gas network. In both analysed scenarios, the maximum gas flow rate (and therefore compressor duty) corresponds to all the electrolysers are producing at rated production, for which a single compressor could technically be used to handle the total capacity. However, it is recommended to divide the compression service into two parallel compressors, each one handling half of the required flow rate capacity (and thus compression duty), and to have a spare unit (also sized to handle half of the required flow rate capacity). This decision is made for two main reasons. First, according to industry experts, reciprocating compressors have a turndown capability of around 30% of the rated capacity. Thus by having two units with half capacity in parallel, this operational point also decreases by half. Second, the use of two operating units with a spare helps ensure the availability of the compression system; the previous is due to if one of the compressors fails or needs to be taken off for maintenance, only half of the wind farm gas compression stops before the spare units take over. The Compressor Capex cost is calculated using a fitted engineering equation

$$CAPEX_{comp}[M€] = 0.8238\ln\left(Power_{Compressor}\right) + 3.1574$$

Where Power Compressor [MW] is the compressor power (6) The operational cost of the compressor is assumed to be a function of the cost for running the compressor and a fixed maintenance cost as follows

$$OPEX_{comp}[€] = \left(A_0 \frac{t_{year}\, e}{\eta_{iso}\eta_m}\right) W \; + PF_{comp}\, CAPEX_{comp}$$

Where Ao is the availability of the compressor; $tyear$ [h / $year$] are the operating hours per year; e [€ / kwh] is the electricity cost; ηiso & ηm are the isentropic and mechanical efficiency of the compressor, respectively;C$APEXComp$ is the compressor CAPEX, and $PFcomp$ is the maintenance penalty factor of the capital cost (assumed 8 % of the capital cost [87]).

Electric inter-array connection

With the exception of the decentralized offshore configuration, the electricity generated by the wind turbines is transmitted to a substation through inter-array cables. The investment cost of the inter-array cables $ECIA$ depends on the length and cross-section of the cables. A string-based layout is considered, shown in fig. below,

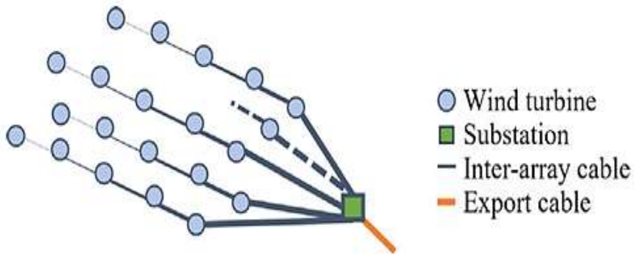

Figure 23. Schematic string-based layout considered for wind farms in centralized offshore electrolysis configuration. The electrolyzers are located on the platform

and the cable cross-section S increases along the array within its capacity limit. The total inter-array cost is estimated using eq. below.

$$EC_{IA} = N_A \cdot \;(\textstyle\sum_i LC_{Si} \cdot L_{Si} \; + LC_{Smax} \; \cdot L_{Smax,HUB} \qquad (14)$$

Where NA is the number of arrays needed, and LCSi and LSi are the linear cost (€/m) and the total length (m) of the inter-array cables of section Si, respectively. *Smax* is the largest cable section needed, and *LSmax*,*HUB* is the length of cable needed to connect the arrays to a sand island hub if needed. The techno-economic parameters of the inter-array cables are shown in Table 9. Both 66 kV and 132 kV cables are considered, since the rated tension increases with the rated power of the turbines. The cable length of section *Si* is calculated as in Eq. The number of wind turbines connected to this section *NSi* depends on the remaining available capacity considering the wind turbines connected to the upstream sections. We limited the number of turbines per array to 8 to limit power losses.

$$Lsi = Nsi \cdot Ll$$

Table 9 Technico-economical assumptions for inter-array cables. Source: [82]

i	Tension (kV)	Section (mm^2)	Resistance (Ω/km)	Capacity (MW)	Cost dynamic (€/m)	Cost static (€/m)	Inst. cost (€/m)
1	66	95	0.25	24	180	113	113
2		150	0.16	30	215	134	121
3		300	0.08	42	298	186	149
4		400	0.06	49	357	223	156
5		630	0.04	59	456	285	171
6		800	0.03	69	577	361	180
1	132	120	0.2	80	288	152	114
2		150	0.16	87	358	188	122
3		300	0.08	123	747	393	216
4		400	0.06	136	900	474	213
5		630	0.04	162	1228	646	226
6		800	0.03	201	1779	936	281

With $$NSi = \frac{\lfloor PSi - \sum_{i-1}{}^{k=1} NSk \cdot PWT \rfloor}{PWT}$$

where LI is the length of the inter-array cable between two turbines (m) and is calculated according to Eq. (18).

$$LI = 2 \cdot 2.6 \cdot h + D_{WT}$$

The distance between two turbines $DWT = \sqrt{\frac{PWT}{CDWT}}$ depends on CDWT and PWT, the capacity density (MW/km²) and the rated power (MW) of the wind turbines, respectively.

Pipeline inter-array connection

In the case of decentralized production, where each turbine has its own electrolyzer, hydrogen is collected using flexible pipes connected to the transport pipe via manifolds. These manifolds have a limited number of connection slots, denoted as NCS, which necessitates cascading the manifolds into Ns connection stages, as calculated by Eq. (14).

$$Ns = \lceil \log_{N_{CS}} (N_{WT}) \rceil \qquad (14)$$

For each stage i, the required length of pipes is estimated using Eq. (15), which depends on the number of pipes Np connected to each of the $N_{MF,i}$ manifolds in that stage i and Ai, the total area covered by the downstream wind turbines (km²). The first pipe stage (from the turbines to the seabed) consists of flexible pipes, while rigid pipes are used in the other stages

$$L_i = \begin{cases} N_{WT} \cdot \left(\frac{\sqrt{A_i}}{\sqrt{2}} + h \right), & \text{if } i = 1 \\ N_p \cdot N_{MF,i} \cdot \frac{\sqrt{A_i}}{\sqrt{2}}, & \text{otherwise} \end{cases} \qquad (15)$$

The cost of inter-array pipeline equipment costs EC_{IAP} is then calculated by Eq. (16).

$$EC_{IAP} = \sum_{i=1}^{Ns} \left(\alpha_s(d_i) \cdot LC_{BA,IAP} + LC_{misc,IAP}(di) \right) \cdot L_I \qquad (16)$$

Where $\alpha s(d)$ and $LCmisc(d)$ are a size factor and miscellaneous cost (details in [88]), and LC_{BA} is the base cost of flexible pipes (€/m) defined in the table.

Values used for pipes (flexible and rigid) and manifold costs estimation [88]

N_{CS}		5	(slots)
LC_{BA}	Flexible	1736.73	(€/m)
	Rigid	173.67	(€/m)
UC_{BA}	Manifold	2.265	(M€)
$UC_{misc,MF}$		0.188	(M€)

The diameter of the pipeline at stage i, denoted as di (m), is recursively calculated based on the diameter of the export pipeline (see Eq. (21)), as defined in Eq. (17). A minimum diameter of 5 cm is considered.

$$di = max\left(0.05, \frac{di-1}{\sqrt{Nc}}\right) \qquad (17)$$

Manifolds group pipes together and connect them to the transmission pipeline. The cost model for manifolds is similar to that for inter-array pipelines, as it depends on the diameter of the connected pipelines. If it is assumed that each manifold has five connection slots, except for the last manifold, which may have fewer slots. The total cost of manifolds denoted as EC_{MF}, is expressed by Eq. (18)

$$EC_{MF} = \sum_{i=1}^{Ns} \left(\alpha_s(di) \cdot \alpha_N(N_{CS}) \cdot UC_{BA,MF} + UC_{misc,MF} \right) \cdot N_{MF,i} \qquad (18)$$

Where $\alpha_s(d)$ and $\alpha_N\ (NCS)$ are factors that depend on the pipe diameter and the number of connection slots, respectively [88]. UC_{BA} and UC_{misc} are the base and miscellaneous costs (€), respectively, defined in the table.

Rigid Pipeline

For offshore electrolyzers, the generated hydrogen must be transported to shore via an export pipeline. The cost modeling for the export pipeline is the same as that used for the inter-array pipes (sec. 5.3.2.3) as illustrated in eq (20).

$$EC_{EP} = (\alpha_s (d) \cdot LC_{BA,EP} + LC_{misc,EP} (d)) \cdot L_{EP} \quad (20)$$

The diameter of the export pipeline grows with both the distance from the coast and the power of the wind farm, as more hydrogen needs to flow through the pipeline and the pressure drop becomes significant. Eq. (21) models the evolution of the export pipeline diameter, denoted as d_{EP} (m). L_{EP} is the length of the pipeline(m).

$$d_{EP} = 0.200 + 0.346 \cdot 10^{-3} \cdot L_{EP} + 0.065 \cdot P_{EP} \cdot 10^{-9} \quad (21)$$

Installation Costs

Turbines

The installation costs of wind turbines, including vessel requirements, transport logistics, and on-site assembly, are comprehensively assessed in WP2. For the purpose of this deliverable, we take these results as input from WP2 and do not replicate the full cost modelling. The detailed methodology, including vessel characteristics, installation time, and related parameters, can be found in the corresponding WP2 deliverables.In the table below are summarizes the input parameters.

Parameters used for turbines installation, source [82]

			Floating		
		Fixed	Trans.	Ancho.	
Vessel		SPIV	Tug	AHV	
Capacity	VC	*	0.3	7	(u/lift)
Speed	v	18.5	7.5	18.5	(km/h)
Load. time	t_{load}	24	5	30	(h/lift)
Inst. time	t_{inst}	144	-	90	(h/u)
Dayrate	DR	200	2.5	40	(k€/d)

Platforms

Fixed platforms are installed using self-propelled installation vessels (SPIVs), similar to fixed wind turbines. Floating substations require heavy-lift cargo vessels (HLCVs). The input parameters are listed in the table below. The equation for cost is given below:

$$C = \left(RSPIV \times (Tload,\ SPIV + Tinstall,\ SPIV)\right) + \left(RHLCV \times (Tload,\ HLCV + Tinstall,\ HLCV)\right)$$

- RSPIV = Day rate for the self-propelled installation vessel.
- *T*load, SPIV = Loading time for the SPIV.
- Tinstall, SPIV = Installation time for the SPIV.
- RHLCV = Day rate for the heavy-lift cargo vessel.
- Tload, HLCV = Loading time for the HLCV.
- *Tinstall, HLCV* = Installation time for the HLCV

Parameters used for platforms installation, source [82]

		Fixed	Floating		
			Trans.	Ancho.	
Vessel		SPIV	HLCV	AHV	
Capacity	VC	1	1	3	(u/lift)
Speed	v	18.5	22.5	18.5	(km/h)
Load. time	t_{load}	24	10	30	(h/lift)
Inst. time	t_{inst}	96	–	90	(h/u)
Dayrate	DR	200	40	40	(k€/d)

For sand island installation, sand needs to be loaded, transported, and unloaded at the farm site using self-unloading bulk vessels (SUBVs). The installation costs for sand islands, denoted as $ICSI$, are estimated using Eq. (23), with input parameters summarized in Table 14.

$$IC_{SI} = \left(\frac{V_{SI}}{VC_{SUBV}} \cdot \frac{2 \cdot DP_{WF}}{v_{SUBV}} + \frac{V_{SI}}{BR_{load}} + \frac{V_{SI}}{BR_{unload}}\right) \cdot \frac{DR}{24} \quad (23)$$

Parameters of vessels for sand island construction, source [82]

		Sand island	
Vessel		SUBV	
Capacity	VC	20,000	(m^3/lift)
Speed	v	25	(km/h)
Load. rate	BR_{load}	2000	(m^3/h)
Unload. rate	BR_{unload}	6000	(m^3/h)
Dayrate	DR	15	(k€/d)

Pipes

Pipe installation costs are modeled by considering that Flex-lay vessels are required for infield pipelines and S-lay vessels for export pipelines. The pipe installation costs, denoted as IC_P, are calculated according to Eq. (24), with the corresponding inputs listed in Table 15**.**

$$IC_P = \frac{L_{EP}}{LR} \cdot DR \tag{24}$$

		Pipeline		
		IA	Exp.	
Vessel		Flex	S-Lay	
Lay. rate	LR	7.0	4.0	(km/d)
Dayrate	DR	400	700	(k€/d)

OPEX

Operational and maintenance (O&M) costs are mainly influenced by the requirement for spare parts and escalate with the distance from the port, as vessels need to travel to the wind farm. These costs are comprised of two key components: material costs MCMC (€), which involve the replacement of equipment parts, and logistics costs LCLC (€). Additionally, energy losses during conversion and transport can be factored into the operating costs.

Repair costs

The repair costs for the various components of the hydrogen production chain, expressed as a percentage of the equipment costs, are presented below:

Maintenance costs as a share of equipment costs, source [83] [82]

	MC (% EC)
Wind turbines	2.5%
Sand island	1.5%
HVDC/HVAC substation	1.5%/3%
Electrolyzers	2%/4%
Power converters	1%/2%
Desalinator	3%
Power cables	0.2%
Pipelines	2%

Logistics costs

Logistics costs correspond to the expense of reaching the turbines for maintenance using specialized vessels. Minor repairs are conducted with light vessels. An onshore-based strategy utilizing crew transfer vessels (CTVs) can be employed if the farm is located near the coast. A mother ship-based strategy using service offshore vessels (SOVs) is more suitable for large parks or those far from the coast, as it avoids very long trips and enhances turbine availability.

The considered maintenance strategy ensures a wind farm availability of 94%, as observed in many existing cases [89]. Logistics costs are modeled to increase linearly up to 150 km from the shore, beyond which a service offshore vessel (SOV) strategy stabilizes costs, as shown in Fig. 6. Major repairs require more extensive intervention; maintenance of fixed wind turbines is performed in situ using a jack-up vessel (JUV), while floating wind turbines must be towed to a port or assembly site for repair. The annual logistics cost for major repairs, denoted as L_oC_{maj}, is calculated using Eq. (25), with the corresponding parameters shown in Table 17.

$$LoCmaj = NWT \cdot \lambda maj \cdot (\frac{2n \cdot DP_{WF}}{v} + t_{rep}) \cdot \frac{DR}{24} \quad (25)$$

Where λmaj is the failure rate, assumed to be 0.08 failures per year [82], and n is the number of round trips required for major maintenance.

Parameters for vessels used in major wind turbine repairs, source [82]

		Fixed	Floating	
Vessel		JUV	Tug	–
Speed	v	18.5	7.5	(km/h)
Repair time	t_{rep}	50	50	(h)
Dayrate	DR	150	2.5	(k€/d)
Roundtrips	n	1	2	–

DECEX

The decommissioning operations are very similar to the installation processes. For simplicity, the cost structure for decommissioning is considered the same as for installation, but the dismantling times are significantly lower.

7. Electrolyzer Sizing

The integration of offshore wind farms with hydrogen production through electrolysis represents a promising pathway towards a sustainable and decarbonized energy future. Offshore wind farms offer a reliable and abundant source of renewable energy, while electrolyzers convert this energy into hydrogen, a versatile and clean fuel. This chapter provides a comprehensive guide on how to size an offshore electrolyzer based on the capacity of an offshore wind farm, ensuring optimal utilization of the available energy and efficient hydrogen production.

Determining the Wind Farm Capacity

The first step in sizing an offshore electrolyzer is to determine the total power output capacity of the offshore wind farm, typically measured in megawatts (MW). This capacity, denoted as P_{WF}, represents the maximum power that the wind farm can generate under ideal conditions.

Calculating the Electrolyzer Size

The electrolyzer should be sized to match the wind farm's nominal power, taking into account the variability in wind energy production. A common practice is to size the electrolyzer to 90–95% of the wind farm's nominal power [57]. This sizing factor ensures that the electrolyzer can efficiently utilize the available energy without being overly large and costly. The electrolyzer size P_{EL} can be calculated using the following equation:

$$P_{EL} = P_{WF} \times f_{size} \tag{26}$$

where f_{size} is the sizing factor, typically ranging from 0.90 to 0.95 for offshore electrolyzers.

Estimating the Annual Energy Production

The annual energy production of the wind farm is taken from earlier WPs.

Determining the Electrolyzer Efficiency

The efficiency of the electrolyzer (η_EL) is a crucial parameter influencing overall hydrogen production. Instead of assuming a fixed efficiency, in this work we apply an **efficiency curve** obtained from literature and public datasets [90]. This curve accounts for the variation of efficiency with operating conditions, providing a more realistic representation than a single constant value.

Calculating the Annual Hydrogen Production

The annual hydrogen production H_{annual} can be calculated using the annual energy production and the electrolyzer efficiency. The energy content of hydrogen is typically around 33.33 kWh/kg [91]. The following equation can be used to determine the annual hydrogen production:

$$H_{annual} = \frac{Eannual \times \eta EL}{33.33} \qquad (28)$$

Sizing the Electrolyzer Based on Hydrogen Production Rate

To size the electrolyzer based on the desired hydrogen production rate, the electrolyzer's power input capacity must match the wind farm's energy output. The electrolyzer size P_{EL} can be calculated using the following equation:

$$P_{EL} = \frac{Hannual \times 33.33}{\eta EL \times 8760} \qquad (29)$$

8. Transportation Of Hydrogen

The levelized cost of transmission (LCOT) for hydrogen transmission from an offshore wind farm and electrolyzer is a critical metric for evaluating the economic feasibility of transporting hydrogen produced offshore to onshore facilities. LCOT takes into account the capital expenditure (CAPEX) for building the transmission infrastructure, such as pipelines or shipping vessels, as well as the operational expenditure (OPEX) associated with maintaining and operating this infrastructure over its lifetime. Factors influencing LCOT include the distance from the offshore site to the onshore destination, the capacity and efficiency of the transmission system, and any additional costs related to compression, storage, and potential losses during transport. By calculating LCOT, stakeholders can assess the overall cost-effectiveness of the hydrogen supply chain and make informed decisions about the viability of offshore hydrogen production and transmission projects.

8.1 Hydrogen Transportation by Ship

With the growing global demand for green hydrogen and ammonia produced from renewable electricity, the need for bulk transportation of these resources from production sites to high-demand consumption areas is set to rise. While repurposing existing infrastructure may offer a cost-effective and technically viable solution, the anticipated growth in supply and demand will inevitably require new developments. According to predictions by the International Renewable Energy Agency (IRENA), hydrogen is poised to become a globally traded commodity, with approximately one-third of its production being traded across borders by 2050 [92]. This projected volume of cross-border trading exceeds the current levels of natural gas trading [92] will require significant offshore transmission development. The "Future of Hydrogen" report [93] from the International Energy Agency (IEA) evaluates various offshore hydrogen transmission technologies based on their effectiveness across different transmission distances.

The electricity powers an electrolyzer to produce hydrogen, which is then liquefied and transported offshore via hydrogen tankers, as shown in Figure

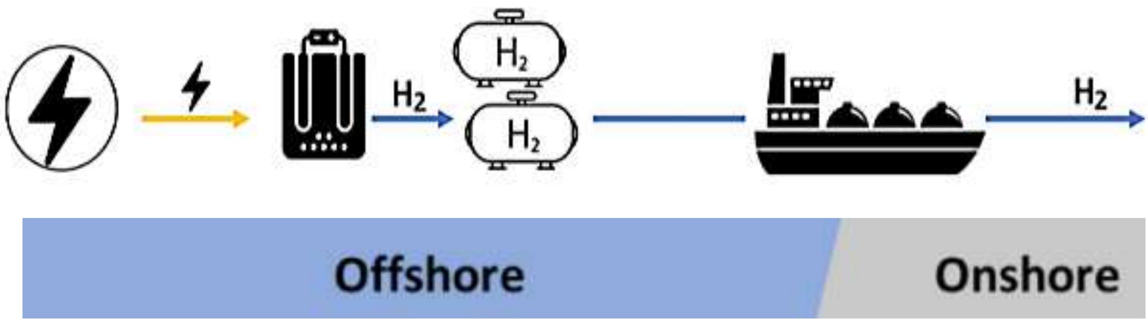

Figure 24 Offshore Hydrogen transportation through ship

Initially, one-time or spot charter vessels could be utilized for hydrogen transportation while production and demand centers are still in development. In general, shipping liquid hydrogen is anticipated to be a more cost-effective option for longer distances compared to pipelines [94].

Transporting liquefied hydrogen is a costly and energy-intensive process due to the need for specialized cryogenic equipment. The design and manufacturing of ships for this purpose are intricate, and currently, only one liquid hydrogen tanker exists, the SUISO Frontier. This vessel was developed in Japan as a demonstration project [95]. Over the next decade, the production of tankers is anticipated to expand significantly, with advancements expected to include increased capacity to match the average size of LNG tankers and the capability to utilize hydrogen boil-off as fuel.

The cost for LH2 tanker transmission is given by Eq. (30) and is composed of three main elements: liquefaction costs (Cliq); storage costs (Csto); and shipping costs (Cship). Only liquid hydrogen (LH2) will be considered for ship transport.

$$CLH2 = Cliq + Csto + Cship \qquad (30)$$

The capital expenditure for hydrogen liquefiers (CAPEXliq) in € was determined using Eq. (31), where Nliq represents the number of liquefiers (with each liquefier capable of supplying up to 200 ton/day), Cliq is the liquefier design capacity in ton H2/day, and I is the overall chemical engineering plant cost index (with I =1.16 for the cost estimates to be presented in USD). The liquefaction plant costs were estimated based on [96], assuming that all hydrogen produced by the electrolyzer plant is liquefied and that the liquefaction plant operates at full capacity continuously.

(Costs converted to present value and to EUR from USD using a conversion rate 1 USD =0.90 EUR.)

$$CAPEXliq = 5{,}600{,}000. Nliq. Cliq\ 0.8. I \qquad (31)$$

The storage capacity of the LH2 tanker, as described by Eq. (32), is determined by several factors, including the tanker capacity (Tcap), the transmission distance (d), the number of vessels in operation (nship), the travel speed of the vessel (Vship), and the production rate of the electrolyzer plant (Prate). The equation assumes that the time between storage unloading is zero. The resulting storage capacity is represented by Scap.

$$S\,cap / 2 = T\,cap = (P\,rate .2. d)/((n\,ship . V\,ship)) \qquad (32)$$

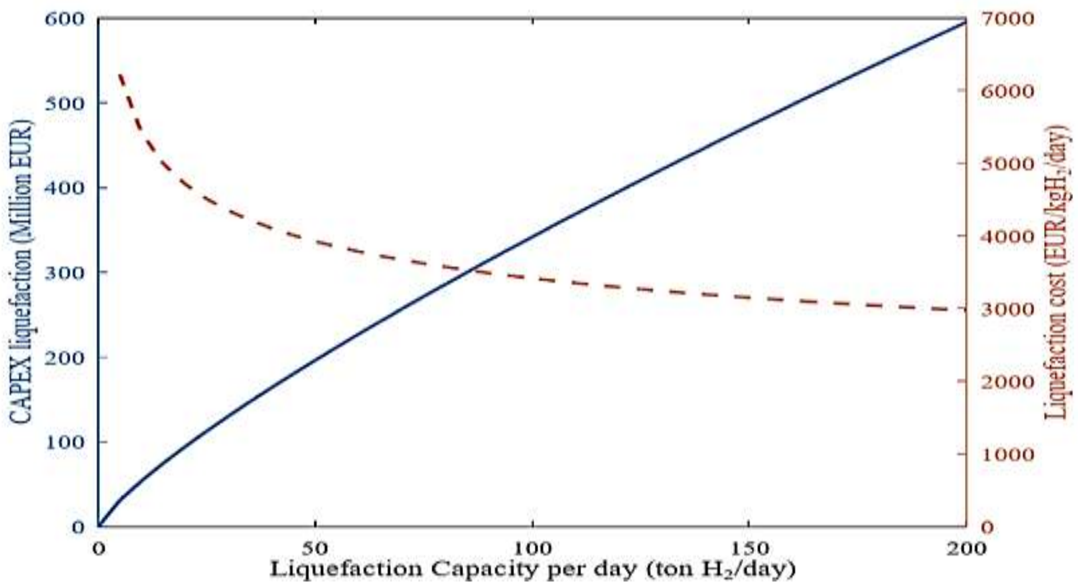

Cost and CAPEX for the installed hydrogen liquefaction plant adjusted for net present value (2020) [96]

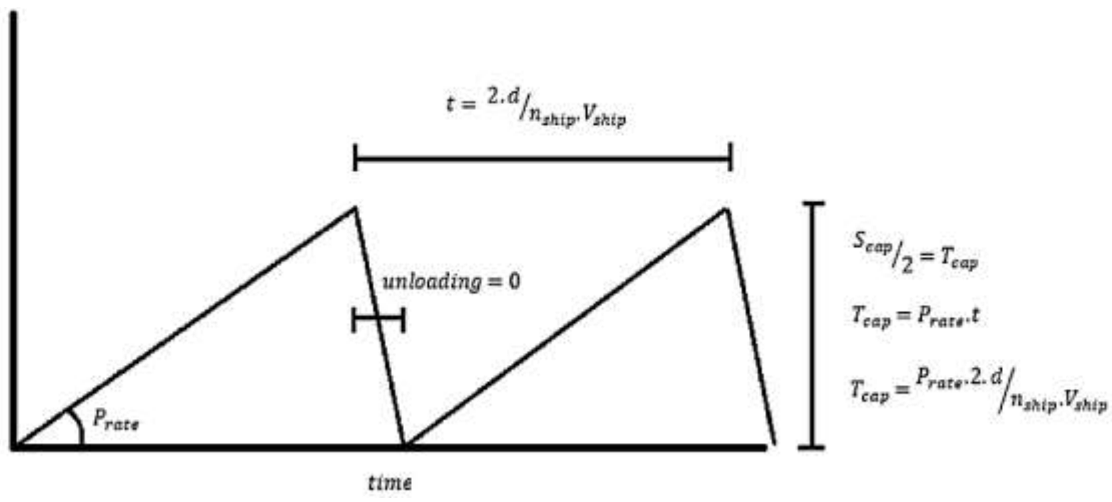

variation of hydrogen storage over time between unloadings

Freight prices (charter rates):

It is anticipated that the market development for LH2 will follow a similar trajectory to that of LNG tankers in the past, until a large-scale green hydrogen market emerges. At present, the charter rates of LNG tankers are determined by the open market, making it challenging to forecast the rates due to fluctuations based on supply and demand. In the past, before the open market, charter rates for LNG tankers were calculated based on shipbuilding prices and ship capacity using net cash flow and discounting methodologies [97].

To begin with, a correlation must be established between the shipbuilding prices and ship capacity. As of 2023, only one LH2 tanker has been constructed, and its cost data is not publicly accessible. As LH2 tankers are still in the early stages of development and share technical similarities with LNG tankers, it is reasonable to assume that the relationship between shipbuilding price and ship capacity used for LNG tankers will also apply to LH2 tankers. The shipbuilding price of a new vessel (PriceA) can be estimated using Eq. (33), which takes into account the shipbuilding price of a benchmark vessel (PriceB), the ship capacity of the new vessel (CapA), and the ship capacity of the benchmark vessel (CapB). The equation assumes that the relationship between shipbuilding price and ship capacity for LNG tankers is also applicable for LH2 tankers.

$$PriceA = \left[PriceB \left(\frac{CapA}{CapB} \right) \right]^{0.623} \quad (33)$$

Using the benchmark LH2 tanker information in Table 1 (data taken from [93]), the shipbuilding cost as a function of ship capacity for LH2 tankers is presented in

Table 10 benchmark LH2 tanker information

Parameter	Units	Value
Capacity / Ship	Ton H_2	11000
CAPEX	Million EUR	371
Ship speed	Km/h	30
Fuel consumption	Kg/km	12.4
Annual OPEX	% of CAPEX	4
Boil-off rate	% per day	0.2%

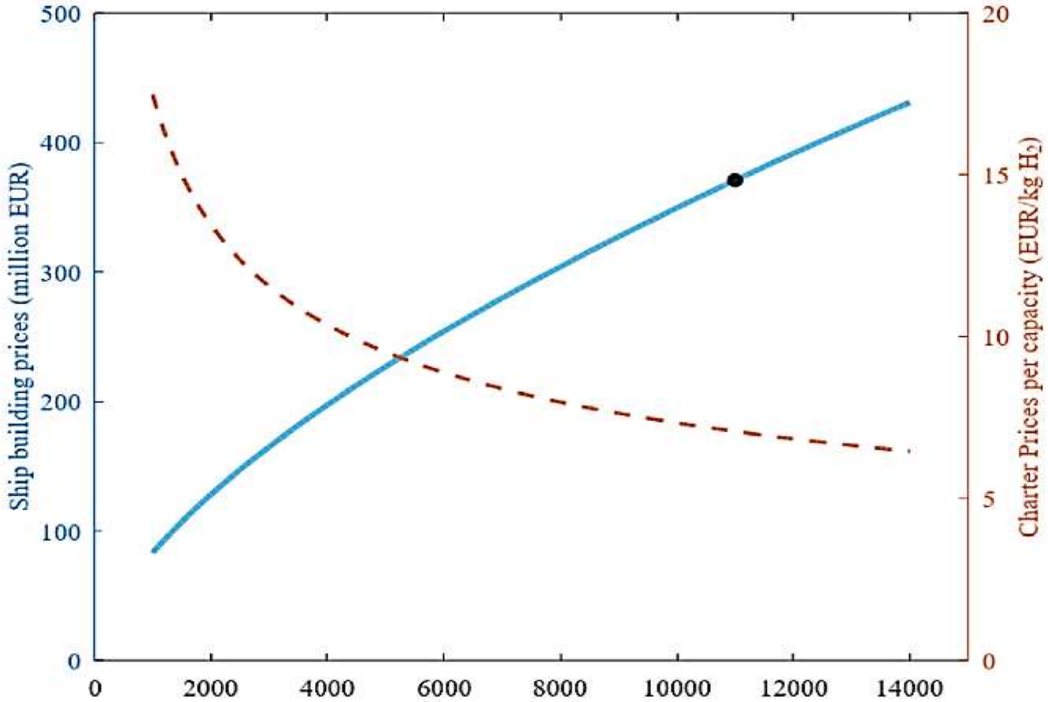

Figure 25. Estimation of ship building costs as a function of ship capacity for LH2 tankers where the highlighted point represents the benchmark LH2 tanker

LH2 tankers with capacities ranging from 1250 m3 (equivalent to the first LH2 tanker built, SUISO Frontier) to 200,000 m3 (equivalent to approximately 100 tons to 14,000 tons of H2, considering the density of LH2 as 70.8 kg/m3) were taken into account. The shipbuilding costs were determined as a function of the LH2 tanker capacity, and subsequently, the charter costs (Chartercost) were estimated using the internal rate of return method. [97]. The internal rate of return method was utilized to estimate the rate that equates the Net Present Value (NPV) of cash flows in investment analysis. In this case, Chartercost was the unknown value, and the internal rate of return (irr) was set at 10%. Several freight prices were tested using Eq. (34) until the NPV of cash flow equaled zero. OPEXship was calculated as a percentage of the CAPEXship given in EUR, while Charter cost represented the freight given in EUR/year. The lifetime (L) was set to start at year 5 to account for the design/construction period, and irr represented the aimed internal rate of return.

$$NPV = CAPEXship + \sum L\_(l = 5) \ \ (OPEXship\ Chartercost)/((1 + irr)l) \ \ = 0 \qquad (34)$$

The CAPEX of the LH2 tanker is determined by combining the CAPEX of the liquefaction and storage plants, as shown in Eq. (35). On the other hand, the OPEX of the LH2 tanker consists of components from the liquefaction, storage, and ship transport, as presented in Eq. (36).

$$CAPEXLH2tanker = CAPEXliq + CAPEXsto \qquad (35)$$

$$OPEXLH2tanker = OPEXliq + OPEXsto + OPEXship + Chartercost \qquad (36)$$

The offshore transmission of hydrogen using LH2 tankers can result in reduced hydrogen delivery due to the hydrogen boil-off phenomenon present in the storage system and LH2 tanker. The annual hydrogen boil-off for storage (Boffsto) and LH2 tanker (Boffship) are calculated as a percentage of their respective capacities using Eq. (8) and Eq. (9), where Boffrate is the boil-off rate given as %/day, Scap is the storage capacity given in kgH2, Tcap is the LH2 tanker capacity given in kgH2, and both are multiplied by the number of operating days in a year (Toper), which is assumed to be 350 days. (drate is the discount rate)

$$Boffsto = Boffrate.Scap.Toper \qquad (37)$$

$$Boffship = Boffrate.Tcap.Toper \qquad (38)$$

$$LCOT\ LH2\ tanker = \frac{CAPEX\ LH2\ tanker + \sum L\ l{=}0 \frac{OPEX\ LH2\ tanker}{(1+drate)l}}{\sum L\ l{=}0\ \frac{ProdH2 - Boffsto - Boffship}{(1+drate)l}} \qquad (39)$$

while pipelines are the cheapest offshore transmission technology for short distances (<c.

200 km) at any electrolyser capacity, LH2 tankers become more economically attractive than pipelines once a certain electrolyser capacity and offshore transmission distance is reached. This highlights the importance of these two parameters in analysing the available options for bulk offshore hydrogen transmission.

Table 11 LH2 tanker assumptions and parameters used

Parameters	Units	Value
Max. liquefaction capacity per unit	kg/day	200
$OPEX_{liq}$	% of $CAPEX_{liq}$	4
Storage capacity	x times the LH2 tanker capacity	2
Storage cost	EUR/kgH2	85
$OPEX_{sto}$	% of CAPEXsto	4
$B_{off,sto}$	%	0.1
LH_2 tanker capacity	kgH 2	Function of Ecap and d
Construction period	Years	5
Internal rate of return	%	15
Charter rate	EUR/day	Function of Ecap and d
OPEXship	% of CAPEXship	4
Boff,ship	%	0.2
Nship	Unitless	Function of Ecap and d
Vship	Km/h	30
Lifetimeship	Years	25

Offshore production of compressed hydrogen is currently the most economically viable option for projects commencing in 2025. However, the feasibility of this scenario is highly dependent on the storage period and the distance between the offshore wind farm and the shore. As we look towards 2050, alternative hydrogen storage and transport scenarios, such as liquefied hydrogen and methylcyclohexane, may become more cost-effective, potentially lowering the levelized cost of hydrogen to approximately £2 per kilogram or less [98]. The following dataset is used for the techno-economic analysis:

Table 12 data used for the techno-economic analysis

Offshore wind farm [99]	**2025**	**2030**	**2050**
Capacity factor (%)	47.5	52	55
Curtailed energy (% total)	6.8	9	18.2
Electrolyser [100]			
Efficiency (%, LHV)	64	65	70.5
Operating lifetime (h)	67,500	75,000	125,000
CAPEX (£/kW)	748.25	511	328.5
O&M (% CAPEX/y)	1.5	1.5	1.5
Replacement (% CAPEX)	14.0	12.0	12.0
Max. output pressure (MPa)	6.3	7.0	10.0
Stand-by battery (£/kW)	41.9	35.5	19.3
Desalination system and freshwater [101]			
$CAPEX_{Desalination}$ (£/(m³/d))	1240.6	1081.9	585.8
$Electricity_{Desalination}$ (kWh/m³)	3.5	3.5	3.5
Operating $lifetime_{Desalination}$ (y)	30	30	30
Freshwater (£/m³)	1.38	1.38	1.38
Hydrogen compressor [102] [103]			
O&M (% CAPEX/y)	3	3	3
Operating lifetime (y)	10	10	10
Replacement (% CAPEX)	100	100	100
Liquefaction unit [104] [105]			
$CAPEX_{Liquefaction}$ (£/(kg/h))	35,971	28,713	20,926
$Electricity_{Liquefaction}$ (kWh/kg_{H2})	10.3	7.6	5.8
Liquid hydrogen yield (%)	75	100	100
$O\&M_{Liquefaction}$ (% CAPEX/y)	4	4	4
Operating $lifetime_{Liquefaction}$ (y)	20	20	20
Storage [106] [107] [104] [105]			
CAPEXComp, storage (£/kgH2)	391.1	373.7	351.1
O&MComp, storage (% CAPEX/y)	2	2	2
Operating lifetimeComp, storage (y)	30	30	30
CAPEXLiq, storage (£/kgH2)	53.3	33.5	23.3

O&MLiq, storage (% CAPEX/y)	2	2	2
Operating lifetimeLiq, storage (y)	20	20	20
Liquid ship tanker [106] [104]			
CAPEX Liquid hydrogen ship tanker (£/m3)	1804.3	1575.7	1273.8
O&M (% CAPEX)	4	4	4
Operating lifetime (y)	25	25	25
CAPEX Ammonia ship tanker (£/m3)	911.3	873.6	807.6
O&M (% CAPEX)	4	4	4
Operating lifetime (y)	25	25	25
CAPEXMCH ship tanker (£/m3)	489.2	429.1	354.9
O&M (% CAPEX)	4	4	4
Operating lifetime (y)	25	25	25
Electricity price [99]			
Offshore electricity (£/kWh)	0.08	0.051	0.037

The amount of hydrogen that could be produced using electricity supplied by the wind farm on an hourly basis, W H2, theoretical (kg H2), was estimated using Equation:

$$WH2\ theoretical(t) = \frac{Pfarm\ (t)}{\frac{Eelec}{nconv} + Eaux} \quad (40)$$

Where nconv is the conversion efficiency, Eelec is the electricity consumed in producing 1 kg of hydrogen (MWh/kgH2), and Eaux is the electricity consumed by auxiliary components (i.e. desalination, hydrogen compression, hydrogen liquefaction, etc.). PEM electrolyzers are considered as they offer high flexibility with substantial variations in operational parameters, making them well-suited for intermittent inputs such as the power generated by offshore wind farms [108].

To account for water losses, a water consumption rate of 15 kg per kg of hydrogen produced by the electrolyzer system, represented as QH2O, was considered. The daily volume of water required by the electrolyzer plant, VH2O (m3/d), can be calculated using the following equation [83]:

$$V_{H2O} = \sum i = 1 \;\; 24 \;\; WH2, prod, i(t).\ Q\ h20\ .\ rho\ \ H2O \quad (41)$$

Where rho H2O is density of water measured in kilograms per cubic meter (kg/m^3). In offshore hydrogen production, the water needed for the electrolyzer is provided by a desalination unit. In this study, reverse osmosis (RO) desalination was considered. The daily energy consumption of the desalination unit, E_des (kWh/d), was calculated according to the following equation :

$$Edes = \ VH2O\ e\ des \ \ (42)$$

where edes is the specific energy consumption of the desalination unit, assumed to be 3.5 kWh per m3 of desalinated water [109]. The CAPEX of the desalination unit was estimated based on the daily volume of water required by the electrolyzer plant, in line with [101]. The O&M costs of the RO desalination unit (with a capacity larger than 100,000 m3/d) included labor, maintenance, chemical, and membrane exchange [110]. The replacement costs were calculated considering a 30-year lifetime of the desalination unit [101].

Freshwater could be used as an alternative to seawater. A constant rate of £1.38/m3 was assumed for the cost per cubic meter of freshwater, represented as C_freshwater (£/m3). A 60% discount for large consumers was considered.

$$CAPEXfreshwater = \ Cfreshwater.(\ 1 - \ 0.6)\ \sum i = 1\ 365\ VH2O \quad (43)$$

Compressor

The CAPEX of the hydrogen compressor was estimated based on the power required at the shaft to pressurize the incoming hydrogen, as shown in the following equation:

$$P = \ Q\ \frac{ZTR}{Mn}.\ \ \frac{Ny}{y-1}\ \left(\frac{Poutlet^{\frac{y-1}{Ny}}}{Pinlet} - \ 1\right) \qquad (44)$$

where P is the required shaft power for a compressor with N stages, Pinlet and Poutlet represent the inlet and outlet pressure (MPa), respectively, Q is the hydrogen flow rate (kg/s), T is the inlet temperature (considered as 298.15 K, corresponding to the outlet pressure of the electrolysis plant), Z is the compressibility factor, M is the molecular mass of hydrogen (g/mol), g is the ratio of the specific heat (1.4), R is the universal ideal gas constant (8.314 J/mol·K), and n is the efficiency of the compressor (assumed as 88% in this study). PEM electrolyzers produce high-purity hydrogen at pressures ranging between 2 and 6 MPa, resulting in the need to compress the produced hydrogen up to 10-20 MPa at the pipeline inlet for offshore application, depending on the required flow rate in the pipeline. Centrifugal compressors, which are commonly used with natural gas pipelines, were considered in this study.

Liquefaction Unit

The specific CAPEX (£/(kg/h)) of liquefaction units was obtained from Refs. [106] [111], refer table 12, considering a decline in CAPEX in the long term. The energy required to liquefy 1 kg of hydrogen varies with the capacity of the liquefaction system, ranging between 8 and 12 kWh for liquefaction systems with a daily capacity of 200 tonnes of hydrogen or less, respectively.

Storage

The CAPEX of compressed gas hydrogen storage was calculated based on the amount of hydrogen produced per day, MH2 (kg/day), and the storage capability, tStorage (days of storage required), which indicates the size of the storage tank. The equation used to calculate the CAPEX of compressed gas hydrogen storage is shown below:

$$CAPEXStorage = CAPEXSpec; storage \,.\, MH2 \,.\, tStorage \qquad (45)$$

Where the specific cost of the compressed hydrogen storage tanks, CAPEXSpec, storage (£/kg), was collected from refs [106] [111]. The compressed hydrogen storage tanks were assumed to have a lifetime of 30 years and an O&M cost of 2% of the CAPEX per year, according to [111] . However, storing a large volume of compressed hydrogen in tanks on offshore platforms could present an additional issue due to the space occupied by the tanks. For example, tanks required for storing the hydrogen produced by a 1 GW electrolyzer for 24 hours would take up a minimum space of 56,000 m3 [44]. Another option for storing hydrogen, we can use specially insulated cryogenic containers to store it in liquid form, which has a much higher density. These tanks are designed with a double wall and reflective heat shields to minimize heat transfer and keep the hydrogen cold. The shape of the tanks is usually spherical to minimize the surface area exposed to the surrounding environment. However, liquid hydrogen storage is not without its challenges. One of the main issues is evaporation, also known as boil-off, which can result in significant losses over time. The rate of boil-off depends on the size and insulation of the tank. For example, a 50 m3 tank may lose 0.4% of its hydrogen per day, while a larger 20,000 m3 tank may only lose 0.06% [112]. To minimize boil-off, we can use active and passive approaches such as accelerating the conversion of ortho- to para-hydrogen during liquefaction, reducing the surface-to-volume ratio of the tank, and improving insulation and cooling techniques.

Shipping

Using ships to transport liquid hydrogen, ammonia, and MCH can be a cost-effective option for long distances, such as for journeys between continents (longer than 1800km) [93] . This makes liquid hydrogen ship tankers a good choice for these types of trips. On the other hand, traditional ship tankers that are used to transport oil and chemicals can be used to distribute ammonia and MCH. However, one downside of using ship tankers to transport these substances is that they will return to the offshore platform empty, without any cargo. This can be a disadvantage unless another use for the ship can be found.

The specific CAPEX (£/m3) for liquid hydrogen, ammonia, and MCH ship tankers were gathered from references [111] [93] [104], table 12. To calculate and compare the total CAPEX for distributing liquid hydrogen, ammonia, and MCH using ship tankers, it was assumed that the capacity of the ship tankers was 160,000 m3, based on current and future ship tanker capacities [113].

The ship tankers were assumed to travel at a speed of 30 km/h, and the fuel consumption data for different ship tankers was obtained from Ref. [93]. The propulsion of the ship tankers would be powered by prime movers that run on heavy fuel oil (HFO) at a cost of

£0.0142 per MJ [114]. It is important to note that liquid hydrogen would experience a loss of 0.2% per day, whereas there would be no loss for ammonia and MCH [111]. The lifetime and the O&M cost of liquid hydrogen, ammonia, and MCH tankers were assumed to be 20 years and 4% of the CAPEX of the tanker per year, respectively.

The following table shows LCOH2 (£/kgH2) estimated for the cases when 100% of the offshore wind electricity was used for hydrogen production offshore and LH2 transport by ship stored over different periods.

Storage Period				
Year	1 day	7 days	14 days	31 days
2025	8.84	8.97	9.13	9.5
2030	4.2	4.26	4.33	4.51
2050	2.78	2.82	2.88	3

8.2 HYDROGEN TRANSPORTATION BY PIPELINE

Transporting hydrogen via onshore pipelines is now well-established and standardized, with approximately 4,500 km of hydrogen pipelines currently in operation, primarily located in Europe and North America [115]. In contrast, there are currently no offshore hydrogen pipelines or established standards for their design.

The future challenge for developing these offshore hydrogen pipelines branches into two scenarios. The first involves utilizing **existing natural gas pipelines** for hydrogen transport to achieve economic savings. The second scenario involves constructing **new pipelines** specifically for hydrogen.

Before considering these scenarios, it is crucial to analyse the physical properties of hydrogen and compare them with those of natural gas:

Energy Content: Natural gases, typically composed of methane (CH_4), have an energy content ranging from 34 to 43 MJ/m³. In contrast, hydrogen has an energy content of approximately 12.7 MJ/m³. Therefore, to transport hydrogen within a pipeline, a larger volume of gas is required to achieve the same energy content.

Flammability: Hydrogen is more flammable compared to natural gases. At normal temperature and pressure, one cubic meter of hydrogen weighs 1/9th of one cubic meter of natural gas. This implies that, at the same pressure difference, the flow rate of hydrogen will be much higher.

Diffusion: Hydrogen is more diffusive through steel compared to natural gas, promoting embrittlement due to cyclic loads. This phenomenon can be mitigated through appropriate material selection and the use of suitable thicknesses. However, this limits the reuse of old pipelines originally used for natural gas transport.

Due to its low volumetric mass density, hydrogen needs to be initially compressed for economically viable transport. Gas compressors are an indispensable part of hydrogen transport.

Compression will occur at the inlet of the pipeline and at intermediate points along the pipeline itself, as there is a need to compensate for pressure losses that occur over long distances.

With PEM electrolyser, hydrogen is produced at pressures of **30 bar**.

NEW PIPELINES

The use of low-strength carbon steels for hydrogen pipelines is typical for both onshore and offshore applications, operating at room temperature. In contrast, austenitic stainless steels are more common in local gas distribution systems such as manifolds. However, these materials come with higher costs associated with their use.

For corrosion protection, both internal and external cathodic protection is employed to mitigate galvanic corrosion risks, essential for ensuring the pipeline's longevity and integrity.

The American Society of Mechanical Engineers (ASME) sets out specific requirements for hydrogen piping and pipelines in the ASME B31.12 standard, ensuring compliance and safety in design and operation.

Steel grades such as API 5L X42, X52, and X60 are commonly chosen for their reliability in safely transporting hydrogen at pressures up to 14 MPa.

These specifications and standards ensure that hydrogen transport pipelines are designed and constructed to handle the unique challenges and requirements associated with hydrogen gas, ensuring safety, reliability, and efficiency in its distribution and transmission.

Onshore pipelines are mainly utilised at 100 bar for long distance transport and at considerably lower levels if the distance is lower, offshore pipelines would need to operate, due to the higher distance, rather at pressure levels around 200 bar.

Furthermore, the European Hydrogen Backbone has assessed that converting old onshore natural gas pipelines into onshore hydrogen pipelines requires between 15% and 30% of the total cost of constructing a new hydrogen pipeline. [116]

However, the cost of offshore pipelines will critically depend on the number of interventions, inspections, and tests required for the purpose, including:

- **Cleaning and Drying (Pigging):** This process removes residual materials and ensures the pipeline is clean and dry.
- **Displacement Purging with Inert Nitrogen Gas:** This step eliminates gaseous and other impurities from the pipeline.
- **Pipeline Monitoring and Inspection:** Regular inspections are essential to detect and locate flaws, cracks, or leaks.
- **Replacement of Old Equipment:** Equipment such as valves that have been in operation for extended periods may need replacement.

Additionally, factors such as the lifespan of existing pipelines, their location, the materials used (which determine maximum supported pressures), and other significant considerations must be taken into account.

These factors collectively influence the cost and feasibility of converting or constructing hydrogen pipelines, both onshore and offshore, highlighting the complex and meticulous planning required for such infrastructure projects.

Offshore pipelines

The input data necessary for the design of an offshore pipeline can be grouped into data related to the installation environment and data related to the nature of the transported fluids:

ENVIRONMENTAL DATA - Geotechnical data, Meteorological and oceanographic data

FLUID DATA - Composition of fluids and water, PVT properties of fluids

THE INPUT DATA FOR THE DESIGN ARE:

1. Composition of fluids and water
2. P, V, T properties of fluids: the pipeline must be designed to ensure a fluid flow with a specific pressure drop!
3. Bathymetry and geotechnical data: The bathymetric survey is necessary to mechanically size the pipeline as the topography of the seabed determines the route and the inflection spans. The route must be chosen to avoid dangers and obstacles on the seabed.

   Note: It is preferable that the starting point of a pipeline is placed lower than the endpoint. This is because in the case of multiphase flows, slugs are easier to manage in "uphill" rather than "downhill" conduits.
4. Meteorological and oceanographic data

THE PIPELINE DESIGN INCLUDES THE DEFINITION OF:

1. Materials
2. Sizing (diameter and thickness)

CONSIDERATIONS INCLUDE:

1. Stress analysis
2. Hydrodynamic stability
3. Inflection spans
4. Thermal insulation
5. Corrosion coating and ballast

BATHYMETRY AND GEOTECHNICAL DATA

A bathymetric survey is necessary to mechanically size the pipeline because the path and the bending clearances depend on the seafloor topography. The route must be chosen to avoid dangers and obstacles on the seabed.

It is preferable for the starting point of a pipeline to be lower than the endpoint. This is because in the case of multiphase slug flows, they are easier to manage in pipelines that ascend rather than descend.

Bathymetry allows identifying segments where the clearance is greater than the maximum possible under unsupported conditions. The seafloor geometry determines the stresses on the pipeline and may require some segments to be placed within trenches and backfilled (which affects thermal exchange differently compared to other segments).

The geological and geotechnical nature of the seabed should be thoroughly investigated: there could be "stable" seabeds that are not subject to erosion or changes, and "loose" seabeds that change over time. For loose seabeds, pipelines are placed below the seabed level at a depth sufficient to exceed the thickness of the superficial covering layer.

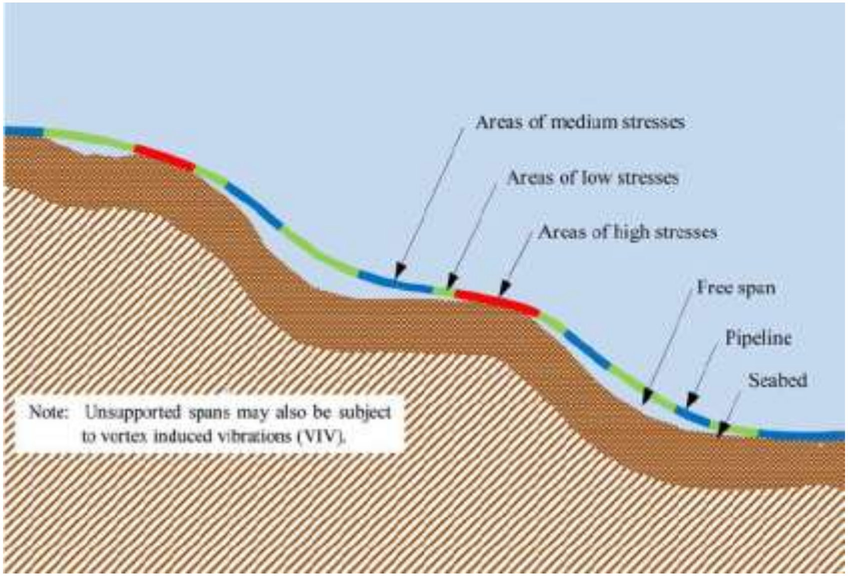

Figure 23: Schematic view of free spanning submarine pipeline and static stress along line [117]

Marine currents and waves are significant factors during both installation and operational phases. Typically considered are waves with return periods of 1 year, 5 years, 10 years, and 100 years, concerning wave height, direction, and velocity, in addition to tidal conditions.

INSTALLATION METHODS

The construction operations of an offshore pipeline are quite complex and rely on different methods:

- S-LAY
- J-LAY
- REEL BARGE
- TOW-IN METHODS

ALL INSTALLATION METHODS REQUIRE SPECIFIC ATTENTION TO:

- External corrosion

- Protection during installation
- Control of stresses and deformations during installation

PIPE PROCUREMENT AND TRANSPORTATION

The pipe laying operations are conducted using a dedicated launch vessel and support vessels that supply it with pipes. The pipes are supplied in single or double lengths of 20 or 40 ft. There are also ships for transporting 80 ft bars that are pre-insulated or pre-coated.

A crane transfers the pipes onto the launch vessel, which has a rack for the automatic transfer of pipes to the welding line located in the hold for S-lay operations and on the deck for J-lay operations.

The launch vessel contains a line that typically has 5 to 12 stations for welding the pipes, inspecting the welds, and coating the joints (for corrosion protection or for ballasting purposes). The number of stations depends on the size of the pipe. Inside the vessel, the bars are butt-welded, and at the welding stations, the insulation/coating in cement is restored.

NOTES ON LAYING VESSELS

The hulls of pipelay vessels can have various layouts. Some have an axial welding line, while others have one or more lateral lines. Vessels with a centered line utilize onboard space less efficiently than those with lateral layouts, but in the latter case, there are greater stresses due to roll and pitch.

Lateral lines require duplication of equipment for pipe handling but are more suitable for launching in rough sea conditions.

Typically, when multiple parallel pipelines need to be launched, one pipeline is launched at a time. For launching two parallel lines of small diameter alongside one large-diameter line, temporary welding lines can be installed on the pipelay vessel.

The launch vessel is assisted by support ships and divers (for shallow waters) or remotely operated submarines for inspecting the launched pipe.

S-LAY

The method is suitable for **shallow to deep seabeds**. Operations begin by placing an anchor on the seabed, which will be connected to the first launched pipe.

The series of welded pipes exits the ship as it advances. The stinger supports the pipes in the initial phase and guides them to submerge, containing flexural stresses.

The pipes touch the seabed, forming an "S" shape, from which the method derives its name.

Controls and devices are necessary to prevent pipe buckling.

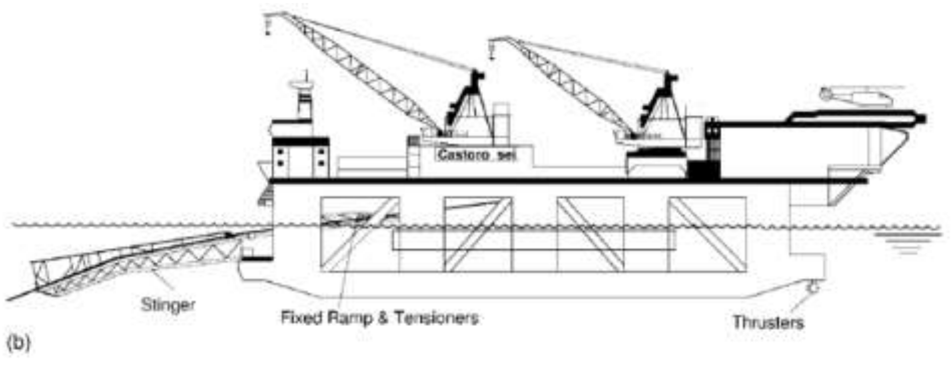

Figure 24 : S-lay vessel [118]

The first stingers for shallow waters were straight, but now they are curved or have differently curved sections for use in deep waters. The stinger is hinged to the hull.

Onboard, there are jacks that balance the tensile force of the pipe.

S-LAY STRESSES

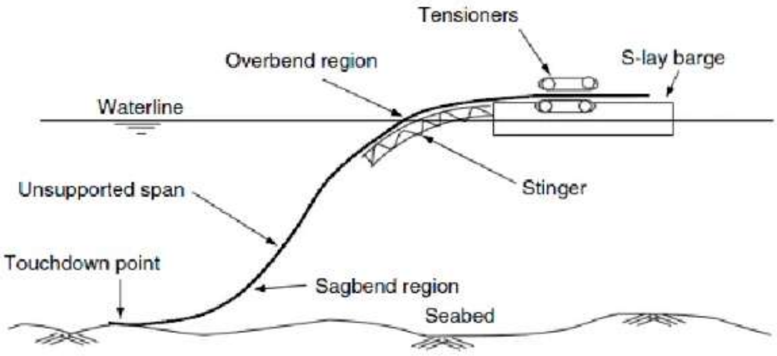

Figure 25 : S-lay vessel bending region [118]

In the overbend area, the curvature of the pipe is controlled by the support structure (STINGER). Generally, the curvature of the stinger is such as not to exceed 85% of the minimum yield strength.

NOTES ON PIPE COATING

In many pipelines, it is necessary to increase the weight of the pipe to counteract hydrodynamic forces on the seabed and to thermally insulate the pipe (see flow assurance). This is achieved with substantial thicknesses of cement that increase the stiffness of the pipe.

When the pipe-cement assembly bends during laying, both steel and cement work in the compressed zone, whereas only steel needs to be considered in the tensile zone because the strength of cement is negligible. The presence of cement increases the stress in the steel in the tensile zone and decreases it in the compressed zone, resulting in a neutral axis of the system that does not pass through the center of the section.

At the butt joint between two pipes, the pipe is bare except for an anti-corrosion coating and any fresh cement, which does not contribute significantly as it is fluid. This causes a more pronounced curvature at the joints and increases stresses specifically at the joint.

Figure 26 : Pipeline coating

J-LAY

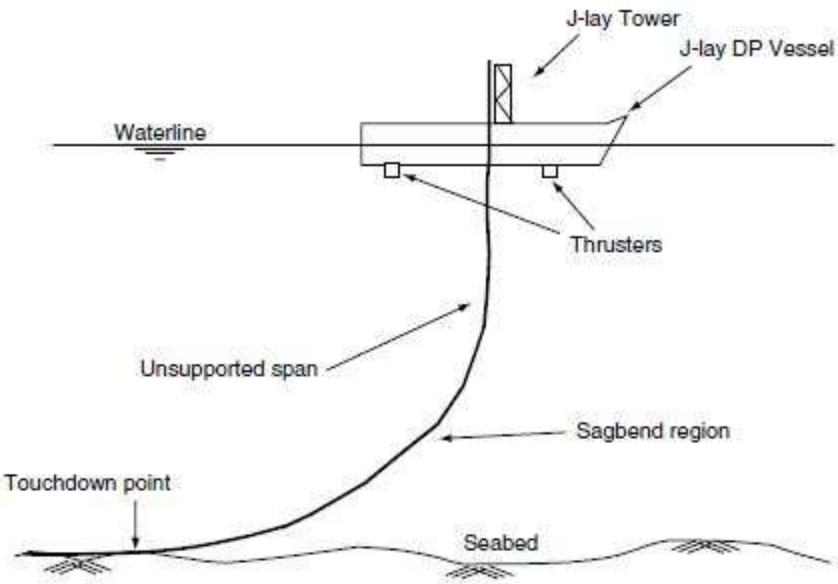

Figure 27 : J-lay vessel [119]

The method is used for **deep waters**.

With J-lay, the pipes are immersed nearly vertically until they touch the seabed. The series of pipes takes on the "J" shape that gives the procedure its name.

The ship has a relatively tall laying tower that allows the use of pre-welded pipe sections up to 240 ft long.

REEL BARGE METHOD

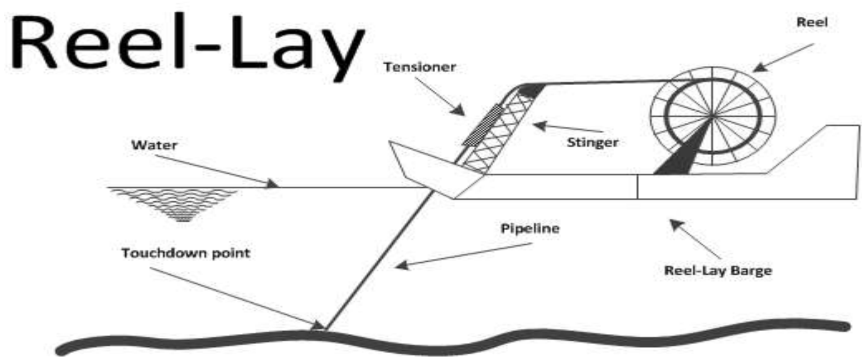

Figure 28 : Reel-lay vessel [120]

The pipe is welded onshore, with welds inspected and then coated. During laying, the reel is unwound.

The reels are loaded onto laying vessels with either horizontal or vertical axes. Reels with horizontal axes generally deploy pipes using S-lay, while reels with vertical axes almost always deploy pipes using J-lay (although they could also use S-lay).

The significant curvatures that the pipe undergoes make it impossible to apply cement coating. To provide stability to the pipeline, thicker steel thicknesses are used.

TOW METHODS

Note: In all cases, pre-assembled pipes on land are towed out to sea with tugboats.

There are four possible variations:

SURFACE TOW

The pipeline is towed on the sea surface using floats.

Often, a head tugboat and a tail tugboat are used to control the trajectory of the pipeline, keeping it under slight tension.

Upon arrival at the laying area, the floats are either removed or flooded, allowing the pipeline to settle on the seabed.

With the below-surface methods, the pipeline is kept buoyant well below the influence of waves. Buoyancy units connected to the pipes with flexible systems are used to limit the transfer of surface actions to the pipeline.

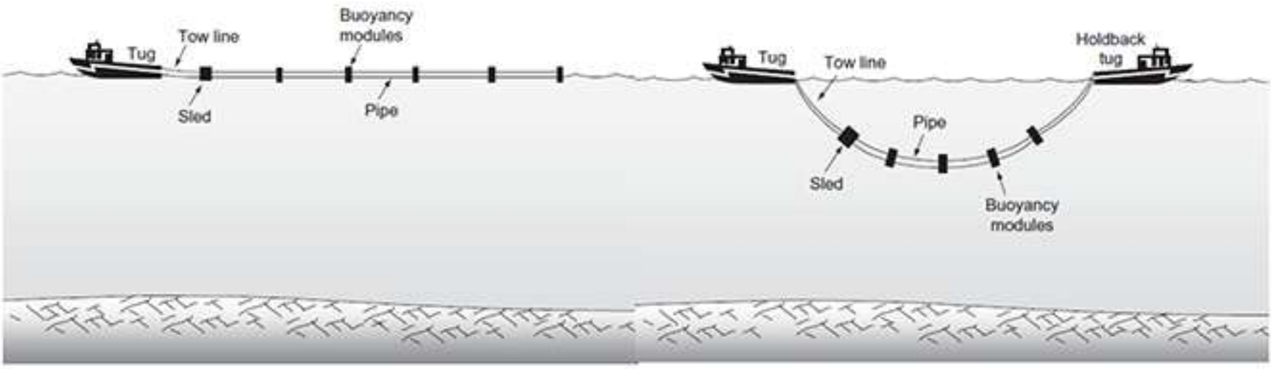

Figure 29 : Surface tow and mid depth tow [121]

MID DEPTH TOW

It requires a smaller number of floats. The pipeline rests on the seabed when the tension is released.

OFF BOTTOM TOW

The off-bottom method is a variation of the below-surface method achieved by adding floats and weighted chains. The chains also provide stability against lateral currents.

The depth at which the pipeline string is transported is predetermined based on the seafloor morphology. It can be adjusted by increasing the pulling force exerted by the head and tail tugboats.

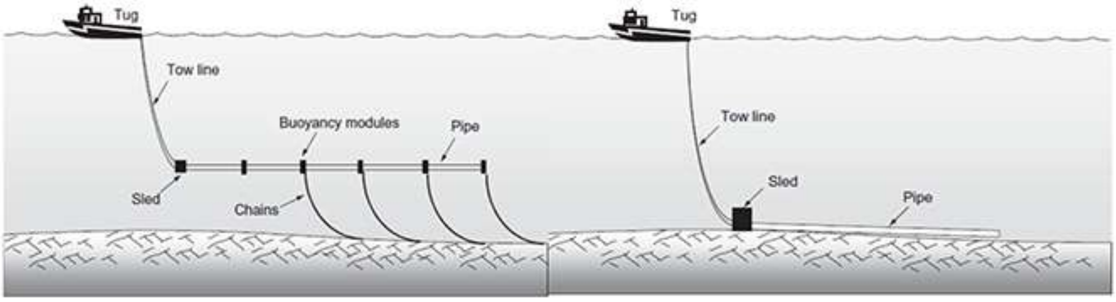

Figure 30 : Off bottom tow [121]

BOTTOM TOW

The bottom tow method is significantly different from the previous ones because it involves dragging the pipeline along the seafloor, thus keeping it in direct contact with it. This means that, unlike other techniques, the transportation route is crucial even during the design phase.

It can only be used in shallow waters with sandy and regular seabeds.

OFFSHORE MATERIALS

The design of a pipeline involves the choice of material, diameter, and thickness. The most commonly used standards are **ANSI B32.8**, Z187 (Canada), DNV (Norway), and IP6 (United Kingdom).

MOST COMMONLY USED MATERIALS: For high pressures and/or deep waters, with diameters less than 30'':

- X-60 (414 MPa)
- X-65 (448 MPa)

For low pressures and/or shallow waters, with large diameters (to reduce investment costs):

- X-42
- X-52

- X-56

In any case, the choice of material must be made with specific studies!

NOTES ON THE DESIGN PROCEDURE

Thickness calculation is done considering either **internal pressure** or **external hydrostatic pressure**. Longitudinal stresses and resultant forces are limited by various standards and must be evaluated considering both installation and operational phases. Generally, this analysis is conducted retrospectively and is not typically used to determine thickness.

Greater thicknesses can provide more stability compared to other ballasting methods (such as heavy coatings), although they are not cost-effective (except for deepwater installations where the use of cement coatings may be incompatible with J-lay methods).

DESIGN PROCEDURE

1. CALCULATE THE MINIMUM THICKNESS FOR INTERNAL PRESSURE (tPI)
2. CALCULATE THE MINIMUM THICKNESS FOR EXTERNAL PRESSURE (tPE)
3. ADD THE CORROSION ALLOWANCE c TO THE GREATER OF THE TWO PREVIOUS THICKNESSES (t = max($t(PI)$, $t(PE)$) + c)
4. IDENTIFY THE CLOSEST GREATER NOMINAL THICKNESS tR TO THE CALCULATED THICKNESS ($tR \geq t$) Note: For significant quantities, it may be possible to choose non-standard thicknesses.
5. VERIFY THAT THE CHOSEN THICKNESS IS SUITABLE FOR THE HYDROSTATIC TESTING OF THE SYSTEM.
6. VERIFY THE OPERATIONAL FEASIBILITY: pipes with D/t > 50 are difficult to handle, and thicknesses less than 0.3 inch are difficult to weld.

INTERNAL PRESSURE CALCULATION -I Standards used:

- **ASME B31.4** (oil lines in North America)

- ASME B31.8 (gas and two-phase flow lines in North America)
- **DNV 1981** (pipeline in the North Sea) The same standards are used in areas of the world that do not have specific regulations.

$$t_{nom} = \frac{P_d\, D}{2\, E_w\, \sigma_y\, F_t\, \eta} + t_a \qquad (46)$$

Pi: internal pressure

Pe: external pressure

Pd: $Pi - Pe$ (differential pressure)

D: nominal outside diameter

ta = c: corrosion allowance

σy: minimum yield strength

Ew: weld efficiency (for seamless, ERW, and DSAW = 1)

Ft: equal to 1 for temperatures below 250°F (120°C)

η: from table 3.1 for oil and table 3.2 for gas

OSCILLATIONS CAUSED BY VORTICES

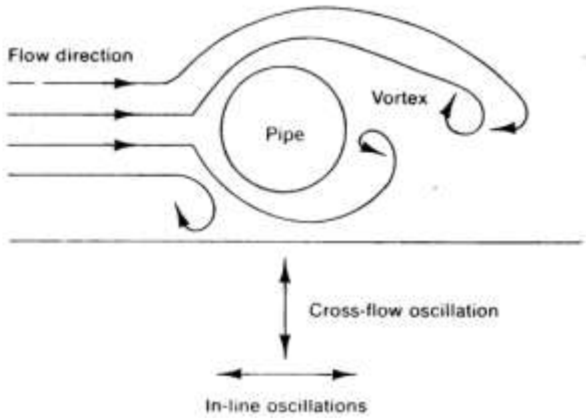

Figure 31 : Pipeline oscillations

When a current impacts the pipeline, vortices are generated due to flow turbulence and downstream instabilities of the pipe. The generation of vortices causes pressure fluctuations on the pipe, which can lead to vibration.

The frequency of these vortices depends on the fluid velocity impacting the pipeline and its diameter. If the vortex shedding frequency matches one of the natural frequencies of the pipeline segment, the pipeline begins to vibrate.

Cross-flow oscillations are more dangerous than in-line oscillations.

The frequency of vortex shedding (often around a Strouhal number of 0.2 for many pipelines) should be sufficiently far from the natural frequency of the pipe. This natural frequency depends on the stiffness of the configuration, boundary conditions, length of the suspended segment, and masses involved.

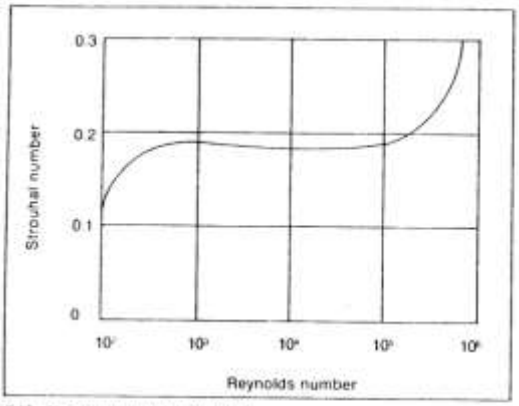

3.12 Variations of Strouhal number

Figure 32 : Variations of Strouhal number

$$f_s = \frac{S\ V}{D} \qquad (47)$$

fS: vortex shedding frequency

S: Strouhal number

V: flow velocity

D: pipeline diameter

$$f_n = \frac{C}{L^2}\sqrt{\frac{E\ I}{M}} \qquad (48)$$

fn: fundamental frequency of vibration

C: constant depending on the type of constraint

L: length of the unsupported span

E: elastic modulus

I: moment of inertia

M: mass of the pipe + insulation + ballast

In-line oscillations begin when the vortex shedding frequency is about 1/3 of the fundamental frequency fn.

PIPE-SOIL STABILITY

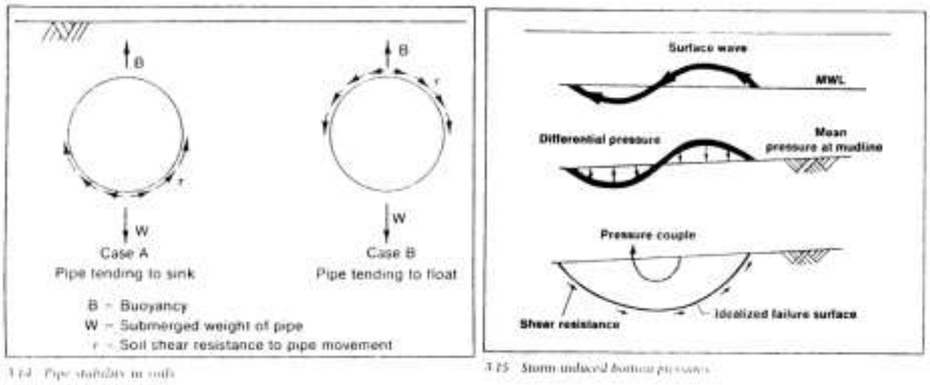

Figure 33 : Pipeline stability

The horizontal and vertical stability of the pipeline (whether resting on the seabed or buried) needs to be carefully verified under both static and dynamic conditions (waves and currents).

A pipeline on the seabed can experience buoyancy, tending to either lift or sink below the seabed level when waves pass over it.

The passage of surface waves creates cyclic depressions and surges on the seabed. This alternation can lead to drained and undrained conditions of the seabed sand and may cause instability, especially during storms where waves of various frequencies occur.

SEABED MOVEMENTS

The seabed can undergo macroscopic changes due to erosion, rapid sand depositions, and the passage of large surface waves.

The interaction mechanism between surface waves and changes in loose seabed sediments (unconsolidated sediment) is quite complex.

Gravity alone generally isn't sufficient to cause instability in underwater slopes, but when combined with the cyclical effect of waves, significant changes in seabed geometry can occur.

The presence of the pipeline on the seabed increases the load. In general, the more buried the pipeline is, the greater the forces acting on it.

As a result, the pipeline should ideally be placed on the seabed or slightly buried to minimize the forces exchanged between the pipeline and the seabed in case of seabed movement.

If the ground movement is limited to the pipeline zone, it can lead to flexural failure, although this case is quite rare.

EFFECTS OF SEABED IRREGULARITIES

The pipeline encounters irregularities on the seabed that can induce excessive bending and shear stresses.

If the span between supports is excessive, interventions are necessary to modify the route or reduce irregularities through pre-levelling.

EROSION

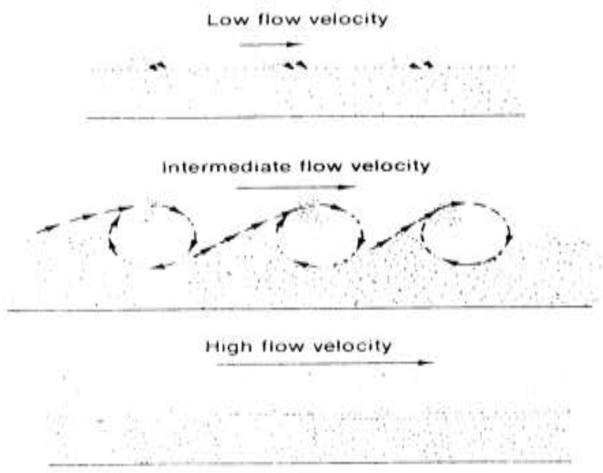

Figure 34 : Seabed erosion

In areas of landing or wherever there are significant currents, sediments can be displaced, suspended, or deposited anywhere. This can cause the pipe to become exposed, lose seabed support, and remain suspended, leading to movements that induce stresses, vibrations, and damage to the pipeline.

If the current velocity is low, sediment grains do not move. As velocity increases, grains start to move, with individual grains shifting and rolling randomly.

As velocity further increases, turbulence increases, and more particles begin to follow trajectories that cause them to lift and then settle back onto the seabed (sedimentation). At consistent velocities, grains are consistently lifted and carried within the fluid flow, causing irregularities on the seabed known as ripples.

Grains continue to be transported until the velocity decreases, allowing them to settle back onto the seabed (settling velocity).

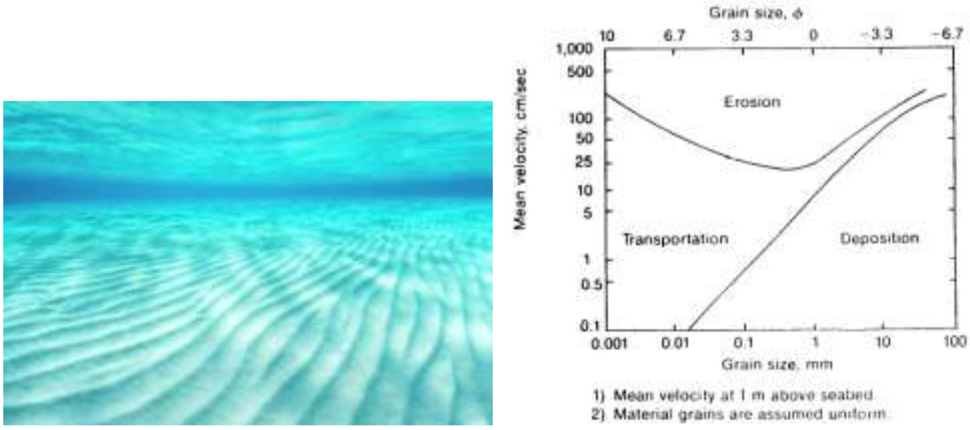

Figure 35 : Sedimentation and grain properties

The phenomenon depends on many factors (grain size, density). Literature contains results that, based on grain size and average velocity, describe the type of phenomenon that occurs (assuming quartz as the material).

Since the forces due to seabed movement are minimal when the pipeline is resting on or slightly buried in the seabed, pipelines must be designed to remain supported (without tending to bury themselves) throughout their operational life. However, when the pipeline is not buried, hydrodynamic forces come into play, and the pipeline's weight must be sufficient to maintain stability even under severe waves and strong currents, preventing the pipe from tending to bury itself.

TRENCHING

For stability reasons, it may be necessary to bury sections of a pipeline on the seabed. Common reasons include:

1. **Hydrodynamic Forces**: The pipeline is designed to remain stable during construction (when it is empty) and throughout its operational life, including the risk of burial on the seabed. Some sections of the pipeline may be lighter than others. Hydrodynamic actions are stronger near the shore, which is why many pipelines are buried in near-shore areas.

2. **Span Length Flexibility**: When spans of the pipeline are exposed to underwater currents, they may vibrate. To reduce the extent of suspended spans or improve boundary conditions, some sections of the pipeline are buried.
3. **Obstacles/Presence of Exposed Rocks**: The presence of obstacles on the seabed can cause excessive stresses on the pipeline. Smoothing the seabed by generating embankments can help reduce these stresses.
4. **Erosion/Seabed Modifications Due to Wave Action**: Pressures on the seabed from passing waves can cause settlements, landslides, or soil liquefaction, which may lift or sink the pipeline. In such cases, burying the pipeline can be a solution.
5. **Interference with Fishing Activities**: One of the main risks comes from trawling activities that can cause impacts against the pipeline (potentially damaging its cement coating) or entangle nets that would then exert force on the pipeline. In these cases, burying the pipeline is recommended.
6. **Risk of Anchor Impact**: This risk exists in known anchorage areas and can also occur during emergency anchoring. The pipeline must be buried at a depth greater than the anchor penetration depth. Different anchor sizes require corresponding burial depths.

TRENCHING METHOD

- JETTING METHOD: This method involves creating a trench on the seabed to bury the infrastructure. High-pressure water jets are used to fluidize the seabed material, allowing cables or pipelines to sink into the trench. Fast and relatively low-impact on the environment. Not effective for harder seabed types (e.g., rock), and can cause reburial issues due to seabed resettlement.

- MECHANICAL CUTTING: Mechanical cutting tools are used to cut into the seabed to create a trench. Can handle harder substrates where other methods fail. More expensive and slower than jetting or ploughing. Requires significant power and is complex to operate.

- FLUIDIZATION METHOD: High-pressure water jets or fluidizing nozzles are directed at the seabed to loosen or "fluidize" the sediment. This temporarily changes the seabed material into a more fluid-like state. Once the trenching operation is complete and the water jets are removed, the fluidized sediment naturally settles back into place, covering the infrastructure and re-solidifying over time. This forms a natural protective cover.

- PLOWING METHOD: A mechanical plough is towed along the seabed to cut a trench into which the pipeline or cable is laid. Robust and capable of trenching to a consistent depth. Suitable for long-distance trenching.

PIPE CONNECTION & POSITIONING SYSTEMS

The issue of connections arises in the following scenarios:

1. During the construction of a new pipeline.
2. For repair needs.
3. Adding a lateral line to the main pipeline.

There is also a need for connections between pipelines and risers, and between pipelines and subsea manifolds.

Connections can be made either on the surface by lifting the pipeline from the seabed, performing the necessary welds, and then redepositing the pipeline on the seabed. Alternatively, connections directly on the seabed are carried out using hyperbaric welding, flanged joints, or mechanical connectors.

The positioning of the ends to be joined is a critical aspect to facilitate the connection. Often, "pipe spools" are used, which are pre-prepared pipes equipped with flanges and all necessary fittings to bridge the gap between the two ends.

There are techniques to eliminate the distance between the ends to be welded, which are used to connect the pipeline to the riser, the wellhead, the subsea manifold, or other subsea resources.

PIPELINE CONNECTION SYSTEM

FLANGED JOINTS

Figure 36 : Flanged joints

The pipes are prepared with flanges in advance, and during laying, an adjustable accessory is brought down to the seabed and connected to the terminal flanges of the two pipeline sections to be joined. The accessory is then brought back to the surface and serves as a template for a rigid pipe spool that will form the connection between the two pipeline sections.

To ensure alignment of the bolt holes between the two flanges to be coupled, special flanges are used that can be radially rotated (swivel ring flanges). The cost of these flanges is limited, but the installations have a long lifespan and can lead to leaks that are difficult to detect.

Flanges are also used at the base of the riser to facilitate replacement when necessary.

ECONOMIC FEASIBILITY

To evaluate the economic feasibility of using a green hydrogen production plant powered by electricity from an offshore wind farm, the Levelized Cost of Hydrogen ($LCOH_2$) is a key parameter. $LCOH_2$ indicates the cost to produce 1 kg of hydrogen, considering both investment and operational costs.[116]

A hydrogen production plant typically consists of an electrolyser, water supply (in this case, seawater), a desalination for treating seawater, an electricity source (from the offshore wind farm), and an intermediate storage facility. To minimize costs, it's crucial to design the plant's capacity to operate as much as possible at its nominal value (full-load hours), with offshore wind offering the highest full load hours.

$LCOH_2$ is influenced by transmission distance, making it essential to evaluate the economic viability of multiple scenarios. In the study published by DNV, "Specification of a European Offshore Hydrogen Backbone," three different scenarios are analysed:

1. Electricity transmission via HVAC with onshore electrolyser (cable)
2. Electricity transmission via HVDC with onshore electrolyser (cable)
3. Offshore electrolyser and hydrogen transmission to onshore (pipeline)

The study assesses the distance in kilometers of the transmission lines to compare these scenarios. It concludes that for distances between 100 km and 150 km, the most cost-effective scenario involves HVAC transmission. HVDC transmission becomes more economical for distances exceeding 150 km, as losses compared to HVAC are nearly halved.

For context, energy losses are approximately 1.7% per 1000 km in a new 48-inch pipeline at 80 bar pressure, while HVDC cables experience losses of 3.5% per 1000 km and HVAC cables 6.7% per 1000 km.

Considering transmission via pipelines necessitates evaluating the offshore hydrogen production plant's capacity, as the pipeline will be sized accordingly.

Figure 37 : LCOH from offshore wind by transmission vector in 2030 [116]

As seen from the graph, in the case where the electrolyser capacity is very large (10 GW), it becomes more economically advantageous to use pipeline transmission compared to HVDC. The reason for this lies in the limited transmission capacity of electrical cables. AC cables have a maximum capacity of 350 MW, while DC cables can handle up to 2 GW. In contrast, for pipeline transmission, it is feasible to increase capacity by interconnecting various offshore wind farms using larger pipe diameters. Increasing the pipe diameter significantly boosts capacity, although the investment cost rises proportionally with diameter, leading to an overall reduction in plant costs. This scalability gives pipelines a greater economic advantage.

Conversely, costs for cables do not decrease with capacity increases. Using cables in parallel is complex due to the vast distances involved, which pose technical limits related to magnetic induction.

HYDROGEN PIPELINE COST

This paragraph provides an economic analysis for the construction of a pipeline for the transmission and distribution of green hydrogen produced offshore via a wind turbine farm. To carry out this analysis, some assumptions will need to be made to simplify the calculation of investment and operating costs.

Initially, the costs for the construction of a natural gas pipeline will be evaluated; subsequently, the calculation will be adapted to a hydrogen pipeline.

From the literature, it is not possible to define a unique cost function as this function is strongly influenced by the bathymetry of the terrain on which the pipeline is to be built.

Referring to this article[122], the costs related to piping and compressors, necessary to compensate for the pressure losses characteristic of pipelines, will be assumed. Engineering, planning, and authorization costs have not been included. Moreover, compared to natural gas transport, hydrogen pipelines will operate at higher pressures, consequently leading to an increase in the thickness of the pipeline. As reported in the article[122] , a 25% increase in the cost of materials, man-labour, and machinery for the hydrogen pipeline will be assumed. Conversely, the increase in cost due to the use of different materials will not be considered. Subsequently, the cost of austenitic steel instead of conventional steel will be considered. For the thickness calculation, Barlow's formula will be used, and a safety factor of 1.6 will be applied.

$$P = \frac{2\,S\,t}{D} \tag{49}$$

From which the thickness equation is obtained.

$$t = \frac{P\,D}{2\,(S\,E + P\,y)} + A \tag{50}$$

P Is the pressure (psi), D is the outside diameter (mm), A is a corrosion factor, E is the welding efficiency, S is the yield strength and y is the fragility factor.

The pipeline in question will consist of a transmission line and a distribution line, as the two will present distinct operating conditions. A natural gas pipeline with a nominal pressure of 10 MPa, a gas velocity of 15 m/s, an operating pressure of 6.5 MPa for the transmission line, and an operating pressure of 3 MPa for the distribution line will be considered as the reference case. As reported in the article[122], the equation for the investment cost in the case of a natural gas pipeline will be a function of the diameter of the pipeline itself and will be distinguished between the transmission line and the distribution line.

At this point, we can use the mass flow rate formula to express the diameter.

$$\dot{Q}_{mass} = \rho\, v\, \frac{\pi\, D^2}{4} \qquad [\text{kg/s}] \tag{51}$$

The first equation is referred to investment cost of the distribution line.

$$Cap\,(D) = 1{,}500{,}000\, D^2 + 860{,}500\, D + 247{,}500 \qquad [€_{2010}/\text{km}] \tag{52}$$

For the calculation of the investment cost of the transmission line, the cost of recompression stations is taken into account.

$$Cap\,(D) = 2{,}200{,}000\, D^2 + 860{,}500\, D + 247{,}500 \qquad [€_{2010}/\text{km}] \tag{53}$$

Taking into account that diameter lower than 100 mm will not be installed, some section of the distribution lines will be overrated. This will lead to an increase in the investment cost.

The polynomial equations for distribution and transmission are as follows.

$$Cap\,(D) = 3{,}400{,}000\, D^2 + 598{,}600\, D + 329{,}000 \qquad [€_{2010}/\text{km}] \tag{54}$$

$$Cap\,(D) = 4{,}000{,}000\, D^2 + 598{,}600\, D + 329{,}000 \qquad [€_{2010}/\text{km}] \tag{55}$$

In this article[123] the simplified model of the previously mentioned cost equation is revisited. It is possible to scale this equation from the onshore case to the offshore case by multiplying it by a factor of two.

$$CAPEX_{offshore} = 2\, CAPEX_{onshore} \qquad [€_{2010}/\text{km}] \tag{56}$$

From this point on, the focus will shift to the electrolyser. Specifically, the mass flow rate[kg/s] of hydrogen will be evaluated based on the capacity[MW] and the production rate[kg_{H2}/s/MW] of the electrolyser.

$$Q_{mass} = E_{cap}\, P_{rate} \qquad [\text{kg/s}] \tag{57}$$

At this point, we will rewrite the diameter and insert it into the investment cost equation. It should be noted that pipelines with a diameter of less than 100 mm will not be installed.

$$D = \sqrt{\frac{4\, \dot{Q}_{mass}}{\rho\, v\, \pi}} \qquad [\text{m}] \tag{58}$$

Additionally, the costs of coated steel with Galvalume are considered to be 950 $€_{2009}$/ton and the reworking of welds is 1200 $€_{2010}$/ton for the natural gas pipeline. The cost of austenitic steel Nirosta 4318 is 3600 $€_{2010}$/ton for the hydrogen pipeline, with a soil temperature of 12°C, hydrogen density of 5.3 kg/m³ for the transmission line and 2.5 kg/m³ for the distribution line.
An average distance of 250 km is assumed between stations recompressing hydrogen from 3.0 to 10.0 MPa. From the base example of a compressor costing $ 7.3 million for a specific throughput of 240 tonnes H2/day, we derive a specific cost of compressors in relation to the mass flow. This leads to an additional approx. 10,500 $€_{2010}$ s/kg for each km of transmission pipeline [122].
A production rate of 0.0055 kg_{H2}/s/MW (for a Siemens – Silyzer 300), a utilization rate of the electrolyser of 75%, so the capacity of the electrolyser is a 33% oversized, and a 30 year of lifetime for the pipe is assumed[121].

We have the function of the distance in function of the electrolyser's capacity.

$$CAPEX_{pipe}\left(E_{cap}\right) = 2\ (16{,}000{,}000\ \frac{E_{cap}\ P_{rate}}{\rho\ v\ \pi} + 1{,}197{,}200\ \sqrt{\frac{E_{cap}\ P_{rate}}{\rho\ v\ \pi}} + 329{,}000) \quad [€_{2010}/\text{km}] \tag{59}$$

Piping (Austenitic steel), materials and compressors (required each 250 km) are considered; engineering, planning and consenting costs were not included [121].

OPEX will be evaluated as a percentage of the CAPEX. [122]

$$OPEX = 2\%\ CAPEX \qquad [€_{2010}/\text{km}] \tag{60}$$

Levelized Cost of Transmission for Hydrogen

We can now define the LCOTH (Levelized Cost of Transmission for Hydrogen) in €/kg_{H2} [122].

Considering a d_{rate} equal to 8%, we have the LCOTH equation.

$$LCOTH = \frac{CAPEX\ d_{rate} + \sum_{l=0}^{L} \frac{OPEX}{(1+d_{rate})^l}}{\sum_{l=0}^{L} \frac{Prod_{H2}}{(1+d_{rate})^l}} \qquad [€_{2010}/kg_{H2}] \tag{61}$$

INSTALLATION COST

For completeness of the analysis, an estimate will be made of the costs associated with transporting and laying the pipelines offshore. These costs are fundamentally a function of the distance the ships need to travel, the time they will spend on installation, and the time on the job.

Installation costs vary between 28% and 33% of the CAPEX for the construction of a facility. The difference depends on the installation site, if it is in deep or shallow water [123].

We can estimate installation costs as a percentage of CAPEX.

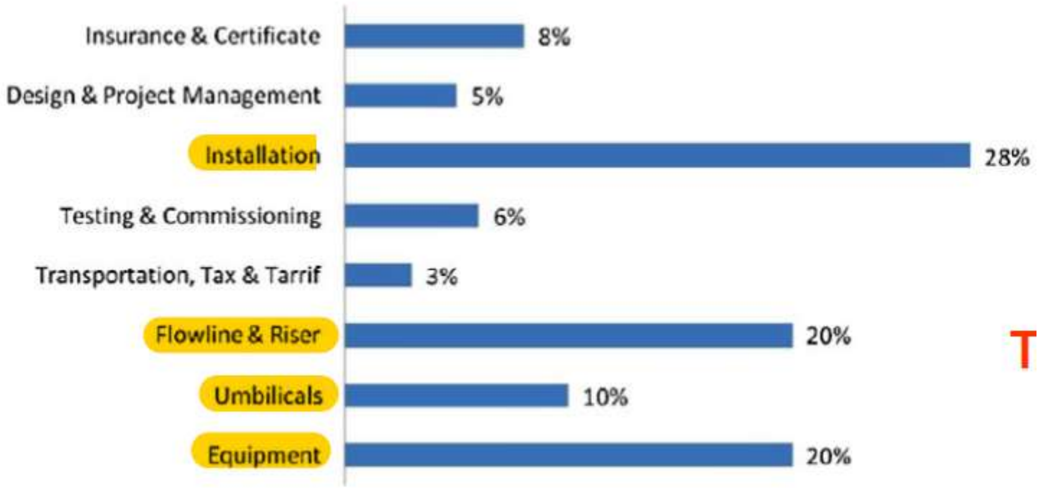

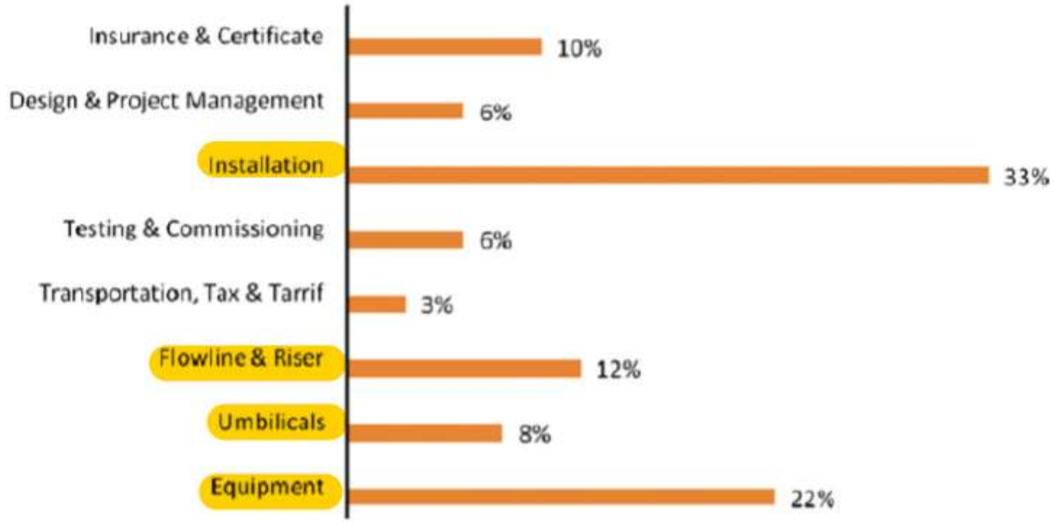

Figure 38 : Shallow and deep water subsea CAPEX breakdown, Subsea Engineering Handbook (Yong Bai, Qiang Bai) [124]

9. Economic Analysis of Ammonia Production From Offshore Wind

Once green hydrogen is produced, it can be converted into ammonia, an energy carrier. To achieve this, nitrogen and hydrogen are required. Nitrogen is obtained using an Air Separation Unit (ASU), followed by a synthesis process for ammonia production via the Haber-Bosch (HB) process.

The Air Separation Unit (ASU) involves a cryogenic distillation process. This technology has a very high level of maturity (TRL 9) and consists of a double-column distillation process. It separates nitrogen, oxygen, and argon contained in the air by exploiting their different boiling points.

Cryogenic distillation of air produces high-purity nitrogen and oxygen (99.999 wt%) in large volumes (250–50,000 Nm^3/h).

Ammonia can be stored in pressurized storage cylinders and refrigerated tanks, both of which are mature technologies available worldwide. Pressurized cylinders are small-scale, with capacities of up to 270 tonnes. In these cylinders, ammonia is stored at 20°C and 10 bar. On the other hand, refrigerated tanks store ammonia at -33°C and 1 bar, with capacities of up to 50,000 tonnes.[125]

The Haber-Bosch (HB) synthesis loop is the most competitive method for producing ammonia on a large scale[126]. Ammonia synthesis is a reversible exothermic reaction. The reaction is shown below:

$$N_2 + 3\,H_2 <-> 2\,NH_3\;\Delta H^{\circ} = -91.8\,\frac{kJ}{mol} = -2.7\,\frac{GJ}{t_{NH_3}} \quad (62)$$

The molecular ratio of the reaction involves one molecule of nitrogen and three molecules of hydrogen. The thermochemical reaction uses iron or ruthenium oxide-based catalysts to convert the hydrogen and nitrogen mixture into ammonia. This process occurs in a range of temperatures between 400 and 550°C and pressures ranging from 100 to 300 bar. [126]

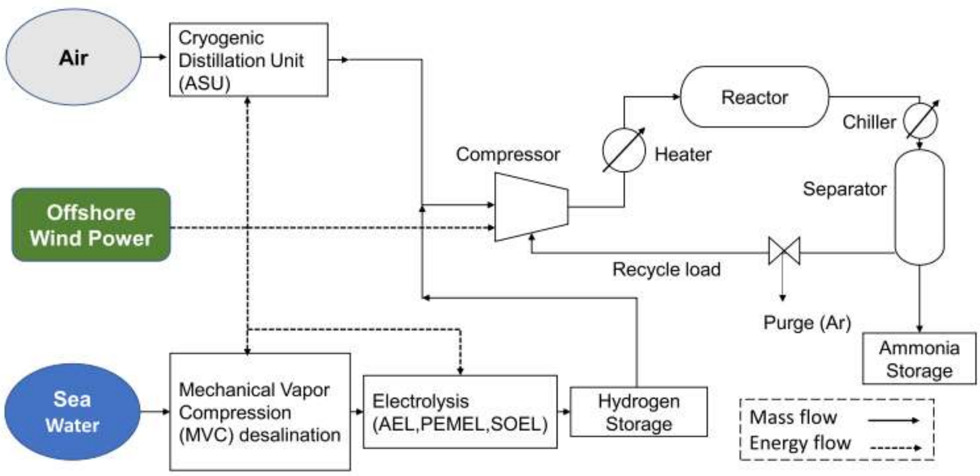

Figure 39: Block diagram of offshore wind-powered ammonia process [126]

Power laws were fitted to the capex estimations **in USD2010** for the synthesis loop (HB), ASU and ammonia storage in respective capacity units. [125]

$$Capex_{synthesis\ loop} = 23850000\left(Capacity\ \frac{t_{NH_3}}{day}\right)^{-1.340} + 173500 \qquad [USD] \qquad (63)$$

$$Capex_{ASU} = 1606000 \left(Capacity\ \frac{t_{N_2}}{day} \right)^{-0.6249} + 9318 \qquad [USD] \qquad (64)$$

$$Capex_{NH_3\ storage} = 46600 \left(Capacity\ t_{NH_3} \right)^{-0.8636} + 536.9 \qquad [USD] \qquad (65)$$

The overall capex of the ammonia plant is calculated by sizing the ASU to the synthesis loop's nitrogen demand and considering 30 days of ammonia storage. Applying a USD/€ exchange rate of **1.12** in 2019.[125]

9.1 Transportation Of Ammonia

Ammonia is commonly transported through carbon steel pipelines with diameters ranging from 0.15 to 0.25 meters, in its liquid state at pressures of approximately 17 bar.[126]

The transportation of ammonia by sea is well-established, relying on vessels specifically designed for this purpose. There are three main types of ammonia carriers: fully pressurized carriers with small capacities of up to 4,000 m^3, semi-refrigerated carriers with capacities ranging from 1,500 to 30,000 m^3, and fully refrigerated carriers with capacities of up to 85,000 m^3.

Ammonia is typically transported using gas carriers originally designed for liquefied petroleum gas (LPG).[127]

9.2 Pipelines

Based on data from the known capacities of ammonia pipelines with four different diameters (10 cm, 15 cm, 20 cm, and 25 cm).

Referring to article [128], we use equation 5 to obtain the diameter of the pipe in centimeters, based on data from the known capacities of ammonia pipelines with four different diameters (10 cm, 15 cm, 20 cm, and 25 cm).

$$Pipe_{capacity} = 15.245\left(\frac{D}{5} - 1\right)^{1.6468} \qquad (66)$$

The cost of onshore ammonia pipelines per kilometre ranges between €0.771 million and €1.322 million ($0.857 million–$1.469 million) for a 25 cm diameter pipeline.
The total cost of a pump station, including two pumps along with the associated buildings and infrastructure, is approximately €1.8 million ($2 million).

According to [128], the optimal spacing between pump stations for long-distance ammonia transmission by pipeline is around 128 km. In this way it is possible to calculate the number of pumps needed considering the total distance to be covered with the pipeline.

The pipeline cost (C_{pipe}) is calculated as follows:

$$C_{pipe} = \frac{D_{pipe}\,C_{25}}{D_{25}} \qquad (67)$$

where the C_{25} (cost per unit length for a 25 cm diameter pipeline) is set to 0.771 M€/km.

Subsea pipelines require stricter standards, particularly in terms of anti-corrosion measures and structural stability. As a result, the cost of offshore pipelines is assumed to be double that of their onshore counterparts.[121]

$$CAPEX_{pipe} = 2\left(C_{pipe}\,d + C_{pump}\,n_{pump}\right) \qquad (68)$$

$$OPEX_{pipe} = \sum_{l=0}^{L}\frac{OPEX_{pipe}}{(1+d_{rate})^{l}} + \sum_{l=0}^{L}\frac{OPEX_{pump}}{(1+d_{rate})^{l}} \qquad (69)$$

9.3 Shipping

The total cost for ammonia tankers (CAPEX_tanker) is expressed as the sum of ship costs (CAPEX_ship) and storage costs (CAPEX_storage), as shown in Equation (70):

$$CAPEX_{tanker} = CAPEX_{ship} + CAPEX_{storage} \qquad (70)$$

The ship costs (CAPEX_ship) are calculated by multiplying the unit cost of a ship (C_ship) by the number of ships required (n_ship), as expressed in Equation (71):

$$CAPEX_{ship} = C_{ship}\, n_{ship} \qquad (71)$$

Similarly, storage costs (CAPEX_storage) are obtained by multiplying the unit cost of a tank (C_tank) by the number of tanks required (n_tank), as shown in Equation (72):

$$CAPEX_{storage} = C_{tank}\, n_{tank} \qquad (72)$$

The number of ships (n_ship) is estimated based on the amount of ammonia produced, the ship capacity, and the time required for transportation. To ensure sufficient storage capacity, the total tank volume is assumed to be larger than the total ship volume. The number of tanks (n_tank) is calculated based on the number of ships, ship capacity, and tank capacity.

The unit cost of a single ship (C_ship) is assumed to be 76.5 million euros (85 million USD), while a tank with a capacity of 34,100 tons of NH3_3 has a cost (C_tank) of 61.2 million euros (68 million USD).

Operational Costs of Tankers

According to [121], the total operational costs of tankers (OPEX_tanker) are defined in Equation (63):

$$OPEX_{tanker} = \sum_{l=0}^{L} \frac{OPEX_{storage}}{(1 + d_{rate})^{l}} + \sum_{l=0}^{L} \frac{OPEX_{ship}}{(1 + d_{rate})^{l}} + \sum_{l=0}^{L} \frac{C_{fuel}}{(1 + d_{rate})^{l}} \qquad (6)$$

The fuel cost (C_fuel) is calculated as shown in Equation (13):

$$C_{fuel} = 2\, d\, n_{trip}\, n_{ship}\, C_{fuel\_km} \qquad (64)$$

The annual operational and maintenance costs of this transportation method combine the costs of storage (OPEX_storage), ships (OPEX_ship), and annual fuel consumption (C_fuel). The annual values of OPEX_storage and OPEX_ship are assumed to be 4% of CAPEX_storage and CAPEX_ship, respectively. The annual fuel consumption is determined based on the number of trips made in a year (n_trip) and the fuel cost per kilometer (C_fuel_km).

The ship and tank capacities used in the calculations are 53,000 tons of NH3_3 and 34,100 tons of NH3_3, respectively. Additionally, the ship operates at a speed of 30 km/h.

Levelized cost of transportation

The Levelized cost of transportation (LCOT) for ammonia tankers and pipelines is given by equation (65)

$$LCOT_{ammonia\ tanker\ ,pipeline} = \frac{CAPEX_{ammonia\ tanker,pipeline} + \sum_{l=0}^{L} \frac{OPEX_{ammonia\ tanker,pipeline}}{(1+drate)l}}{\sum_{l=0}^{L} \frac{Prod_{NH3}}{(1+drate)l}} \qquad (65)$$

Levelized cost of Ammonia

The Levelized Cost of Ammonia (LCOA) is a metric used to evaluate and compare the profitability of ammonia production, such as using hydrogen derived from offshore wind farms. It is calculated based on the total costs and total ammonia production over the project's lifetime, as shown in the following equation:

$$\mathrm{LCOA} = \sum \mathrm{l}_{\ t=0} \frac{\frac{\mathrm{CAPEXt+OPEXt+DECEXt}}{(1+\mathrm{r})^{t}}}{\sum \mathrm{L}_{\ t=0} \frac{\mathrm{Prod}_{\mathrm{NH3}}}{(1+\mathrm{r})^{t}}} \qquad (66)$$

In this equation, CAPEX represents the capital expenditures, OPEX represents the operational expenditures, DECEX represents the decommissioning costs, and Total Ammonia Production refers to the amount of ammonia produced over the project's lifetime. This formula simplifies the calculation by aggregating all lifetime costs and dividing them by the total ammonia output, providing a normalized cost per unit of ammonia produced.

Tables and figures

List of sources

[1] S. J. P. Hill, O. Bamisile, L. Hatton, I. Staffell, and M. Jansen, "The cost of clean hydrogen from offshore wind and electrolysis," *J. Clean. Prod.*, vol. 445, p. 141162, Mar. 2024, doi: 10.1016/j.jclepro.2024.141162.
[2] "Wind-to-Hydrogen Tech Goes to Sea - IEEE Spectrum." Accessed: Jun. 12, 2024. [Online]. Available: https://spectrum.ieee.org/green-hydrogen-2663997448
[3] "Integration of offshore wind clusters to weak grids using PtX and BESS." Accessed: Jun. 29, 2024. [Online]. Available: https://upcommons.upc.edu/handle/2117/400190
[4] M. Aneke and M. Wang, "Energy storage technologies and real life applications – A state of the art review," *Appl. Energy*, vol. 179, pp. 350–377, Oct. 2016, doi: 10.1016/j.apenergy.2016.06.097.
[5] M. C. Carbo, "Global Technology Roadmap for CCS in Industry".
[6] N. Kittner, S. Castellanos, P. Hidalgo-Gonzalez, D. M. Kammen, and S. Kurtz, "Cross-sector storage and modeling needed for deep decarbonization," *Joule*, vol. 5, no. 10, pp. 2529–2534, Oct. 2021, doi: 10.1016/j.joule.2021.09.003.
[7] F. Dawood, M. Anda, and G. M. Shafiullah, "Hydrogen production for energy: An overview," *Int. J. Hydrog. Energy*, vol. 45, no. 7, pp. 3847–3869, Feb. 2020, doi: 10.1016/j.ijhydene.2019.12.059.
[8] R. Ge *et al.*, "A $NiCo_2O_4$@Ni–Co–Ci core–shell nanowire array as an efficient electrocatalyst for water oxidation at near-neutral pH," *Chem. Commun.*, vol. 53, no. 55, pp. 7812–7815, 2017, doi: 10.1039/C7CC03146G.
[9] A. Valentini, "Green shift to create 1 billion tonne 'green ammonia' market?," 2020.
[10] A. T. Wijayanta, T. Oda, C. W. Purnomo, T. Kashiwagi, and M. Aziz, "Liquid hydrogen, methylcyclohexane, and ammonia as potential hydrogen storage: Comparison review," *Int. J. Hydrog. Energy*, vol. 44, no. 29, pp. 15026–15044, Jun. 2019, doi: 10.1016/j.ijhydene.2019.04.112.
[11] A. Valera-Medina, H. Xiao, M. Owen-Jones, W. I. F. David, and P. J. Bowen, "Ammonia for power," *Prog. Energy Combust. Sci.*, vol. 69, pp. 63–102, Nov. 2018, doi: 10.1016/j.pecs.2018.07.001.
[12] P. Rentschler, C. Klahn, and R. Dittmeyer, "The Need for Dynamic Process Simulation: A Review of Offshore Power-to-X Systems," *Chem. Ing. Tech.*, vol. 96, no. 1–2, pp. 114–125, Jan. 2024, doi: 10.1002/cite.202300156.
[13] B. Nastasi and G. Lo Basso, "Power-to-Gas integration in the Transition towards Future Urban Energy Systems," *Int. J. Hydrog. Energy*, vol. 42, no. 38, pp. 23933–23951, Sep. 2017, doi: 10.1016/j.ijhydene.2017.07.149.
[14] A. Buttler and H. Spliethoff, "Current status of water electrolysis for energy storage, grid balancing and sector coupling via power-to-gas and power-to-liquids: A review," *Renew. Sustain. Energy Rev.*, vol. 82, pp. 2440–2454, Feb. 2018, doi: 10.1016/j.rser.2017.09.003.
[15] Y. Guo, G. Li, J. Zhou, and Y. Liu, "Comparison between hydrogen production by alkaline water electrolysis and hydrogen production by PEM electrolysis," *IOP Conf. Ser. Earth Environ. Sci.*, vol. 371, no. 4, p. 042022, Dec. 2019, doi: 10.1088/1755-1315/371/4/042022.
[16] A. Singlitico, J. Østergaard, and S. Chatzivasileiadis, "Onshore, offshore or in-turbine electrolysis? Techno-economic overview of alternative integration designs for green hydrogen production into Offshore Wind Power Hubs," *Renew. Sustain. Energy Transit.*, vol. 1, p. 100005, Aug. 2021, doi: 10.1016/j.rset.2021.100005.
[17] "Requirements for Offshore Substations and Electrical Service Platforms," 2023.
[18] "VindØ – The world's first energy island." [Online]. Available: https://www.windisland.dk/
[19] *Wind Power Hub*. [Online]. Available: https://northseawindpowerhub.eu/key-concepts
[20] "HYDROGEN ISLAND BrintØ." Accessed: Jun. 26, 2024. [Online]. Available: https://www.cip.com/approach/our-projects/hydrogen-island/

[21] *Lhyfe H2 floating elestrolyzer*. [Online]. Available: https://www.lhyfe.com/our-production-units/offshore-ecological-hydrogen/
[22] "ITM Power - Oyster Project." Accessed: Sep. 30, 2024. [Online]. Available: https://oysterh2.eu/partner/itm-power/
[23] "HYPORT®: green hydrogen plant in Ostend | DEME Group." Accessed: Sep. 30, 2024. [Online]. Available: https://www.deme-group.com/news/hyportr-green-hydrogen-plant-ostend
[24] "AquaVentus | Hydrogen projects of RWE." Accessed: Sep. 30, 2024. [Online]. Available: https://www.rwe.com/en/research-and-development/hydrogen-projects/aquaventus/
[25] "ERM | Sustainability is our business," ERM. Accessed: Sep. 30, 2024. [Online]. Available: https://www.erm.com/
[26] "Zenith Energy, EI-H2 plan 2.7-GW green hydrogen facility in Ireland." Accessed: Sep. 30, 2024. [Online]. Available: https://renewablesnow.com/news/zenith-energy-ei-h2-plan-27-gw-green-hydrogen-facility-in-ireland-746801/
[27] T. Watts, "ER.A.2.4 Project Description," 2024.
[28] K. Ligęza, M. Łaciak, and B. Ligęza, "Centralized Offshore Hydrogen Production from Wind Farms in the Baltic Sea Area—A Study Case for Poland," *Energies*, vol. 16, no. 17, 2023, doi: 10.3390/en16176301.
[29] M. Zhang, L. Tao, M. Nuernberg, A. Rai, and Z.-M. Yuan, "Conceptual design of an offshore hydrogen platform," *Int. J. Hydrog. Energy*, vol. 59, pp. 1004–1013, Mar. 2024, doi: 10.1016/j.ijhydene.2024.02.077.
[30] F. D. C. Moreno, "Design of an Electrolyzer Integrated in an Offshore Wind Turbine System," Oct. 2021, Accessed: Sep. 30, 2024. [Online]. Available: https://research.utwente.nl/en/publications/design-of-an-electrolyzer-integrated-in-an-offshore-wind-turbine-
[31] "Report:," ISPT. Accessed: Sep. 30, 2024. [Online]. Available: https://ispt.eu/publications/a-one-gigawatt-green-hydrogen-plant/
[32] Gottfried Wilhelm Leibniz Universität Hannover, Institut Für Stahlbau, "Substructures for offshore wind turbines Current trends and developments," Technische Informationsbibliothek u. Universitätsbibliothek, 2014. doi: 10.2314/GBV:77999762X.
[33] A. Robertson *et al.*, "Definition of the Semisubmersible Floating System for Phase II of OC4," NREL/TP-5000-60601, 1155123, Sep. 2014. doi: 10.2172/1155123.
[34] "Review of next generation hydrogen production from offshore wind using water electrolysis", doi: https://doi.org/10.1016/j.jpowsour.2023.233904.
[35] "Europe's first offshore hydrogen pilot saw electrolyser performance 'as high as on land.'" [Online]. Available: https://www.hydrogeninsight.com/production/europes-first-offshore-hydrogen-pilot-saw-electrolyser-performance-as-high-as-on-land/2-1-1590319
[36] "1-s2.0-S2542435120300325-main.pdf."
[37] V. N. Dinh, P. Leahy, E. McKeogh, J. Murphy, and V. Cummins, "Development of a viability assessment model for hydrogen production from dedicated offshore wind farms," *Int. J. Hydrog. Energy*, vol. 46, no. 48, pp. 24620–24631, Jul. 2021, doi: 10.1016/j.ijhydene.2020.04.232.
[38] O. Schmidt, A. Gambhir, I. Staffell, A. Hawkes, J. Nelson, and S. Few, "Future cost and performance of water electrolysis: An expert elicitation study," *Int. J. Hydrog. Energy*, vol. 42, no. 52, pp. 30470–30492, Dec. 2017, doi: 10.1016/j.ijhydene.2017.10.045.
[39] H. Wang, P. Daoutidis, and Q. Zhang, "Harnessing the Wind Power of the Ocean with Green Offshore Ammonia," *ACS Sustain. Chem. Eng.*, vol. 9, no. 43, pp. 14605–14617, Nov. 2021, doi: 10.1021/acssuschemeng.1c06030.
[40] W. Musial, D. Heimiller, P. Beiter, G. Scott, and C. Draxl, "2016 Offshore Wind Energy Resource Assessment for the United States," NREL/TP--5000-66599, 1324533, Sep. 2016. doi: 10.2172/1324533.
[41] K. Eurek, P. Sullivan, M. Gleason, D. Hettinger, D. Heimiller, and A. Lopez, "An improved global wind resource estimate for integrated assessment models," *Energy Econ.*, vol. 64, pp. 552–567, May 2017, doi: 10.1016/j.eneco.2016.11.015.
[42] "Key World Energy Statistics 2020".

[43] S. Dresp, F. Dionigi, M. Klingenhof, and P. Strasser, "Direct Electrolytic Splitting of Seawater: Opportunities and Challenges," *ACS Energy Lett.*, vol. 4, no. 4, pp. 933–942, Apr. 2019, doi: 10.1021/acsenergylett.9b00220.
[44] G. Calado and R. Castro, "Hydrogen Production from Offshore Wind Parks: Current Situation and Future Perspectives," *Appl. Sci.*, vol. 11, no. 12, p. 5561, Jun. 2021, doi: 10.3390/app11125561.
[45] N. B. Negra, J. Todorovic, and T. Ackermann, "Loss evaluation of HVAC and HVDC transmission solutions for large offshore wind farms," *Electr. Power Syst. Res.*, vol. 76, no. 11, pp. 916–927, Jul. 2006, doi: 10.1016/j.epsr.2005.11.004.
[46] M. van Schot, C. Jepma, J. Koornneef, and M. Halter, "D1.6 Offshore Hydrogen roadmap D. 1.7 Analysis of current offshore market failures and the respective role of existing policy D. 1.8 Recommendations on required policies to achieve a socially optimal state".
[47] A. Alassi, S. Bañales, O. Ellabban, G. Adam, and C. MacIver, "HVDC Transmission: Technology Review, Market Trends and Future Outlook," *Renew. Sustain. Energy Rev.*, vol. 112, pp. 530–554, Sep. 2019, doi: 10.1016/j.rser.2019.04.062.
[48] P.-M. Heuser, D. S. Ryberg, T. Grube, M. Robinius, and D. Stolten, "Techno-economic analysis of a potential energy trading link between Patagonia and Japan based on CO2 free hydrogen," *Int. J. Hydrog. Energy*, vol. 44, no. 25, pp. 12733–12747, May 2019, doi: 10.1016/j.ijhydene.2018.12.156.
[49] P. Xiao, W. Hu, X. Xu, W. Liu, Q. Huang, and Z. Chen, "Optimal operation of a wind-electrolytic hydrogen storage system in the electricity/hydrogen markets," *Int. J. Hydrog. Energy*, vol. 45, no. 46, pp. 24412–24423, Sep. 2020, doi: 10.1016/j.ijhydene.2020.06.302.
[50] P. Hou, P. Enevoldsen, J. Eichman, W. Hu, M. Z. Jacobson, and Z. Chen, "Optimizing investments in coupled offshore wind -electrolytic hydrogen storage systems in Denmark," *J. Power Sources*, vol. 359, pp. 186–197, Aug. 2017, doi: 10.1016/j.jpowsour.2017.05.048.
[51] R. Loisel, L. Baranger, N. Chemouri, S. Spinu, and S. Pardo, "Economic evaluation of hybrid off-shore wind power and hydrogen storage system," *Int. J. Hydrog. Energy*, vol. 40, no. 21, pp. 6727–6739, Jun. 2015, doi: 10.1016/j.ijhydene.2015.03.117.
[52] J. Eichman, A. Townsend, and M. Melaina, "Economic Assessment of Hydrogen Technologies Participating in California Electricity Markets," NREL/TP--5400-65856, 1239543, Feb. 2016. doi: 10.2172/1239543.
[53] M. Scolaro and N. Kittner, "Optimizing hybrid offshore wind farms for cost-competitive hydrogen production in Germany," *Int. J. Hydrog. Energy*, vol. 47, no. 10, pp. 6478–6493, Feb. 2022, doi: 10.1016/j.ijhydene.2021.12.062.
[54] T. R. Lucas, A. F. Ferreira, R. B. Santos Pereira, and M. Alves, "Hydrogen production from the WindFloat Atlantic offshore wind farm: A techno-economic analysis," *Appl. Energy*, vol. 310, p. 118481, Mar. 2022, doi: 10.1016/j.apenergy.2021.118481.
[55] A. Kim, H. Kim, C. Choe, and H. Lim, "Feasibility of offshore wind turbines for linkage with onshore green hydrogen demands: A comparative economic analysis," *Energy Convers. Manag.*, vol. 277, p. 116662, Feb. 2023, doi: 10.1016/j.enconman.2023.116662.
[56] T. Nguyen, Z. Abdin, T. Holm, and W. Mérida, "Grid-connected hydrogen production via large-scale water electrolysis," *Energy Convers. Manag.*, vol. 200, p. 112108, Nov. 2019, doi: 10.1016/j.enconman.2019.112108.
[57] G. Calado, R. Castro, A. J. Pires, and M. J. Marques, "Assessment of hydrogen-based solutions associated to offshore wind farms: The case of the Iberian Peninsula," *Renew. Sustain. Energy Rev.*, vol. 192, p. 114268, Mar. 2024, doi: 10.1016/j.rser.2023.114268.
[58] "Hydrogen is vital to tackling climate change," HyDeploy. Accessed: Jul. 24, 2024. [Online]. Available: https://hydeploy.co.uk/
[59] S. Fields, "Heavenn - Projects." Accessed: Jul. 24, 2024. [Online]. Available: https://heavenn.org/heaven-projects/
[60] "North Sea Wind Power Hub." Accessed: Jul. 24, 2024. [Online]. Available: https://northseawindpowerhub.eu/

[61] "H2RES: State-of-the-art-green hydrogen production," State of Green. Accessed: Jul. 24, 2024. [Online]. Available: https://stateofgreen.com/en/solutions/h2res-green-hydrogen-production/
[62] "The HySeasIII Project." Accessed: Jul. 24, 2024. [Online]. Available: https://www.hyseas3.eu/the-project/
[63] "Safety | Hydrogen Program." Accessed: Jun. 29, 2024. [Online]. Available: https://www.hydrogen.energy.gov/program-areas/safety
[64] I. A. for H. Safety, "HySafe – International Association for Hydrogen Safety." Accessed: Jun. 29, 2024. [Online]. Available: https://hysafe.info/
[65] S. Eck, P.E., C. ■ M. D. Snyder, and P. E. ■ D. P. Safety, "Hydrogen Safety Fundamentals." Accessed: Jun. 29, 2024. [Online]. Available: https://www.aiche-cep.com/cepmagazine/december_2021_cep/MobilePagedArticle.action?articleId=1747851
[66] "Hydrogen Storage," Energy.gov. Accessed: Jun. 29, 2024. [Online]. Available: https://www.energy.gov/eere/fuelcells/hydrogen-storage
[67] M. Genovese, V. Cigolotti, E. Jannelli, and P. Fragiacomo, "Current standards and configurations for the permitting and operation of hydrogen refueling stations," *Int. J. Hydrog. Energy*, vol. 48, no. 51, pp. 19357–19371, Jun. 2023, doi: 10.1016/j.ijhydene.2023.01.324.
[68] "ISO/TC 197 - Hydrogen technologies," ISO. Accessed: Jun. 29, 2024. [Online]. Available: https://www.iso.org/committee/54560.html
[69] 14:00-17:00, "ISO 19880-1:2020," ISO. Accessed: Jun. 29, 2024. [Online]. Available: https://www.iso.org/standard/71940.html
[70] "J2601_202005: Fueling Protocols for Light Duty Gaseous Hydrogen Surface Vehicles - SAE International." Accessed: Jun. 29, 2024. [Online]. Available: https://www.sae.org/standards/content/j2601_202005/
[71] "EN 17127:2020 - Outdoor hydrogen refuelling points dispensing gaseous hydrogen and incorporating filling protocols," iTeh Standards. Accessed: Jun. 29, 2024. [Online]. Available: https://standards.iteh.ai/catalog/standards/cen/dd394609-b196-4fba-8c9b-1e6c8bd7d282/en-17127-2020
[72] V. Negro, M. Noussan, and D. Chiaramonti, "The Potential Role of Ammonia for Hydrogen Storage and Transport: A Critical Review of Challenges and Opportunities," *Energies*, vol. 16, no. 17, p. 6192, Aug. 2023, doi: 10.3390/en16176192.
[73] "Safety Assessments of Ammonia as a Transportation Fuel," Ammonia Energy Association. Accessed: Jun. 29, 2024. [Online]. Available: https://ammoniaenergy.org/articles/safety-assessments-of-ammonia-as-a-transportation-fuel/
[74] "Ammonia Refrigeration - Overview | Occupational Safety and Health Administration." Accessed: Jun. 29, 2024. [Online]. Available: https://www.osha.gov/ammonia-refrigeration
[75] "International Code for the Construction and Equipment of Ships carrying Dangerous Chemicals in Bulk (IBC Code)." Accessed: Jun. 29, 2024. [Online]. Available: https://www.imo.org/en/OurWork/Environment/Pages/IBCCode.aspx
[76] H. Jang *et al.*, "Regulatory gap analysis for risk assessment of ammonia-fuelled ships," *Ocean Eng.*, vol. 287, p. 115751, Nov. 2023, doi: 10.1016/j.oceaneng.2023.115751.
[77] "NEN Connect - PGS 12." Accessed: Jun. 29, 2024. [Online]. Available: https://connect.nen.nl/Family/Detail?name=PGS%2012
[78] A. Wang, J. Jens, D. Mavins, and M. Moultak, "Analysing Future Demand, Supply, and Transport of Hydrogen," Jun. 2021, Accessed: Jul. 25, 2024. [Online]. Available: https://www.h2knowledgecentre.com/content/policypaper2256
[79] O. S. Ibrahim, A. Singlitico, R. Proskovics, S. McDonagh, C. Desmond, and J. D. Murphy, "Dedicated large-scale floating offshore wind to hydrogen: Assessing design variables in proposed typologies," *Renew. Sustain. Energy Rev.*, vol. 160, p. 112310, May 2022, doi: 10.1016/j.rser.2022.112310.
[80] Z. Luo, X. Wang, H. Wen, and A. Pei, "Hydrogen production from offshore wind power in South China," *Hydrog. Sourced Renew. Clean Energy Feasibility Large-Scale Demonstr. Proj.*, vol. 47, no. 58, pp. 24558–24568, Jul. 2022, doi: 10.1016/j.ijhydene.2022.03.162.

[81] C. Rodriguez, B. Yeter, S. Li, F. Brennan, and M. Collu, *A critical review of challenges and opportunities for effective design and operation of offshore structures supporting green hydrogen production, storage, and transport*. 2023. doi: 10.5194/wes-2023-143.
[82] A. Rogeau, J. Vieubled, M. De Coatpont, P. Affonso Nobrega, G. Erbs, and R. Girard, "Techno-economic evaluation and resource assessment of hydrogen production through offshore wind farms: A European perspective," *Renew. Sustain. Energy Rev.*, vol. 187, p. 113699, Nov. 2023, doi: 10.1016/j.rser.2023.113699.
[83] A. Singlitico, J. Østergaard, and S. Chatzivasileiadis, "Onshore, offshore or in-turbine electrolysis? Techno-economic overview of alternative integration designs for green hydrogen production into Offshore Wind Power Hubs," *Renew. Sustain. Energy Transit.*, vol. 1, p. 100005, Aug. 2021, doi: 10.1016/j.rset.2021.100005.
[84] "Technology Data for Renewable Fuels," The Danish Energy Agency. Accessed: Jul. 25, 2024. [Online]. Available: https://ens.dk/en/our-services/technology-catalogues/technology-data-renewable-fuels
[85] A. One-GigaWatt, "Hydrohub Innovation Program".
[86] A. H. Reksten, M. S. Thomassen, S. Møller-Holst, and K. Sundseth, "Projecting the future cost of PEM and alkaline water electrolysers; a CAPEX model including electrolyser plant size and technology development," *Int. J. Hydrog. Energy*, vol. 47, no. 90, pp. 38106–38113, Nov. 2022, doi: 10.1016/j.ijhydene.2022.08.306.
[87] F. D. Chico Moreno, "Design of an Electrolyzer Integrated in an Offshore Wind Turbine System," University of Twente. [Online]. Available: https://ris.utwente.nl/ws/portalfiles/portal/267465220/PDEng_Report_FDCM.pdf
[88] Y. Bai and Q. Bai, "Chapter 6 - Subsea Cost Estimation," in *Subsea Engineering Handbook*, Y. Bai and Q. Bai, Eds., Boston: Gulf Professional Publishing, 2010, pp. 159–192. doi: 10.1016/B978-1-85617-689-7.10006-8.
[89] D. Cevasco, S. Koukoura, and A. J. Kolios, "Reliability, availability, maintainability data review for the identification of trends in offshore wind energy applications," *Renew. Sustain. Energy Rev.*, vol. 136, p. 110414, Feb. 2021, doi: 10.1016/j.rser.2020.110414.
[90] "Offshore Wind Outlook 2019 – Analysis," IEA. Accessed: Jul. 29, 2024. [Online]. Available: https://www.iea.org/reports/offshore-wind-outlook-2019
[91] "The Future of Hydrogen: Seizing Today's Opportunities - Event," IEA. Accessed: Jul. 29, 2024. [Online]. Available: https://www.iea.org/events/the-future-of-hydrogen-seizing-todays-opportunities
[92] "Geopolitics of the Energy Transformation: The Hydrogen Factor." Accessed: Jul. 15, 2024. [Online]. Available: https://www.irena.org/publications/2022/Jan/Geopolitics-of-the-Energy-Transformation-Hydrogen
[93] "The Future of Hydrogen – Analysis," IEA. Accessed: Jul. 15, 2024. [Online]. Available: https://www.iea.org/reports/the-future-of-hydrogen
[94] Q. V. Dinh, P. H. T. Pereira, V. N. Dinh, A. J. Nagle, and P. G. Leahy, "Levelised cost of transmission comparison for green hydrogen and ammonia in new-build offshore energy infrastructure: Pipelines, tankers, and HVDC," *Int. J. Hydrog. Energy*, vol. 62, pp. 684–698, Apr. 2024, doi: 10.1016/j.ijhydene.2024.03.066.
[95] "News & Events," Kawasaki Heavy Industries, Ltd. Accessed: Jul. 15, 2024. [Online]. Available: https://global.kawasaki.com/en/corp/newsroom/news/detail/?f=20191211_3487
[96] "Current Status of Hydrogen Liquefaction Costs," Department of Energy, USA, Aug. 2019. [Online]. Available: https://www.hydrogen.energy.gov/docs/hydrogenprogramlibraries/pdfs/19001_hydrogen_liquefaction_costs.pdf?Status=Master
[97] Y. Li, "Optimising liquefied natural gas [LNG] supply chains : a case study for China," *World Marit. Univ. Diss.*, Jan. 2002, [Online]. Available: https://commons.wmu.se/all_dissertations/378
[98] A. Giampieri, J. Ling-Chin, and A. P. Roskilly, "Techno-economic assessment of offshore wind-to-hydrogen scenarios: A UK case study," *Int. J. Hydrog. Energy*, vol. 52, pp. 589–617, Jan. 2024, doi: 10.1016/j.ijhydene.2023.01.346.
[99] I. Irena, "Future of wind: Deployment, investment, technology, grid integration and socio-economic aspects," *Abu Dhabii*, 2019.
[100] A. Spyroudi, D. Wallace, G. Smart, K. Stefaniak, S. Mann, and Z. Kurban, "Offshore wind and hydrogen: solving the integration challenge," 2020.

[101] U. Caldera and C. Breyer, "Learning Curve for Seawater Reverse Osmosis Desalination Plants: Capital Cost Trend of the Past, Present, and Future," *Water Resour. Res.*, vol. 53, no. 12, pp. 10523–10538, 2017, doi: 10.1002/2017WR021402.
[102] M. Penev, J. Zuboy, and C. Hunter, "Economic analysis of a high-pressure urban pipeline concept (HyLine) for delivering hydrogen to retail fueling stations," *Transp. Res. Part Transp. Environ.*, vol. 77, pp. 92–105, Dec. 2019, doi: 10.1016/j.trd.2019.10.005.
[103] J. André, S. Auray, D. De Wolf, M.-M. Memmah, and A. Simonnet, "Time development of new hydrogen transmission pipeline networks for France," *Int. J. Hydrog. Energy*, vol. 39, no. 20, pp. 10323–10337, Jul. 2014, doi: 10.1016/j.ijhydene.2014.04.190.
[104] Z. Abdin, C. Tang, Y. Liu, and K. Catchpole, "Large-scale stationary hydrogen storage via liquid organic hydrogen carriers," *iScience*, vol. 24, no. 9, p. 102966, Sep. 2021, doi: 10.1016/j.isci.2021.102966.
[105] J. Ikäheimo, J. Kiviluoma, R. Weiss, and H. Holttinen, "Power-to-ammonia in future North European 100 % renewable power and heat system," *Int. J. Hydrog. Energy*, vol. 43, no. 36, pp. 17295–17308, Sep. 2018, doi: 10.1016/j.ijhydene.2018.06.121.
[106] B. A. Franco, P. Baptista, R. C. Neto, and S. Ganilha, "Assessment of offloading pathways for wind-powered offshore hydrogen production: Energy and economic analysis," *Appl. Energy*, vol. 286, p. 116553, Mar. 2021, doi: 10.1016/j.apenergy.2021.116553.
[107] F. Baldi *et al.*, "Optimisation-based system designs for deep offshore wind farms including power to gas technologies," *Appl. Energy*, vol. 310, p. 118540, Mar. 2022, doi: 10.1016/j.apenergy.2022.118540.
[108] M. Patel, S. Roy, A. P. Roskilly, and A. Smallbone, "The techno-economics potential of hydrogen interconnectors for electrical energy transmission and storage," *J. Clean. Prod.*, vol. 335, p. 130045, Feb. 2022, doi: 10.1016/j.jclepro.2021.130045.
[109] C. MacGregor, "The future of Hydrogen," presented at the Energy, COVID, and Climate Change, 1st IAEE Online Conference, June 7-9, 2021, International Association for Energy Economics, 2021.
[110] G. Azinheira, R. Segurado, and M. Costa, "Is Renewable Energy-Powered Desalination a Viable Solution for Water Stressed Regions? A Case Study in Algarve, Portugal," *Energies*, vol. 12, no. 24, Art. no. 24, Jan. 2019, doi: 10.3390/en12244651.
[111] S. Song *et al.*, "Production of hydrogen from offshore wind in China and cost-competitive supply to Japan, Nat. Commun., 12, 6953," 2021.
[112] M. Hurskainen, "Liquid organic hydrogen carriers (LOHC): Concept evaluation and techno-economics," 2019.
[113] M. Al-Breiki and Y. Bicer, "Comparative cost assessment of sustainable energy carriers produced from natural gas accounting for boil-off gas and social cost of carbon," *Energy Rep.*, vol. 6, pp. 1897–1909, Nov. 2020, doi: 10.1016/j.egyr.2020.07.013.
[114] "Oil price manufacturing industry in Great Britain 2022," Statista. Accessed: Jul. 17, 2024. [Online]. Available: https://www.statista.com/statistics/372315/price-of-oil-per-tonne-manufacturing-industry-in-the-united-kingdom-uk/
[115] "Hydrogen pipelines vs. HVDC lines: Should we transfer green molecules or electrons?" THE OXFORD INSTITUTE FOR ENERGY STUDIES, Nov. 2023. [Online]. Available: https://www.connaissancedesenergies.org/sites/connaissancedesenergies.org/files/pdf-pt-vue/ET27-Hydrogen-pipelines-vs.-HVDC-lines_HG_AP_2.pdf
[116] "Specification of a European Offshore Hydrogen Backbone." DNV, Feb. 17, 2023. [Online]. Available: https://www.gascade.de/fileadmin/downloads/DNV-Study_Specification_of_a_European_Offshore_Hydrogen_Backbone.pdf
[117] "Journal of Pipeline Systems Engineering and Practice," *Free-Spanning Submarine Pipeline Response to Severe Ground Excitations: Water-Pipeline Interactions*, Nov. 2012. [Online]. Available: https://www.researchgate.net/publication/262619294_Free-Spanning_Submarine_Pipeline_Response_to_Severe_Ground_Excitations_Water-Pipeline_Interactions
[118] *Pipelay Vessel Des. Optim. Using Genet. Algorithms*, [Online]. Available: https://gigatskhondia.medium.com/pipelay-vessel-design-optimisation-using-genetic-algorithms-506aa04212f1

[119] “Pipeline Installation Methods (Lay Methods).” [Online]. Available: https://anakkelautan.wordpress.com/2014/01/31/pipeline-installation-methods-lay-methods/
[120] “Offshore Pipeline Installation.” [Online]. Available: https://nfatmala.blogspot.com/2016/02/offshore-pipeline-installation_5.html
[121] “Pipe-laying Method in Offshore / Subsea Construction.” [Online]. Available: https://indonesiare.co.id/id/article/pipe-laying-method-in-offshore-subsea-construction
[122] “International Journal of Hydrogen Energy,” *Levelised cost of transmission comparison for green hydrogen and ammonia in new-build offshore energy infrastructure: Pipelines, tankers, and HVDC*, Apr. 10, 2024. [Online]. Available: https://www.sciencedirect.com/science/article/pii/S0360319924008553
[123] “International Journal of Hydrogen Energy,” *GIS-based scenario calculations for a nationwide German hydrogen pipeline infrastructure*, pp. 3813–3829, Apr. 01, 2013.
[124] (Yong Bai, Qiang Bai), *Subsea Engineering Handbook (Yong Bai, Qiang Bai)*.
[121] «International Journal of Hydrogen Energy», Levelised cost of transmission comparison for green hydrogen and ammonia in new-build offshore energy infrastructure: Pipelines, tankers, and HVDC, 10 aprile 2024. [Online]. Disponibile su: https://www.sciencedirect.com/science/article/pii/S0360319924008553
[122] «International Journal of Hydrogen Energy», GIS-based scenario calculations for a nationwide German hydrogen pipeline infrastructure, pp. 3813–3829, 1 aprile 2013.
[123] (Yong Bai, Qiang Bai), Subsea Engineering Handbook (Yong Bai, Qiang Bai).
[124] Mahdi Fasihi , Robert Weiss , Jouni Savolainen , Christian Breyer, «Applyed Energy», Global potential of green ammonia based on hybrid PV-wind power plants, 2021.
[125] Armando Díaz-Motta , Francisco Díaz-Gonz´alez , Manuel Villa-Arrieta, «Journal of Cleaner Production», Energy sustainability assessment of offshore wind-powered ammonia, 2023.
[126] Tansu Galimova , Mahdi Fasihi , Dmitrii Bogdanov , Christian Breyer, «Journal of Cleaner Production», Feasibility of green ammonia trading via pipelines and shipping: Cases of Europe, North Africa, and South America, 2023.

List of tables

List of figures

SPOWIND

Interreg
Euro-MED

Co-funded by
the European Union

Politecnico
di Torino

University
of Cyprus

ΕΠΙΣΕΥ
ICCS

ENVPRO

SAPIENZA
UNIVERSITÀ DI ROMA

EIHP

edp